POLITECNICO DI TORINO

Corso di Laurea Magistrale in Ingegneria Civile

Tesi di Laurea Magistrale

Investigating the thermo-mechanical performance of energy geo-structures using numerical approaches

Master's degree thesis

Mateo Garcia Bertaina

Supervision:
Marco Barla (Politecnico di Torino)

Co-supervision:
Guillermo Narsilio (University of Melbourne)
Nikolas Makasis (University of Melbourne)

Marzo, 2020

Abstract: *Shallow geothermal energy systems can be used to provide renewable energy for heating and cooling purposes by utilizing the ground as a thermal source/sink. An innovative application that can minimize capital costs is to incorporate this technology in structural foundations, such as piles, retaining walls and tunnels. Due to the large variations in geometry and conditions, there exist a lack of understanding of how these structures can be most optimally and efficiently designed and how/if their structural performance can be affected. This study will incorporate finite element numerical modelling approaches, developed within the University of Melbourne, to further investigate the thermal and mechanical performance of energy geo-structures, in particular retaining walls.*

TABLE OF CONTENTS

LIST OF TABLES

LIST OF FIGURES

1 Introduction

1.1 Overview of work

Energy *geo-structures* are used to provide thermal energy in addition to their primary aim, the structural stability. The different structures can be optimally and efficiently designed depending on their geometry and structural purpose and based on the same reasons, their structural performance can be affected due to the appearance of thermal activity.

Since the first purpose of the geotechnical structure is stability, the incorporation of a thermal use of the same, which is a secondary objective of the system, should be done ensuring that extra solicitations are considered in the calculation of the respective structure and the soil stability. In the case where extra solicitations were found, they should be minimum to avoid damaging both, the structure and soil, and avoid the enlargement of the designing cost of the structure.

This study is focused essentially on diaphragm walls, which have not been researched deeply in comparison to other types of geotechnical structures as tunnels or piles. The study will incorporate Finite Element Numerical modelling approaches, developed with the software *COMSOL*, within the University of Melbourne.

The expected research outcomes will provide valuable information regarding the viability of diaphragm walls, specifically in structures founded over the water table level, which is a first step to start the research in this kind of structures as, in this case, the hydraulics are basically uncoupled to the rest of the physics (mechanics and thermodynamics).

1.2 Organization of Thesis

This thesis consists in five chapters. Chapter 1 describes the motivation and scope for the work. Chapter 2 presents the literature as relevant to energy consumption, geo-structures, GSHPs, and theory that need to be managed for the fully understanding of this work (both for geotechnics and thermodynamics). Chapter 3 describes the specific case of study. Chapter 4 presents the FEM model of the case of study, including mechanical, thermal and thermomechanical. Chapter 5 outlines the research results and conclusions.

2 Literature Review

2.1 Today's energy

2.1.1 Sources

Nowadays, the energy provision is a huge topic to focus on as the living standards, the technology development and the population are increasing, with the consequent increase of energy consumption. With this quick step, the energy consumption may overpass the amount of energy offered, and then, special care should be taken to manage this situation.

The source of the energy provided worldwide varies region to region, including also the importation of energy from other parts of the world as well. Now, natural fossil fuels are the biggest source of energy worldwide with about 80 % of the participation, while only a 10 % is taken by modern renewables sources. These numbers can be seen in Figure 1 Principal energy sources (taken from www.ren21.net) with more clarity.

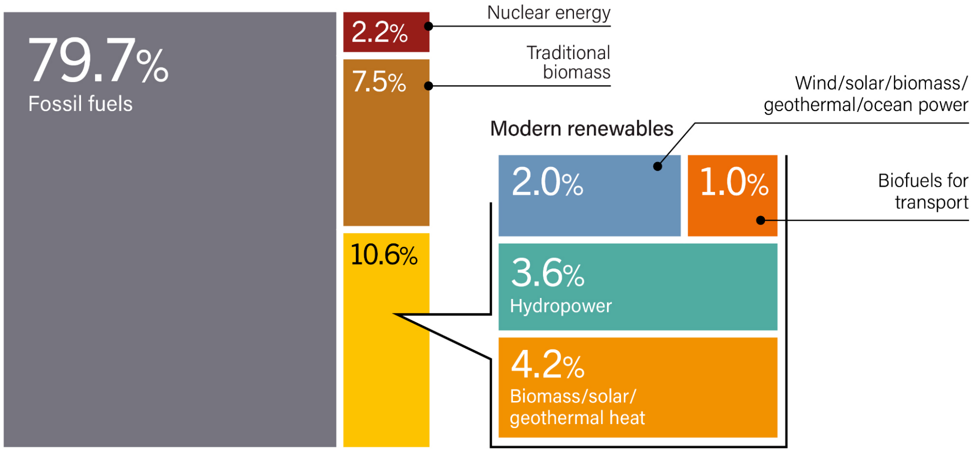

Figure 1 Principal energy sources (taken from www.ren21.net)

In the figure, are shown the main sources of energy, included:

- *Solar energy*: accounts for the solar power, harnessing the sun's energy to produce electricity through photovoltaic cells.

- *Wind energy*: conversion of wind motion by wind turbines into useful means of energy, as electricity or mechanical energy.

- *Biomass*: uses living and recently dead biological material as fuels or for industrial production.

- *Geothermal:* harness the increased temperature located in the layers of soil to either condition buildings in case of shallow geothermal system or produce electricity for the case of deep ones.

- *Hydro power*: produces power using gravitational forces of falling or flowing water. Includes wave and hydrological power.

- *Nuclear energy*: its principle lays on splitting atoms in a called reactor, to heat water into steam to run turbines, and in this way, generate electricity.

- *Fossil fuels*: comes from the biomass produced in former eras, like geologic deposits of organic material formed from decayed plants or animals, that have been converted to oil, coal, natural gas or heavy oils.

Nowadays the last source, as was mentioned before, is the main one. Since the use of fossil fuels impacts on climate change, urban heat island phenomenon, and involves a limited source, a big consideration of this situation should be taken. The mentioned fact calls for the need of renewable energy, which has already started to be developed in many countries.

An outlook of the development of renewable energies worldwide can be seen in the following chart:

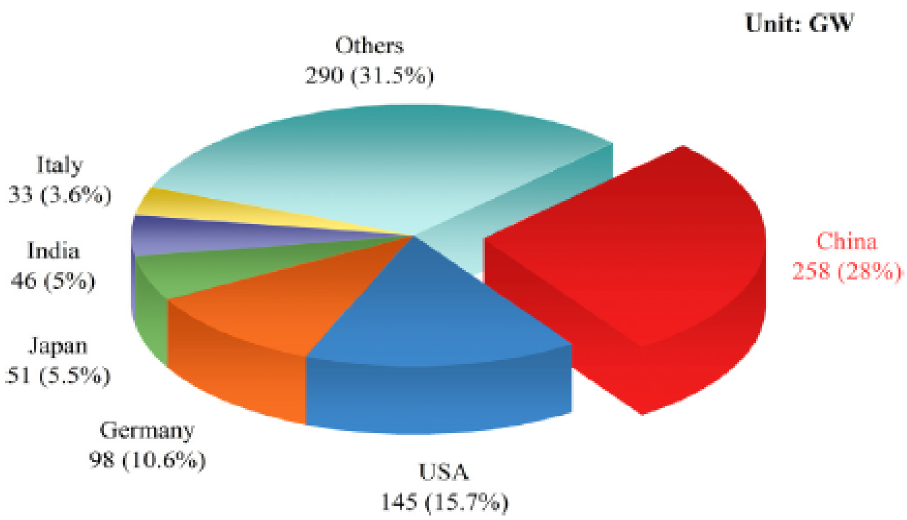

Figure 2 Top six renewable energy power generation capacities in the world in 2016 (taken from www.ren21.net)

2.1.2 **Application**

While considering the development of new green and clean energy sources it is of vital importance the consideration of the destination of this energy, because this destination, condition the source that suits the best for it.

In Figure 3 Renewable energy in total final energy consumption,2016 (taken from www.ren21.net) can be seen the different destinations of the energy and the different sources involved on them.

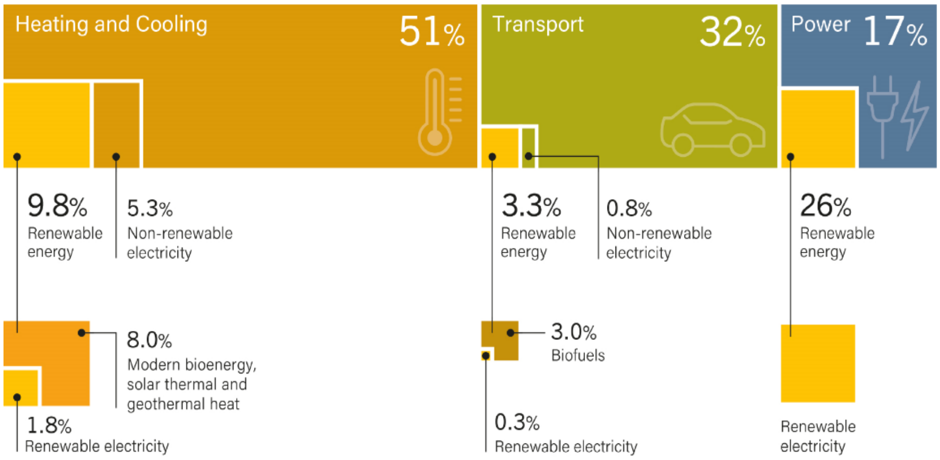

Figure 3 Renewable energy in total final energy consumption,2016 (taken from www.ren21.net)

An interesting fact to point out, is that most of the energy is going to Heating and Cooling purposes, taking more than the half of the amount of energy consumed. In a second plane, the transportation is taking a little more than a quarter of the total energy, leaving the power purpose of energy in a last place with only 17 % of participation.

This fact is showing that there is a huge opportunity for renewable energies to take place in the heating and cooling destination.

2.2 Geothermal energy

2.2.1 Application

Geothermal resources provide electricity and thermal energy services also known as processed heat and space heating and cooling respectively. These two different destinations of the geothermal source have totally different principles, and consequently, technologies and costs involved.

For the case of electricity services (or processed heat), in terms of costs, this source involves high research and installation cost. In particular, has high inherent risk for the exploration and the project development. One of the main risks involves the high capital that must be mobilised for the exploratory drilling that needs to be done to establish the size, temperature and other parameters that define the viability of this resource. Nevertheless, new methods of resource exploration and extraction are helping to overcome this problem, but still there is a great field of study to be focused on for a great advancement in this energy.

Among the different renewable energy sources, geothermal energy for electricity production, also must face with high project costs as said. An important aspect to counterbalance the high cost is the fact that geothermal brine can contain relatively high penetrations of rare earth minerals and metals, and the recovery of these can add extra value to the geothermal extraction.

Respect to the thermal energy services (or space heating and cooling) coming from geothermal systems, this source is likely to be applied in any environmental condition, which means that is quite flexible. The main costs involved are related to the installation of its components at a very first stage, with almost no cost related to maintenance. These first costs are mitigated if this technology is applied in the means of geothermal structures as will mention ahead.

Based on the two different destinations of these geothermal energy, the same can be subdivided between two main categories:

- Deep geothermal energy
- Low enthalpy systems

2.2.1.1 Deep geothermal energy

In this category can be found the geothermal power plants which harness the temperature found at large depths to produce big amounts of energy to generate electricity.

The plants can operate in different ways to obtain this energy. Between them could be found "dry steam" operations, where the heated water vapor is used to drive an electrical generator while on the other hand there is the "wet steam" operation, in which a binary cycle is designed, using a mixture of hot water and steam extracted from the ground to produce the energy.

In both cases, to be able to produce electrical power, the water should be at a temperature above the 175 °C to be economically convenient. To obtain this order of temperature, the system must reach between 3.5 and 4.5 km. This last requirement is the reason of its name, and, the reason of the high costs involved.

The principle in which this procedure relies is injecting a fluid into the ground to enhance the transmissivity of it and maintain a reservoir of this fluid that will capture the heat from the ground eventually. This heated fluid will be pumped afterwards to the surface through the called production wells, and will end up in the power plant, where a turbine generator is powered by this geothermal fluid producing energy, able to be distributed to different points of usage.

The use of deep geothermal system is limited to hot areas around the world. As an example of a hot area can be mentioned the border of the called ring of fire in the United States.

These systems have many advantages, being the two main ones:

- independent on the weather (can be used properly in the whole year round)

- totally reliable and predictable
- high lifetime
- great efficiencies levels

For a better understanding of deep geothermal systems, a simple scheme is shown in Figure 4 Deep geothermal system (taking from blog.arcadiapower.com).

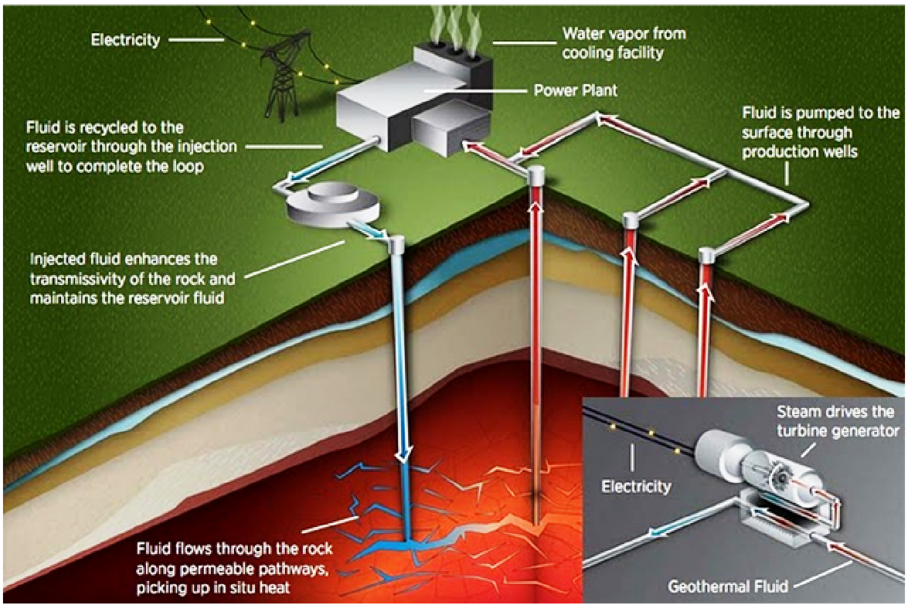

Figure 4 Deep geothermal system (taking from blog.arcadiapower.com)

2.2.1.2 Low enthalpy systems

These systems are totally different from the previous one in terms of the amount of temperature that they manage, and the depth at which they operate.

Low enthalpy systems take advantage of the first tens of meters of soil (<400 m depth) where the temperature is relatively constant through the year, allowing the extraction and injection of heat for cooling and heating purposes. The order of energy at which they operate is between 2 and 35 degrees, with a limit of 40 degrees to avoid damages in the system involved in the heat exchange (limits to the lowest temperatures also exist due to the freezing of the carrying liquid). Due to the order of magnitude of the energy harnessed by these systems, the same are used mainly for cooling and heating of building as was said before.

Special attention should be taken to these systems. As said in paragraph 2.1.2, the main destination of the energy nowadays is Heating and Cooling, and since this energy source manage orders of magnitude proper for this purpose, a good use of Low enthalpy systems can be the answer for a big reduction of the use of non-renewable energy.

When talking about low enthalpy systems, the use of the term “Ground Source Heat Pump systems (GSHP)”, refers to the use of this energy for heating and cooling buildings. Between the rest of the uses of these systems, can be mentioned greenhouse heating, aquaculture pond heating, agricultural drying, industrial uses, bathing and swimming, cooling/snow melting between others.

2.2.2 **Worldwide Geothermal energy**

Nowadays, there are many countries involved in the development and usage of geothermal systems, either deep or shallow ones.

In terms of deep geothermal systems, the countries with the largest amounts of geothermal power generating capacity at the end of 2017 were the United States, the Philippines, Indonesia, Turkey, New Zealand, Mexico, Italy, Iceland, Kenya and Japan. The amounts involved in this worldwide distribution can be observed in Figure 5 Geothermal power capacity (taken from www.ren21.net)

In the other hand, regarding to low enthalpy systems, the main distribution worldwide in terms of continents is shown in Table 1 Distribution of direct geothermal energy utilization by continent (taken from (Lund and Boyd 2016), while the distribution among the main producers is shown in Table 2 Worldwide leaders in the direct utilization of geothermal energy (taken from (Lund and Boyd 2016).

It is important to consider, that the last two tables mentioned involve all the different uses of the low enthalpy systems, already mentioned before.

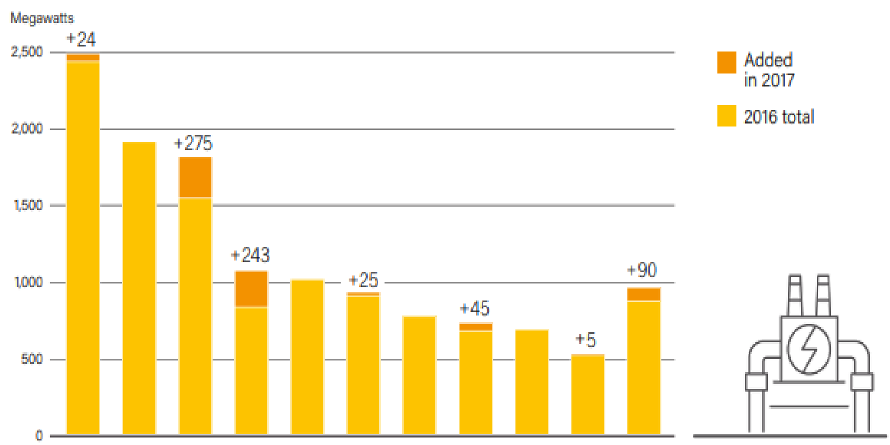

Figure 5 Geothermal power capacity (taken from www.ren21.net)

Table 1 Distribution of direct geothermal energy utilization by continent (taken from (Lund and Boyd 2016)

Continent	# Countries	%MWt	%TJ/year
Africa	8	0.2	0.4
Americas	16	27.7	16.9
Asia	18	35.8	43.9
Europe[a]	37	35.6	37.3
Oceania	3	0.7	1.5

Table 2 Worldwide leaders in the direct utilization of geothermal energy (taken from (Lund and Boyd 2016)

MWt	TJ/year
China (17,870)	China (174,352)
USA (17,416)	USA (75,862)
Sweden (5,600)	Sweden (51,920)
Turkey (2,937)	Turkey (45,892)
Germany (2,849)	Iceland (26,717)

2.2.3 Ground source heat pumps (GSHPs)

As said before, Ground Source Heat Pumps are low enthalpy geothermal energy systems used mainly for heating and cooling purposes of civil buildings. Three main components are found on them:

1) The primary circuit

2) The heat pump, and the

3) Secondary circuit

The first one is composed by a series of Ground Heat Exchangers (GHEs) which take or put energy from or to the ground. The second component, the heat pump, is the one that pumps the carrying fluid from the ground to the building or the other way round, acting as a connection component between the primary circuit and the secondary one, which has the purpose to transfer the heat to and from the building using air or water as a medium (among other carrying fluids). An example of a GSHP is shown in Figure 6 Low enthalpy system during cooling and heating mode (taking from Makasis 2018).

These types of systems provide paybacks in less than 4 years of operation and work as a good option for conditioning houses. The installation of GSHP can be done directly through trenches or boreholes made only for this purpose.

Another option to install a GSHP, is coupling the GHE to any geotechnical structure involved in the building, allowing to reduce the expenses of the installation and reducing the time to obtain the payback.

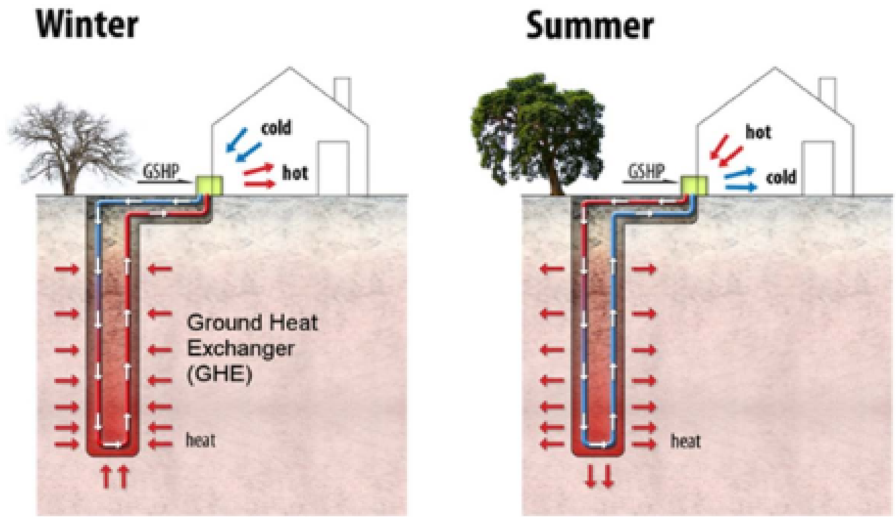

Figure 6 Low enthalpy system during cooling and heating mode (taking from Makasis 2018)

As can be observed in Figure 6 Low enthalpy system during cooling and heating mode (taking from Makasis 2018)these systems can operate during winter and summer, conditioning where the heat is going. In this way, during winter, the GSHP harness the heat from the ground and extracts it heating the building, using the soil as a source. In the other hand, during summer, the GSHP injects heat into the ground, cooling the building, using the soil as a sink.

These systems are based on the fact that the first tens of meters of soil are found roughly at a constant temperature during the whole year, while the need of heat inside the building is changing due to the season. Then, having a temperature gradient between the inside of the building and the ground, a heat flux can be ensured, allowing to condition the building with the heat provided from or to the ground.

It is important to stand that the GSHP can be found in different conditions due to the energy needed. In other terms, these systems can be balanced, when the need of heating and cooling are balanced during the year, keeping the ground roughly in his original main temperature. In the other hand, unbalanced systems are the ones where the heating or the cooling is predominant over the other, raising or lowering the ground’s main temperature.

Ground Source Heat Pump systems can be divided into open and closed systems. The first ones use separate trenches or wells for extraction and for injection, while the second ones use HDPE pipes to circulate fluid into a unique GHE. Open systems are more dependent on the balance of the provided energy but can be installed in more diverse environments.

For the case of closed systems, they can be installed vertically or horizontally, having different cost and production of energy. In the case of vertical systems, the cost is higher in the sense that need a lot of drilling but at the same time they obtain higher amounts of heating, reducing the length of the GHEs needed (HDPE pipes). In the other hand, horizontal systems are cheaper in the sense that don't need drilling, but they do need larger areas and larger lengths of pipes since the order of magnitude of temperature that they manage is smaller, requiring more area of heat exchange to capture the heat.

An increasing installation of these systems has been done in the last years due to its economical characteristics and the increasing conscientisation on climate change. In Table 3 Worldwide leaders in the installation of geothermal heat pumps are shown the main leaders in the installation of the GSHP worldwide.

Table 3 Worldwide leaders in the installation of geothermal heat pumps

MWt	TJ/year
USA (16,800)	China (100,311)
China (11,781)	USA (66,670)
Sweden (5,600)	Sweden (51,920)
Germany (2,590)	Finland (18,000)
France (2,010)	Germany (16,200)

2.3 Energy geo-structures

Regarding the low enthalpy systems, the cost of boring and trenching for the installation of the GHEs is the main cost of them, mainly in vertical ones. To overcome this economic disadvantage, have appeared the energy geo-structures, which harness any kind of geotechnical structure used as a primarily underground structural element (i.e. retaining walls, tunnel linings and piles) to incorporate the GHEs at small extra cost. In this way these geotechnical structures have as a primary purpose the provision of structural stability, and as a second purpose the energy production.

Nowadays, the most common energy geos-structure implemented are piles. The main cause of this may be the fact that have the most likely geometry to a borehole, which is a great geometry to capture the heat from the ground. After them, the other structures used as GHEs are tunnel's linings and earth retaining structures (mainly flexible earth retaining walls and soldier pile retaining walls)

The researches have been focused on investigating the thermal performance of these structures and the geo-mechanical effects induced due to thermal activity.

Regarding the second investigation purpose, research has shown that no significant issues arise in most of the cases of energy piles, but there is limited information about earth retaining systems and tunnels.

The cases of tunnel's linings and earth retaining walls are more complex in the sense that don't involve a completed surrounded structure by ground, as the case of piles, giving a non-symmetric consideration of the problem.

2.3.1 Energy piles

Energy piles involve the coupling of GHEs with piles, giving to the last one the secondary objective of providing energy in a very simple, low cost and time saving solution,

These structures, further than providing structural support to the superstructure, are equipped with pipes that have a heat carrier fluid circulating to harness the thermal storage capabilities of the ground surrounding the foundation. The typical scheme of an energy pile involves loops of pipes connected to a GSHP. These loops can be attached to the structural reinforcement cages being installed within the foundation, adding little additional cost.

A single energy pile may delivery between 25 to 50 W/m depending on its size, construction details, the surrounding soil types and how the system is operated (Bourne-Webb, 2013).

This technology is not new, has been applied before, pioneered in Austria in the 1980s (Brandl, 2006) and taken up in a number of other northern European Countries (e.g. Koene et al, 2000, Pahud & Hubbuch, 2007, Desmedt & Hoes, 2007).

In the case of pile foundations, many piles may be found for the same superstructure involved. Then, the interaction between them and with other energy structures is of important consideration. An example of an energy piles system is shown in Figure 7 Example of pile energy system (taken from www.gsho.org.uk)

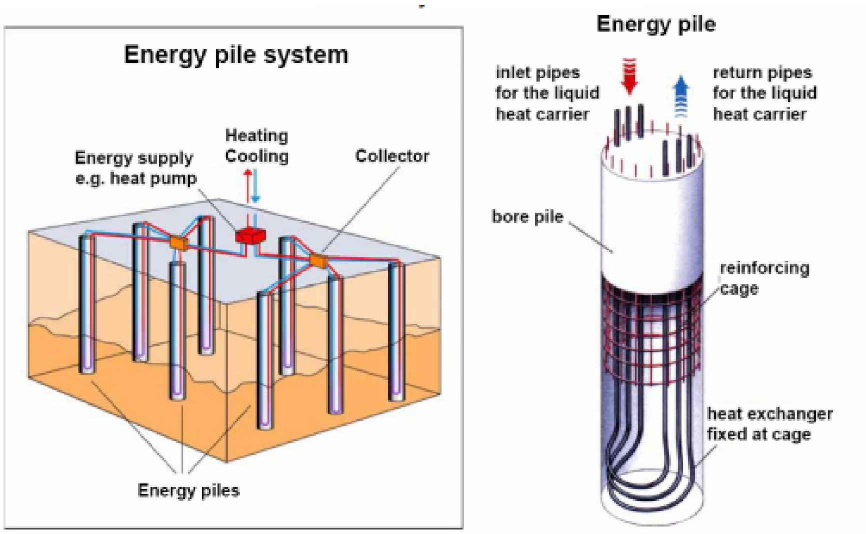

Figure 7 Example of pile energy system (taken from www.gsho.org.uk)

2.3.2 Energy tunnels

When mechanized tunnelling is used, the tunnel segmental lining is precast in factory and then placed on site by the tunnel boring machine (TBM). The segments can therefore be prepared and optimized for heat exchange. In the case of energy tunnels, the heat exchanged at the tunnel level can be transferred to the surface by placing pipes into the ventilation shafts or through the portals. The stations of metro tunnels can also be used for this purpose (Barla and Di Donna 2018)

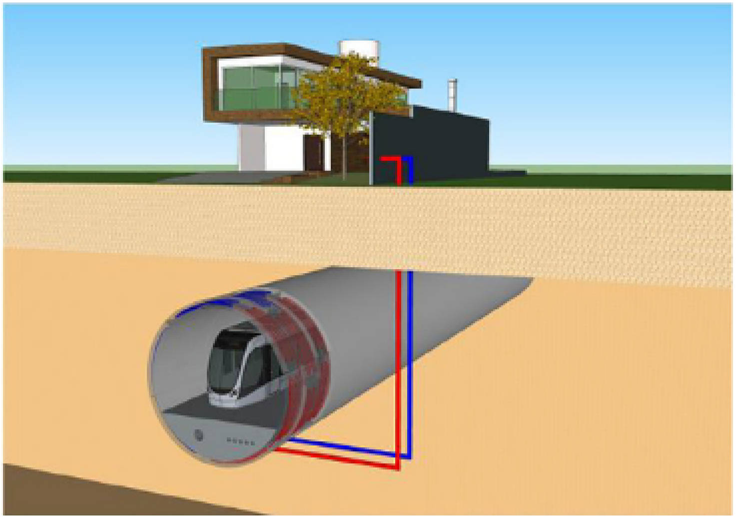

Figure 8 Example of energy tunnel (taken from (Barla and Di Donna 2018)

For the case of energy tunnels, as a difference with energy piles, the heat coming from the air inside the lining can be used as an extra heat source available to be harnessed. For the special case of urban tunnels (underground railways), they usually show high internal temperatures given the rapid cycle frequency of trains and the crowd found in train stations. This increasing temperature can also warm the ground as well.

2.3.3 Energy walls

The fact that these structures involve a big contact area with the surrounded soil gives a great opportunity to obtain big quantities of heat exchanged.

For the application of a GHEs into a diaphragm wall, the type of retaining wall and the construction method involved are of important consideration. The most suitable earth retaining walls are the cast in situ reinforced diaphragm walls.

As in the same case of tunnels, these structures are not totally surrounded by soil. Which means that an extra heat source may be considered due to the air at one of the wall's side, or not, depending of the heat generated due to the activity performed close to it.

These structures, as a difference with the piles, are mainly subjected to horizontal pressures contrasted by its flexural response and by the supporting action of possible anchors and struts.

Variations of pressures induced by the material's thermal contraction or expansion could be of interest, while the possible detrimental action induced by cyclic thermal loads could be neglected, (since the interface shear resistance is not a key factor in the structural behaviour of the wall). In addition, temperature gradients in the wall plane develop not only in the vertical direction, but also in the horizontal direction, due to the non-negligible distance that usually exists between cool and warm portions of the heat exchangers (Coletto and Sterpi 2016)

A simple scheme of a single energy wall panel is shown in Figure 9 Sketch of a single energy wall panel (taken from (Coletto and Sterpi 2016).

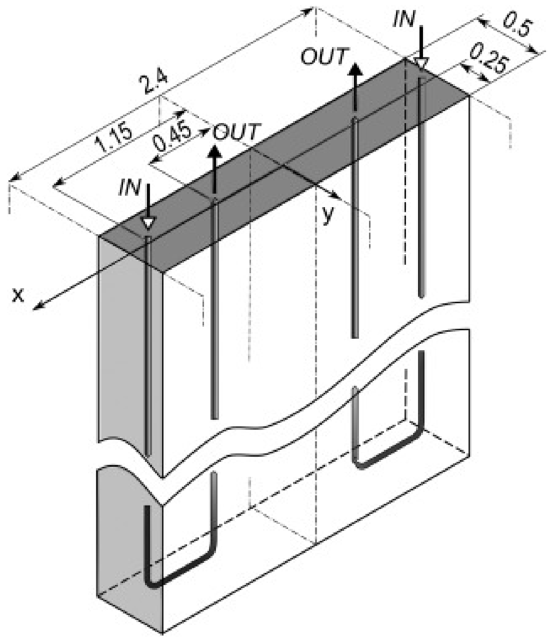

Figure 9 Sketch of a single energy wall panel (taken from (Coletto and Sterpi 2016)

2.4 Continuum mechanics

At a very first stage, the concept of solid continuum should be managed. The so-called continuum mechanics is the kinematic analysis and mechanical behaviour of materials modelled considered as continuous.

The same considers that the discrete composition of material bodies is ignored if the substance of such bodies is distributed uniformly throughout the same, filling completely the space that occupies. If this body is divided into smaller portions, each of them retains all the physical properties of the parent body.

Since the size of the structural elements are many times the order of magnitude of the atoms that compose them, and because the experimental data in structures and geotechnics available for the modelling of the structural components and soil is referred to large size specimens, the application of continuum mechanics suits perfectly for modelling a wide range of geotechnical structures.

Continuum mechanics is divided in two main topics of interest:

- derivation of fundamental equations
- development of constitutive equations

2.4.1 **Fundamental equations**

For the case of Equilibrium equations, from a mathematical point of view, may be developed in two separate but equivalent formulations. The integral (or global) form, derives from a consideration of the basic principles being applied to a finite volume of the material. In the other hand, the differential, leads to equations resulting from the basic principles being applied to an infinitesimal element of volume. It is often useful and convenient to deduce the field equations from their global form.

If the continuum assumption of the material is considered, the field quantities of the problem and material involved, should be a continuum functions as well, dependent of the space and time coordinates.

The following paragraphs will be referenced to a homogeneous isotropic material.

2.4.1.1 Force Equilibrium

Forces equilibrium condition requires that the summation of all forces acting on the body be equal to zero. Employing a force balance on the body are derived the local equilibrium equations. This set of three differential equations must hold for every point in any continuum body that is in equilibrium. Expressed by the global equation, the resulting expression is the following one:

$$\int_S t_i^{(n)}\, dS + \int_V \rho b_i dV = 0 \tag{2.1}$$

Where ti and bi are surface and body forces respectively, dS is the differential element of the surface S and dV that of volume V.

Using the divergence theorem and considering the surface force as a projection of the stress tensor, the resulting expression is:

$$\int_V \left(\sigma_{ji,j} + \rho b_i\right) dV = 0 \tag{2.2}$$

As this equation must be valid for the whole, requires the integrand itself to vanish, and is obtained the so-called local equilibrium equations

$$\sigma_{ji,j} + \rho b_i = 0 \tag{2.3}$$

Or

$$\nabla.\sigma + \rho b = 0 \tag{2.4}$$

for Cauchy's stress tensor

$$\nabla.(FS)^T + \rho b = 0$$

for Second Piola Kirchhoff's nomenclature

For the case of the stress tensor σ, different measures can be defined. Between them, can be founded:

1) The Kirchhoff stresses
2) The Nominal stress
3) The first Piola-Kirchhoff stress (this stress tensor is the transpose of the nominal stress)
4) The second Piola-Kirchhoff stress
5) The Biot stress

In the case of Cauchy stresses, this measure is the one of the forces acting on an element of area in the deformed configuration. Then, it is the measure of the so-called "true stress". In the other hand, the Second Piola Kirchhoff stress tensor, express the forces acting on an element of area in the reference configuration. It is important to consider that Cauchy's tensor is defined in a spatial frame and Second Piola Kirchhof's one, in a material frame. Both, Cauchy's and Second Piola Kirchhoff are symmetric stress tensors.

All the stress tensors coincide in a geometrically linear analysis.

The relation between Cauchy's stress tensor and Second Piola Kirchhof's one is:

$$S = (JF^{-1}\sigma F^{-T})$$

With σ Cauchy's stress tensor, scalar defined as J= det F, and F deformation gradient defined as $F = I + \nabla U$ (this allows the conversion between spatial and material frames)

This vector S, may include different contributions, as shown in equation **(2.5**

$$\mathrm{S} = \mathrm{Sad} + J_i F_{inel}^{-1}(C{:}\,\varepsilon_{el})F_{inel}^{-T} \tag{2.5}$$

$$S = \left(S_0 + S_{ext} + S_q\right) + J_i F_{inel}^{-1}(C{:}\,\varepsilon_{el})F_{inel}^{-T}$$

As seen, the same may have the contribution of initial stresses, external stresses, the ones related with constitutive models of materials, between others. For the case of a ILE material, the stresses due to the constitutive behaviour of the same are the associated with equation **(2.5**)

2.4.1.2 Moment Equilibrium

Equilibrium also requires the sum of moments to be zero with respect to any fixed point. This condition is used, together with the local equilibrium equations, to deduce the fact that the stress tensor is symmetric (for the case of some of the stress measurements). This equilibrium condition holds true as long as there is absence of concentrated body moments.

Taking the origin of coordinates as the centre for moments, and xi as the position vector for the typical elements of surface and volume, the balance of moments for the body is:

$$\int_S \varepsilon_{ijk} x_j t_k^{(n)} dS + \int_V \varepsilon_{ijk} x_j \rho b_k dV = 0 \tag{2.6}$$

As before, considering the divergence theorem and the surface force as a projection of the stress tensor, the resulting expression is:

$$\int_V \varepsilon_{ijk}[(x_j\sigma_{qk})_{,q} + x_j\rho b_k]dV = 0 \tag{2.7}$$

Considering that there are forces equilibrium (second term of integral equal to zero), the following expression reduces to the following one after vanishing de integral (as the volume is arbitrary):

$$\varepsilon_{ijk}\sigma_{jk} = 0 \tag{2.8}$$

Concluding that:

$$\sigma_{jk} = \sigma_{kj} \tag{2.9}$$

That means that the balance of moments for a body in which concentrated body moments are absent holds true. As a consequence, for some stress measurements, the stress tensor is symmetric, giving the final expressions for the equilibrium:

$$\sigma_{ij,j} + \rho b_i = 0 \tag{2.10}$$

Or

$$\nabla.\sigma + \rho b = 0 \tag{2.11}$$

2.4.2 **Balance laws**

These are expressions of the conservation of some physical quantity, applicable to all continuum materials and result in equations that must always be satisfied.

2.4.2.1 Conservation of mass

Physically, the mass of the body is associated with its inertial property (its tendency to resist a change in motion). Mass may be a function of the space variables and time. Assuming a continuum material, the limit of this property into an infinitesimal volume is the so-called density of the material.

$$m = \int_{V^o} \rho_0(x,t)dV^0 \tag{2.12}$$

The law of conservation of mass states that the mass of a body, is invariant under motion, that is, remains constant in every configuration

$$\dot{\mathrm{m}} = \frac{d}{dt}\int_V \rho(x,t)dV = 0 \tag{2.13}$$

or

$$\dot{\mathrm{m}} = \int_V (\dot{\rho} + \rho v_{ij})dV = 0 \tag{2.14}$$

These expressions, after a mathematical rearrangement, state the principle of conservation of mass, which looks like:

$$\frac{\partial \rho}{\partial t} + (\rho v_i)_{,i} = 0 \tag{2.15}$$

2.4.2.2 Linear momentum conservation

The principle of linear momentum states that the time rate of change of the linear momentum is equal to the resultant force acting on the body:

$$\frac{d}{dt}\int_V \rho v_i dV = \int_S t_i^{(n)} dS + \int_V \rho b_i dV \tag{2.16}$$

Applying a mathematical rearrangement and vanishing the integral (as the volume is arbitrary), the final expression of linear momentum conservation becomes:

$$\sigma_{ji,j} + \rho b_i = \rho \dot{v}_i$$

It is important to observe, that in absence of motion, the second term disappeared, and the equilibrium of forces is obtained.

2.4.2.3 Angular momentum conservation

Angular momentum represents the moment of the momentum with respect to some point. This principle states that the time rate of change of the moment of momentum of a body with respect to a given point, is equal to the moment of the surface and body forces with respect to that point.

Taken the origin of any coordinates system as the point of reference, the angular momentum expression has the following aspect:

$$\frac{d}{dt}\int_V \varepsilon_{ijk}x_j\rho v_k \, dV = \int_S \varepsilon_{ijk}x_j t_k^{(n)} dS + \int_V \varepsilon_{ijk}x_j\rho b_k dV \tag{2.17}$$

After some mathematical rearrangement, and vanishing the integral as the volume is arbitrary, the angular moment conservation equation is obtained:

$$\varepsilon_{ijk}\sigma_{kj} = 0 \tag{2.18}$$

It is important to state that in the moment of momentum equilibrium equation no external moment was considered. In the case that was considered, the last equation doesn't remain true and the material is said to be a polar material.

As can be seen, the angular momentum equilibrium in absence of external moments, express the equilibrium of moments expressed in 2.4.1.2.

2.4.2.4 Energy conservation

For the case of the energy conservation law, first a purely mechanical balance will be done. After this, an energy balance that includes both mechanical and thermal energies will be performed. This last one is a statement of the first law of thermodynamics.

For the first purely mechanical energy, the energy conservation expresses that the material time derivative of the kinetic energy plus internal energies is equal to the sum of the rate of work of the surface and body forces. The expression related is:

$$\dot{K} = \int_V \rho b_i v_i dV + \int_S t_i^{(n)} v_i dS - \int_v \sigma_{ij} D_{ij} dV \tag{2.19}$$

Or

$$\dot{K} + S = P \tag{2.20}$$

With S the stress work

$$S = \int_V \sigma_{ij} D_{ij} dV = \int_V tr(\sigma.D) dV \tag{2.21}$$

And P the work done by external forces (body and surface ones)

$$P(t) = \int_S t_i^{(n)} v_i dS + \int_V \rho b_i v_i dV \tag{2.22}$$

Putting the stress work in terms of internal energy:

$$S = \dot{U} = \frac{d}{dt}\int_V \rho u dV = \int_V \rho \dot{u} dV \tag{2.23}$$

The final expression becomes:

$$\dot{K} + \dot{U} = P \tag{2.24}$$

This expression states that from the total work done by the external forces, a portion goes toward increasing the kinetic energy, and the remainder appears as work done by the internal stresses.

For the case in which thermal energy is also included, the material time derivative of the kinetic energy plus internal energy is equal to the sum of the rate of work of the surface and body forces, plus all thermal energies that enter or leave the body per unit time.

The thermomechanical continuum considered, will have a rate of thermal energy added to the body, expressed as:

$$Q = \int_V \rho r dV - \int_S q_i n_i dS \tag{2.25}$$

With scalar r the rate at which heat per unit mass is produced by internal sources (known as the heat supply) and vector qi the heat flux vector (measure of the rate at which heat is conducted into the body per unit area per unit time across the element of surface). The heat flux, in the case of conduction, is often assumed to obey Fourier's law (but it depends on the material behaviour)

With the addition of the thermal energy consideration, the expression for energy conservation becomes:

$$\dot{K} + \dot{U} = P + Q \tag{2.26}$$

Or

$$\int_V (\rho\dot{u} - \sigma : D - \rho r + \nabla . q) dV = 0 \tag{2.27}$$

2.4.3 **Compatibility equations**

For the mechanical study in a continuum, the condition of continuity and the fact that each point in the space is occupied by a unique point of the material domain should hold true. In another words the fact that no holes or overlapping in the domain exist should be ensured.

Given a continuum domain, there is a strain field associated at each point of the same, function of the field of displacements. Since the number of strain components are 6 and the number of displacement components is 3, these last three components are not independent. In fact, they must respect the already called compatibility equations. Then, can be shown mathematically that for a compatible displacement field to exist, all the components of strain and their derivatives must exist and be continuous to at least the second order.

This condition can be studied focusing on the strain components at each point of the domain. Assuming small strain theory, the condition for compatibility of displacements can be written in function of the field displacement components u, v, w as follows:

$$\frac{\partial^2 \varepsilon_x}{\partial y^2} + \frac{\partial^2 \varepsilon_y}{\partial x^2} = \frac{\partial^2 \gamma_{xy}}{\partial x \partial y} \tag{2.28}$$

$$\frac{\partial^2 \varepsilon_y}{\partial z^2} + \frac{\partial^2 \varepsilon_z}{\partial y^2} = \frac{\partial^2 \gamma_{yz}}{\partial y \partial z} \tag{2.29}$$

$$\frac{\partial^2 \varepsilon_z}{\partial x^2} + \frac{\partial^2 \varepsilon_x}{\partial z^2} = \frac{\partial^2 \gamma_{xz}}{\partial x \partial z} \tag{2.30}$$

$$\frac{\partial^2 \varepsilon_x}{\partial y \partial z} = \frac{\partial}{2\partial x}\left(-\frac{\partial \gamma_{yz}}{\partial x} + \frac{\partial \gamma_{zx}}{\partial y} + \frac{\partial \gamma_{xy}}{\partial z}\right) \tag{2.31}$$

$$\frac{\partial^2 \varepsilon_y}{\partial z \partial x} = \frac{\partial}{2\partial y}\left(-\frac{\partial \gamma_{yz}}{\partial x} - \frac{\partial \gamma_{zx}}{\partial y} + \frac{\partial \gamma_{xy}}{\partial z}\right) \tag{2.32}$$

$$\frac{\partial^2 \varepsilon_z}{\partial x \partial y} = \frac{\partial}{2\partial z}\left(\frac{\partial \gamma_{yz}}{\partial x} + \frac{\partial \gamma_{zx}}{\partial y} - \frac{\partial \gamma_{xy}}{\partial z}\right) \tag{2.33}$$

2.4.4 **Constitutive equations**

From a point of view of the determination of a continuum mechanical problem, they are the link between stress and strain fields, given the remaining equations to have a determinate equations system for the respective study.

Given a 3D problem, before the introduction of the constitutive equations, the number of equations and unknowns was the following one:

- Unknowns:

  6 stress components + 6 strain components + 3 displacement components = 15 unknowns

- Equations

  3 equilibrium equations + 6 compatibility equations = 9 equations

As can be seen, there are missing 6 equations to be able to have a determinate system for the study of the continuum mechanic problem. This last mentioned equations are the constitutive ones.

They define idealized behaviours based on the internal constitution of a material. It is important to consider that they do define behaviours and not materials, as many materials behave differently under changing levels of loading (mechanical or thermal). In another words, define their response to force or temperature load. At the same time, these equations specify the mechanical and thermal properties of the materials based upon their internal constitution.

Stated in mathematical terms, these equations describe the relationships among the kinematic, mechanical and thermal field equations and formulate a couple problem if needed.

2.4.4.1 Elasticity Theory

Elastic behaviour of materials is characterized by:

1) Stresses is a unique function of the strains

2) Material has the property to complete recovery to a “natural” shape upon removal of the applied forces.

The relation involving the first condition of an elastic model can be linear or no linear. Reference to the first one will be done in this case.

The respective constitutive equation for this elastic behaviour can be expressed in its most general form as:

$$\sigma = G(\varepsilon)$$

Where G is a symmetric tensor and ε is any one of the various strain tensors.

For the case of linear elasticity, the stress tensor, which is also a response function, express a linear relation between stresses and strains.

When the time to talk about strains comes, it is important to stay the difference between small a large strain theory.

- **Small strain theory**

The ε strains, under the assumption of small strain theory, involve small displacement gradients compared with the unit, and then, the infinitesimal strain tensor can be used. Its components are defined as follows:

$$\varepsilon_{ij} = \frac{1}{2}\left(\frac{\partial u_i}{\partial X_j} + \frac{\partial u_j}{\partial X_i}\right) = \frac{1}{2}\left(\frac{\partial u_i}{\partial x_j} + \frac{\partial u_j}{\partial x_i}\right) = \frac{1}{2}\left(u_{i,j} + u_{j,i}\right) \tag{2.34}$$

Respecting the mentioned assumptions, the constitutive equation for a linear elastic behaviour can be expressed through the generalized Hooke's law as:

$$\sigma_{ij} = C_{ijkm}\varepsilon_{km} \tag{2.35}$$

Or

$$\sigma = C\varepsilon \tag{2.36}$$

With C_{ijkm} the tensor of elastic coefficients relating the stresses and strains, which has 81 components. Due to the symmetry of the strain and stress tensors, this tensor containing the elastic coefficients reduces from 81 components to 36 and after considering the existence of a strain energy function reduces from 36 to 21. These elastic coefficients C_{ijkm} may depend upon temperature and on strain-rate effect. The mentioned fact, can be disregarded considering adiabatic and isothermal conditions, and considering the coefficients C_{ijkm} as only a function of position . In this way, neglecting the thermal effects, the energy balance equation

$$\int_V (\rho\dot{u} - \sigma{:}D - \rho r + \nabla.q)dV = 0 \tag{2.37}$$

Is reduced to the following for:

$$\dot{u} = \frac{1}{\rho}\sigma_{ij}D_{ij} \tag{2.38}$$

Including a small-deformation theory, the expression becomes:

$$\dot{u} = \frac{1}{\rho}\sigma_{ij}\dot{\varepsilon}_{ij} \tag{2.39}$$

This expressed internal energy u, is purely mechanical as disregard all the thermal terms, and is called strain energy per unit mass. For a small displacement gradient assumed, the strain energy is a function of the strain components only, and can be written as:

$$\dot{u} = \frac{\partial u}{\partial\varepsilon_{ij}}\dot{\varepsilon}_{ij} \tag{2.40}$$

If these elastic coefficients are constants, the material is known as homogeneous. In this case these constants are the ones describing the elastic properties of the material.

For the specific situation where, summed to the condition to linear elasticity, the material is also an isotropic media, which means that the elastic properties are the same in every set of reference axis at any point, the elastic coefficients tensor is reduced to two components. In this case the material has an Isotropic Linear Elastic (ILE) behaviour. The associated Hooke’s law for this specific behaviour looks like:

$$\sigma_{ij} = \lambda\delta_{ij}\varepsilon_{kk} + 2\mu\varepsilon_{ij} \tag{2.41}$$

As can be seen, the two elastic components are λ and μ, known as the Lamé constants, which can be related to the elastic engineering constants E (Young’s modulus) and v (Poisson’s ratio) as follows:

$$E = \frac{\mu(3\lambda + 2\mu)}{\lambda + \mu} \tag{2.42}$$

$$v = \frac{\lambda}{2(\lambda + \mu)} \tag{2.43}$$

Then, the constitutive expression with these constants looks like:

$$\varepsilon_{ij} = \frac{1}{E}[(1+v)\sigma_{ij} - v\delta_{ij}\sigma_{kk}] \tag{2.44}$$

And the matrix expression for an ILE is:

$$\begin{bmatrix} \epsilon_{11} \\ \epsilon_{22} \\ \epsilon_{33} \\ 2\epsilon_{23} \\ 2\epsilon_{13} \\ 2\epsilon_{12} \end{bmatrix} = \frac{1}{E} \begin{bmatrix} 1 & -\nu & -\nu & 0 & 0 & 0 \\ & 1 & -\nu & 0 & 0 & 0 \\ & & 1 & 0 & 0 & 0 \\ & & & 2(1+\nu) & 0 & 0 \\ & symm & & & 2(1+\nu) & 0 \\ & & & & & 2(1+\nu) \end{bmatrix} \begin{bmatrix} \sigma_{11} \\ \sigma_{22} \\ \sigma_{33} \\ \sigma_{23} \\ \sigma_{13} \\ \sigma_{12} \end{bmatrix}$$

- **Large strain theory**

It is applied when geometric non linearities are present. In this case, the use of a material frame stress tensor is of great help. The constitutive law for the case of an ILE material with the presence of geometric non linearities is shown in equation **(2.45**:

$$\sigma = G(\varepsilon) = J_i F_{inel}^{-1}(C : \varepsilon_{el}) F_{inel}^{-T} \tag{2.45}$$

With $\varepsilon_{el} = \frac{1}{2}(F_{el}^T F_{el} - I), \quad F_{el} = F F_{inel}^{-1}$

And $\varepsilon = \frac{1}{2}[(\nabla u)^T + (\nabla u) + (\nabla u)^T \nabla u]$

It is important to notice that when geometric non linearities exist, the obtention of the elastic strain that will interact in the constitutive relation is not done through the substruction of the inelastic strain by means of a rest, but through a matrix multiplication between the deformation gradients.

Elasticity theory has some shortcomings that will be treated with other constitutive theories. Phenomena such as irreversibility of a portion of the strains, stress-path dependency, coupling effects such as volume changes due to shear stresses, referred to as shear-dilatant, rotation of principal stress axes and, and most behaviour patterns near and beyond failure can't be handled by elasticity theory (Lade 2005).

2.4.4.2 Elastoplastic models

Elasticity theory can predict with good accuracy the behaviour of soils for stress states not approaching failure. To face the shortcomings mentioned about elasticity theory, the plasticity theory is introduced.

In this way, the soil behaviour shown far from failure favours elastic theory, while the behaviour closer to failure is best simulated by plasticity theory. It is important to consider that all the realistic constitutive models for modelling the behaviour of soils involve both components of deformation, elastic, and plastic.

Then, for the complete modelling of a soil behaviour, as said, the elastic and plastic part must be included. For this full definition, the following components should be defined:

Table 4 Components and physical significance for EP models (taken from (Lade 2005)

	Component	Function
Elastic Behavior	Hooke's Law	Produces elastic strains whenever the stresses change
Plastic Behavior	Failure Criterion	Imposes limits on stress states that can be reached
	Plastic Potential Function	Produces relative magnitudes of plastic strain increments (similar function as Poisson's ratio for elastic strains)
	Yield Criterion	Determines when plastic strain increments occur: Only when yield surface is pushed out/in (hardening/softening)
	Hardening/Softening Relation	Determines magnitudes of plastic strain increments (similar function as Young's modulus for elastic strains)

The main components shown in the previous table are explained below:

1) **Elastic stress-strain relationship**

The same can be either linear or nonlinear. The one related to the first one (ILE) was explained in section **Error! Reference source not found.**.

2) **Failure criterion**

As said before, both elastic and plastic behaviour must be modelled in an elastoplastic behaviour of a soil. This criterion imposes the limit for the stresses that a material can reach. Usually this is confused with the yielding criterion in brittle materials. With the purpose of limiting the stresses states that a material can reach this surface is prescribed.

3) **Plastic potential function**

Provides the direction of the plastic strains, which occurs only when the stress state lays on the yield surface ($f(s) = 0$) and remains there (consistency condition).

This plastic potential function can be defined in correspondence to the yield surface in the stress space. Assuming this, an associated plastic flow rule is imposed, and the related plastic strain increment directions can be defined as normal to the plastic yield surface. In other words, implementing this assumption, the direction or relative magnitude of the plastic strain increments can be determined from the yield surface through derivative mathematical expressions. This simplifies the mathematical framework of the plastic constitutive models.

This new concept of the associated plastic flow doesn't fit well for frictional materials, as them predict bigger volume dilation compared to experimental data. This difference is more pronounced for frictional materials with high effective friction angles (Lade 2005).

4) **Yield criterion**

Indicates the onset of plastic strain. Usually is a scalar function of stress defining a surface, expressed in terms of stress components or stress invariants. In this way, all the stress state laying below this surface belong to the elastic behaviour part of the soil, while the ones laying on this surface respond elastoplastically (with irrecoverable or permanent deformations).

A simple scheme explaining this is shown below:

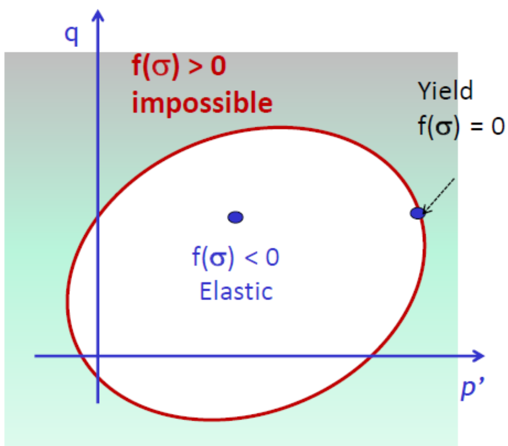

Figure 10 Failure criterion simple scheme

Then, the mentioned failure criterion separates domains where the behaviour is purely elastic, from the ones where the behaviour is elastoplastic. Expressing this in a simple mathematical form:

a) $f(\sigma) < 0$

$f(\sigma) = 0 \; and \; df = \frac{\partial f}{\partial \sigma}.d\sigma < 0$ The behaviour is elastic

b) $f(\sigma) = 0 \; and \; df = \frac{\partial f}{\partial \sigma}.d\sigma = 0$ The behaviour is elasto-plastic

c) $f(\sigma) > 0$ Is an impossible condition as the material can take that state of stress

5) Hardening/softening relation

This accounts for the expansion or contraction of the yield surfaces in the stress space. For the case of hardening plastic models, the expansion occurs, while for softening plastic models the contraction takes place. In another words, this rule tells how the yield surface evolves. Usually, this is obtained by relating the size of the yield surface to the plastic strain.

To clarify these components, a summary of some usual elastic plastic constitutive models is shown in the following tables:

Table 5 EP constitutive models (taken from (Lade 2005)

Type of Model	Model	References	Types of Soil			Failure Surface	Curved Failure Surface in Triaxial Plane?	Yield Surface	Plastic Potential: Associated or Nonassociated?	Hardening Parameter
			Sand	Clay	Cemented Soil					
Elastic	Hooke's Law	Textbook	Yes	Yes	Yes	NA	NA	NA	NA	NA
	Hyperbolic	Duncan and Chang (1970)	Yes	Yes	Yes	Mohr-Coulomb	Yes, see Duncan et al. (1980)	NA	NA	NA
Simple Elastic Plastic	Drucker-Prager	Drucker and Prager (1952)	Yes	Yes	Yes	Extended von Mises	No	= Failure surface	Associated	None
	Drucker's Cap	Drucker et al. (1957)	Yes	Yes	Yes	Extended von Mises	No	Spherical Cap	Associated	Plastic Work
	Stress-Dilatancy	Rowe (1962)	Yes	No	No	Mohr-Coulomb +Dilation Effect	Yes	Mohr-Coulomb	Nonassociated	NA
	Mohr-Coulomb	Smith & Griffiths (1982) Brinkgreve and Vermeer (1997)	Yes	Yes	Yes	Mohr-Coulomb	No	= Failure Surface	Nonassociated	None
	DiMaggio-Sandler	Dimaggio and Sandler (1971) Sandler et al. (1976)	Yes	Yes	Yes	Curved Extended von Mises	Yes	Elliptical Cap	Associated	Plastic Volumetric Strain
	PLAXIS Soft Soil	Brinkgreve and Vermeer (1997)	No	Yes	Yes	Mohr-Coulomb	No	Elliptical Cap	Associated	Plastic Shear & Vol. Strain
	Lade and Duncan	Lade and Duncan (1975)	Yes	Yes	No	Smooth Triangular, Conical	No	Smooth Triangular, Conical	Nonassociated	Plastic Work

Table 6 EP constitutive models (taken from (Lade 2005)

Type of Model	Model	References	Types of Soil			Failure Surface	Curved Failure Surface in Triax. Plane?	Yield Surface	Plastic Potential: Associated or Nonassociated?	Hardening Parameter
			Sand	Clay	Cemented Soil					
Critical State	Modified Cam Clay	Roscoe and Burland (1968)	No	Yes	No	Extended von Mises	No	Elliptical Cap	Associated	Plastic Volumetric Strain
	Elasto-Viscoplastic	Adachi and Oka (1982)	No	Yes	No	Smooth Triangular, Conical	No	Bullet-shaped (Orig. Cam Clay)	Associated	Plastic Volumetric Strain
	Structured Cam Clay	Liu and Carter (2002)	No	Yes	No	Extended von Mises	No	Elliptical Cap	Associated	Plastic Volumetric Strain
	Anisotropic Cam Clay	Sekiguchi and Ohta (1977)	No	Yes	No	Extended von Mises	No	Bullet-shaped (Orig. Cam Clay)	Associated	Plastic Volumetric Strain
	Anisotropic Plasticity	Dafalias et al. (2003)	No	Yes	No	Rotated, Extended von Mises	No	Distorted Ellipse	Nonassociated	Plastic Vol. & Shear Strain
	Nor-Sand	Jefferies (1993)	Yes	Yes	No	Smooth Triangular, Conical	No	Bullet-shaped (Orig. Cam Clay)	Associated	Plastic Work
	Unified SMP	Matsuoka et al. (1999)	Yes	Yes	No	Smooth Triangular, Conical	No	Modified Elliptical Cap	Associated	Product of Stress Funct. & Plastic Vol. Strain
	t_{ij}-Concept	Nakai and Matsuoka (1986) Nakai (1989)	Yes	Yes	No	Smooth Triangular, Conical	No	Modified Bullet-shape (Mod. Orig. Cam Clay)	Associated in t_{ij}-Space (Nonassoc.)	Plast. Vol. Strain(clay "Plastic Work" in t_{ij}-Space (sand)

2.5 **Heat Transfer**

It is well known that heat is the transfer of thermal energy across a defined boundary, within a thermodynamic system. The mechanisms of this possible heat transfer are different. They are mentioned below:

1) Radiation: energy is transferred through emissions of electromagnetic radiation
2) Advection: transport mechanism of a fluid from one location to another, depending on motion and momentum of this fluid
3) Convection: transfer of energy between a domain and its surrounding environment due to a fluid motion
4) Conduction: transfer of energy between two domains that are in contact

Each of this mechanism has different equations involved. Considering all the mechanism of heat transfer and the thermoelastic effects in a continuum medium, the resultant governing equation is the following one:

$$\rho C_p\left(\frac{\partial T}{\partial t}+u_{trans}.\nabla T\right)+\nabla.(q+q_r)=Q \tag{2.46}$$

With:

ρ density

C_p specific heat capacity at constant stress

T absolute temperature

u_{trans} velocity vector of translational motion

q heat flux by conduction

q_r heat flux by radiation

Q additional heat sources

In the sited equation, the term $\rho C_p \left(\frac{\partial T}{\partial t}\right)$ stays for heat transfer in solids and the term $\rho C_p (u_{trans}.\nabla T)$, stays for heat transfer in fluids.

To give an idea of the terms involved in the heat flux by conduction, Fourier's law which express the relation for this heat mechanism of energy exchange is shown below:

$$q = -k\nabla T \tag{2.47}$$

With

k thermal conductivity

∇T temperature gradient

2.6 Thermo-mechanical models of soils

2.6.1 Linear Thermoelasticity

If the effects of temperature are also considered with the mechanical loads on the elastic behaviour of bodies, the themoelasticity is a simple constitutive model to be applied. The same is relatively simple in the fact that is an uncoupled theory for which temperature changes brought about by elastic straining are neglected, and then the equation **(2.40**) doesn't apply.

With this theory, the linear elastic strains are the sum of two contributions:

$$\varepsilon_{ij} = \varepsilon_{ij}{}^{(M)} + \varepsilon_{ij}{}^{(T)} \tag{2.48}$$

where M is the contribution from the mechanical forces and T are the temperature-induced strains.

This thermal strain term, when consider the result from a change in temperature of a completely unconstrained isotropic volume have the following aspect:

$$\varepsilon_{ij}{}^{(T)} = \alpha(T)(T - T_{ref}) \tag{2.49}$$

Where α is the secant coefficient of thermal expansion (m/m/°C).

It is important to consider that shear strains are not induced by a temperature change in an unconstrained body

When heat conduction in an elastic solid is governed by the Fourier law:

$$q_i = -k\nabla T \tag{2.50}$$

Introducing the specific heat shown in equation (**2.51**) can be obtained the heat conduction equation for this linear elastic uncoupled theory. This last equation summed to the thermo elastic one, constitute the basic set of field equations for uncoupled, quasi-static, thermos elastic problems

$$-q_{i,i} = \rho c\dot{T} \tag{2.51}$$

Again, in the case of thermal strains, it is important to refer to the right frame, either material or spatial. For a general approach, which can be applied even with non-geometrical linearities, the following formulation can be used:

$$F_{inel}^{-1} \rightarrow F_{th}^{-1}F_{inel}^{-1} \; with \;\; F_{th} = I + \varepsilon_{th} \tag{2.52}$$

2.6.2 **Thermoelastic damping**

For the case in which the thermal behavior of a material is coupled with the mechanical one of the same, the thermoelastic damping is a simple model to stand this coupling. This phenomenon acts in correspondence with thermoelastic materials, adding an extra term due to the thermal expansion to the respective heat transfer equation. The resulting heat transfer equation with this new thermoelastic damping terms is shown below:

$$\rho C_p\left(\frac{\partial T}{\partial t} + u_{trans}.\nabla T\right) + \nabla.(q + q_r) = -\alpha T{:}\frac{dS}{dt} + Q \tag{2.53}$$

With:

$\propto$ coefficient of thermal expansion

S second Piola-Kirchhoff stress tensor

2.7 **Diaphragm walls**

Earth retaining walls are structures with the aim of supporting lateral loads coming from the soil. Them can be rigid or flexible, defining in this way different resistance and failure mechanism. In the case in which the wall is flexible and is partially embedded into the ground, the structure is called diaphragm wall.

Diaphragm walls maintain stability relying on the resistance of the ground below the excavation level and on the resistance forces provided by any props or anchors. The more flexible the wall is, the smaller the bending moment and larger the deformation, particularly if no props or anchors are used.

These structures are subjected to the called lateral earth pressure coming from the retained soil mass. Analytically, this pressure can be defined by two main theories, Coulomb (1776) and Rankine (1857) which will be explained below. At the end, some comments about the diaphragm wall analysis with numerical modelling will be done.

2.7.1 **Rankine's theory**

Considering the stress states of the soil surrounded a vertical wall retaining a soil mass, Rankine formulated his theory based on the following assumptions:

1) The earth retaining wall is vertical
2) The interface between the wall and soil is frictionless
3) The soil surface is horizontal, and no shear stress acts on horizontal and vertical boundaries
4) The wall is rigid and extends to an infinite depth in a dry, homogeneous, isotropic soil mass
5) The soil is loose and initially in an at rest state

Assuming a rotation about the bottom of the wall enough to produce a slip place in the soil mass at both sides of the wall, Rankine studied the lateral effective stress that brings the soil to the condition of failure with the Mohr's circle. Schemes of the active and passive states and the slip planes studied are shown below:

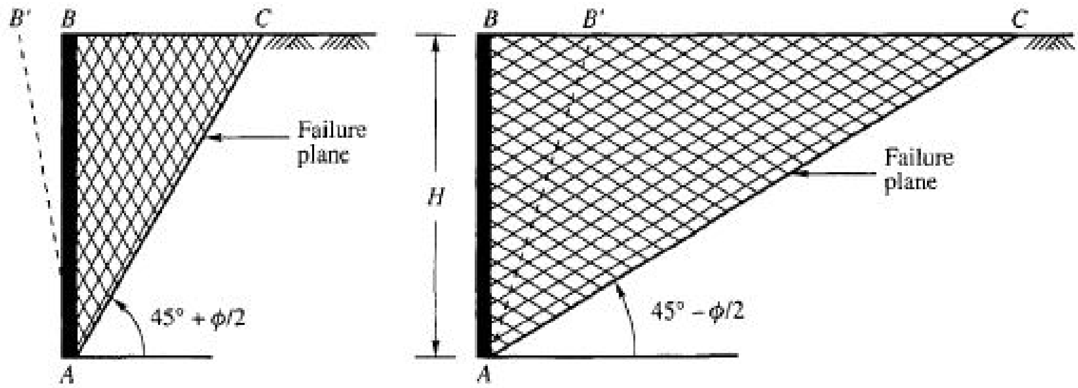

Figure 11 Slip planes within a soil mass near a retaining wall

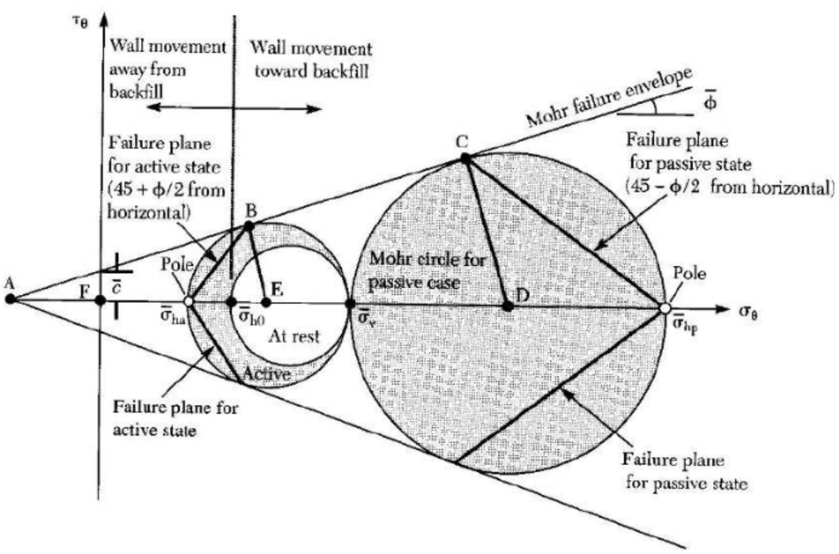

Figure 12 Mohr's circles at rest, active and passive states (Al-Khafaji & Andersland, 1992)

In this way, Rankine demonstrate that the lateral earth pressure on retaining walls are related directly to the vertical effective stress through two coefficients, the active and passive earth pressure ones, shown below:

$$K_a = tan^2\left(45 - \frac{\emptyset}{2}\right) = \frac{1 - \sin(\emptyset)}{1 + \sin(\emptyset)} \qquad (2.54)$$

$$K_p = tan^2\left(45 + \frac{\emptyset}{2}\right) = \frac{1 + \sin(\emptyset)}{1 - \sin(\emptyset)} \qquad (2.55)$$

2.7.2 **Coulomb's theory**

Coulomb is the pioneer of the earth pressure theory. His approach lays on the limit equilibrium method, which can include or not the soil-wall friction. The assumptions for his theory were the following ones:

1) Isotropic and homogeneous soil (with internal friction and cohesion)
2) The rupture and backfill surfaces are planar
3) Friction resistance uniformly distributed along the failure surface
4) Consider an infinite long wall, assuming the problem as a plane strain one

He proposed that the soil mass behind a vertical earth retaining wall experience a tendency to slip along a plane inclined an angle ϑ to the horizontal, defining a limit equilibrium condition. After this assumption he determine this slip plane by searching for the plane in which the thrust acts. The steps included in his study are the ones of a typical limit equilibrium method, which are listed below:

1) Selection of a failure criterion
2) Determination of forces acting on the failure surface
3) Use of equilibrium equations (don't to determine the maximum thrust in this case)

Using the LEM, Coulomb arrived at the same expression than Rankine, but he analyzed the problem as a failure mechanism, while Rankine proposed a stress analysis. The equilibrium condition assumed by Coulomb can be sketched in the following figure:

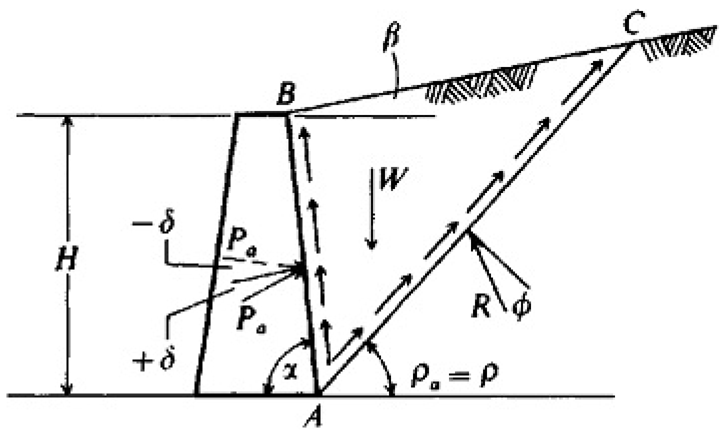

Figure 13 Limit equilibrium for Coulomb's theory (taken from www.civilengineeringbible.com)

This solution is a upper bound one because is usually greater than the true one. This can be since a more efficient failure mechanism may be possible than the one assumed, which usually is curved. This curved failure surface is due to the wall friction that causes the slop planes in both the active and passive states to be curved. In this way the passive earth pressure is overestimated while the active has a small error and can be neglected. To reduce the passive error, a friction for the wall-soil interface is assumed as $\delta<\phi'/3$ (in practice, generally $\delta>\phi'/3$).

Poncelet (1840), used Coulomb's theory to analyse the problem where wall friction was present and the wall face and backfilling were inclined, obtaining the following expressions:

$$K_{ac} = \frac{cos^2(\emptyset' - \eta)}{cos^2\eta \cos(\eta+\delta)\,[1 + \left\{\frac{\sin(\emptyset'+\delta)\sin(\emptyset'-\beta)^{1/2}}{\cos(\eta+\delta)\cos(\eta-\beta)}\right\}]^2} \tag{2.56}$$

$$K_{pc} = \frac{cos^2(\emptyset' - \eta)}{cos^2\eta \cos(\eta-\delta)\,[1 - \left\{\frac{\sin(\emptyset'+\delta)\sin(\emptyset'+\beta)^{1/2}}{\cos(\eta-\delta)\cos(\eta-\beta)}\right\}]^2} \tag{2.57}$$

2.7.3 **Numerical modelling of flexible walls**

The complexity involved in the analysis of a retaining wall increases with the degree of soil-structure interaction, An aspect of total importance that needs to be taking into account during the study is the excavation construction method and neighbored structures interaction, which condition the state of stress involved in the problem, since the load at which the structure is subjected depends on those stresses.

To be able to consider the whole outlook of the problem and obtain a solution as close to reality as possible, a continuum study can be performed with numerical methods. With a continuum mechanic study introduced through numerical methods, the construction process and the interaction with other structures can be considered. Added to this advantage, the case in which slabs, struts or anchors are involved in the problem can be analyzed with ease.

In this case, with a numerical model of the retaining wall, the earth pressure is considered because of the soil deformation and stress state involved in the problem itself. The failure surface at which the soil will tend to fail will be a consequence of the failure criterion adopted for the soil domain and related to the wall stiffness as well.

2.8 Numerical methods

The numerical modelling is a method born to solve boundary value problems. In mathematics, in the field of differential equations, a boundary value problem is a differential equation with a set of restraints called boundary conditions. The solution to a boundary value problem is the solution of the differential equation which satisfies the boundary conditions as well

. Between them, for the field of geotechnical engineering, there are available different numerical methods, in which each one involves a different treatment of the problem:

- Finite element method (FEM)- Continuous method

- Finite difference method (FDM)- Continuous method

-Distinct element method (DEM)- Discontinuous method

-Finite discrete element method (FDEM)- Equivalent-continuous method

-Limit equilibrium method (LEM)- Discontinuous method

-Boundary element method (BEM)

As can be seen above, the numerical methods are divided in three big categories, related to the way in which they consider the domain of study. For that differentiation, the concept of Representative Volume Element (REV) should be considered. The same is the smallest volume over which a measurement can be made and would give a value representative of the whole.

Depending on the relation between the volume of the geometry of the problem and the one of the components of the material that deserve the attention in the problem will define different REV values. Then, can be agreed that when the value of the REV is big compared to the domain volume, the study can be performed through a discontinuous method with good approximation, while when the value is small, the method to be used should be the continuous or equivalent continuous one. It is important to say that the choice of each one depends on the problem that is solved and the calculation cost that wants to be faced.

The numerical method used for this case of study is Finite Element Method, since the physics involved in the same need to be model in a continuous representation of the domain. In particular. was decided to be used a FEM method instead of a FDM because the software requested to be used was a FEM one.

2.8.1 Finite element method

The finite element method (FE) is a differential continuum method developed for solving boundary value problems in continuum mechanics. To solve a boundary value problem in Continuum Mechanics, the following conditions need to be considered:

-Equilibrium equations
-Compatibility equations

-Constitutive law
-Boundary conditions

For the case of a Heat Transfer problem, the conditions that need to be considered are:

-Energy conservation equation
-Boundary conditions
-Heat transfer mechanism equations

In the case of FEMs, the domain is subdivided into discrete elements called finite elements, that provide the approximation to the main variable fields within the continuum. During the application of this method, the governing equations of the problem are written and solved for preliminary points called nodes.

The FEM formulation of the problem results in a system of algebraic equations, for each element of the mesh, that will be assembled into a larger system of equations that model the entire problem. Then, the variational methods are used to approximate a solution minimizing an associated error function. It is important to bear in mind that the FEMs give an exact solution to a differential approximation of the given problem.

The basic steps composing most of the FEM problems are:

1) Domain discretization: model the geometry of the problem and assign a FEM mesh to the same, representing in this way the nodes that the problem will be solved for;

2) Primary variable approximation: as said, the algebra equations of the problems are solved for the nodes. The solution is given in the primary variables selected. Those variables should be assigned and also the way in which they vary over each FE;

3) FE equations: use of an appropriate variation principle to derive element equations;

4) Global equations: combine the FE equations of the whole domain to form the global system equations to be solved;

5) Boundary condition: defined in the boundaries of the problem to set values of the variables on them, modifying the global equations;

6) Solve the global equations; to obtain the values of the primary variables, from which secondary quantities would be calculated.

The previously mentioned primary variables depends on the physics that are solved. For the case of Mechanics, the primary variables are displacements, while for the case of Heat Transfer, the primary variable is temperature. With these primary variables, after been interpolated through the whole domain, they can be derivate to obtain the so called secondary quantities as strain for the case of Mechanics (with which will be obtained stress through the introduction of constitutive equations) or temperature gradients for the case of Heat Transfer, with which, the heat transfer mechanism and the conservation of energy can be applied.

3 Case of study

The following thesis is focused in a fictitious geo-thermal diaphragm wall sited in the city of Melbourne, Australia. The geometry and the soil is based on a case studied already by Barla, Di Donna et al. 2018. This work takes that geometry and soil properties and applies a thermal load correspondent to the city of Melbourne, Australia.

This study includes a different treatment of the thermal modelling adding an extra dimension to the problem as well, consequence of the mentioned treatment of the thermodynamics.

3.1 Geometry

The geometry of the problem involves a 15.5 meters diaphragm wall made of reinforced concrete supporting a 9.5 meters excavation, with a founding slab at the excavation depth.

The same is representative of an underground basement. The activity developed in the surrounding of the wall are the ones related to the movement of a parking transit. The definition of this activity may seem trivial but is going to condition some assumptions during the modelling.

The dimensions of the wall can be observed in the following figure:

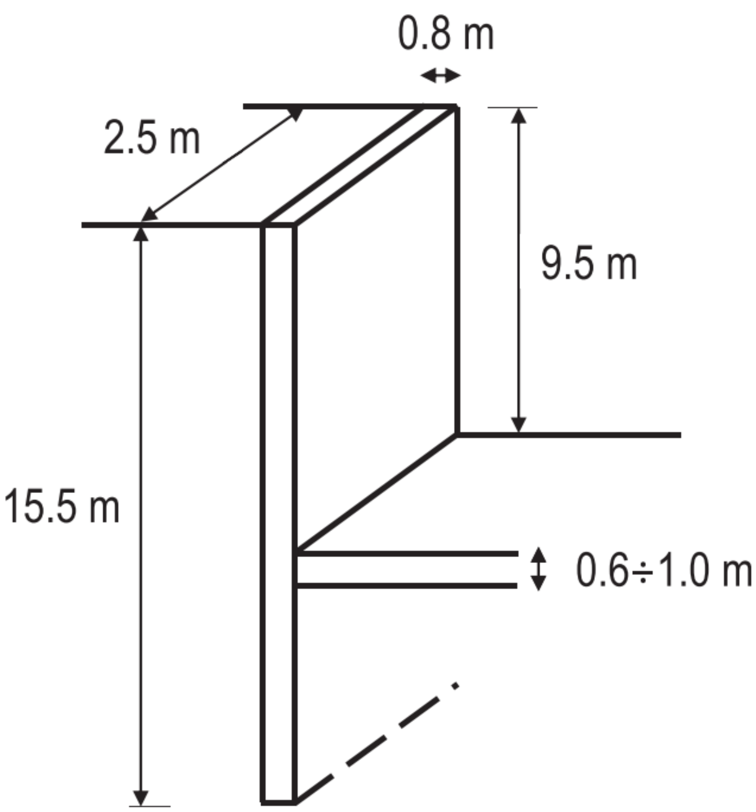

Figure 14 Case study geometry (Barla, Di Donna et al. 2018)

That geometry is the representation of a geothermal diaphragm wall with absorber pipes of HDPE composing the GSHP installed only at the side of the wall correspondent to the unexcavated part. The same is made of reinforced concrete with non-anchors or struts further than the foundation slab. Consequently, this wall can be defined as a cantilever retaining wall or just flexible earth retaining wall.

3.2 Ground water

In this case of study, the ground water has been considered below the structure. The purpose of not considering the ground water is because there is no much research about energy walls, and not including the water coupling in the problem would give a clearer outlook of the outcomes of the mentioned topic.

3.3 Thermal load distribution

The thermal load distribution represents the amount of thermal energy that the system is aimed to provide.

For a thermo mechanical analysis, this is of vital importance in geothermal systems, since they define not only the thermal energy that is provided but the thermal solicitations induced to the structure as well.

The thermal load distribution adopted was the one used by (Makasis 2018) during a research in the city of Melbourne, scaled to match the dimensions of this wall and make sure that the GSHP worked between its operation limits. The same is shown in

Figure 15 **Thermal load distribution to be provided by the geothermal system**.

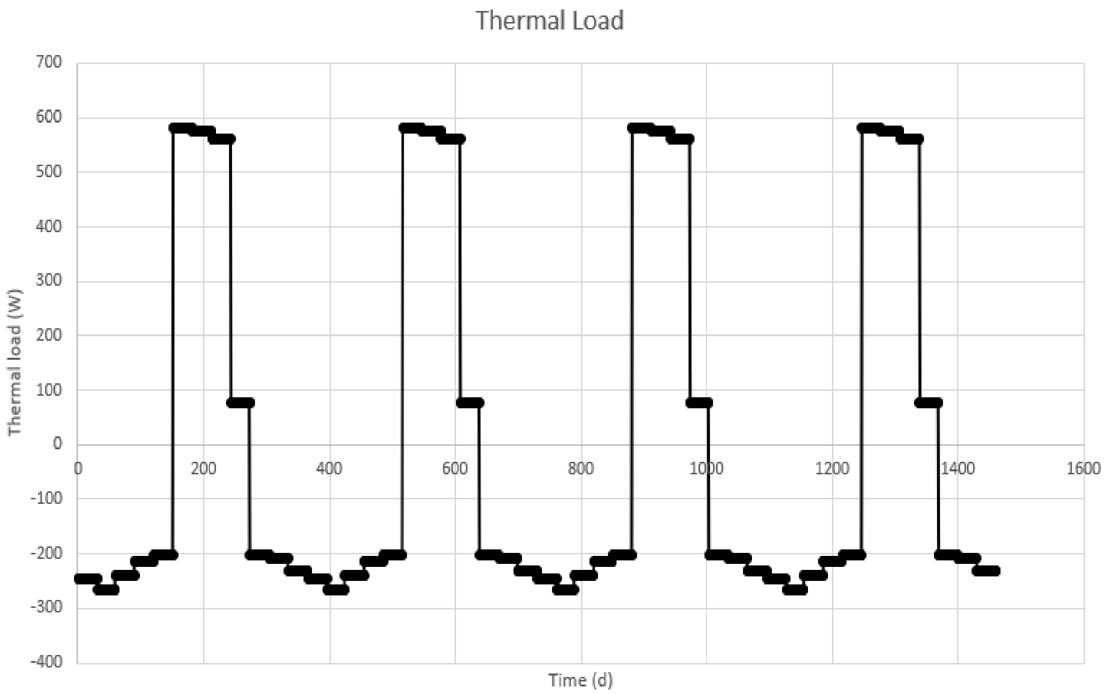

Figure 15 Thermal load distribution to be provided by the geothermal system

The fact that the thermal load used by Makasis was scaled lays in the fact that these low enthalpy systems, specially the pump (the second component of them as described in paragraph 2.2.3),have a certain range of temperature that they can work. Usually they can't sustain temperatures of the carrying fluid over the 40 ˚C. In the other hand, the lower limit of the temperature is conditioned due to the freezing condition of the carrying fluid, that when talking about water, the lower limit is 0 ˚C.

To account for the GSHP operation safety, the numerical model was run with an initial guess of 15 W/m^2 of energy production per square meter of wall. Then, considering that the wall captured heat only through the largest unexcavated side, the calculation was:

$$Thload_{max} = 15 \frac{W}{m^2}\ x\ 15.5m\ x\ 2.5m = 581.25\ W$$

In this way, the thermal load from Makasis was scaled to ensure a maximum thermal load of 581.25 W.

After running the numerical model (only thermal one) for a time scale of four years with the mentioned thermal load, the inlet temperature of the pipe loop was plotted and checked that was within the limits. The main limit that was checked was the one respective to the upper limit for the pump itself, since the lower limit can be extended to a lower value adding some ant freezing liquids to the carrying fluid (even though was checked to be as close to the 0 ˚C limit as possible).

The output obtained for the inlet temperature can be seen in Figure 16 Inlet temperature

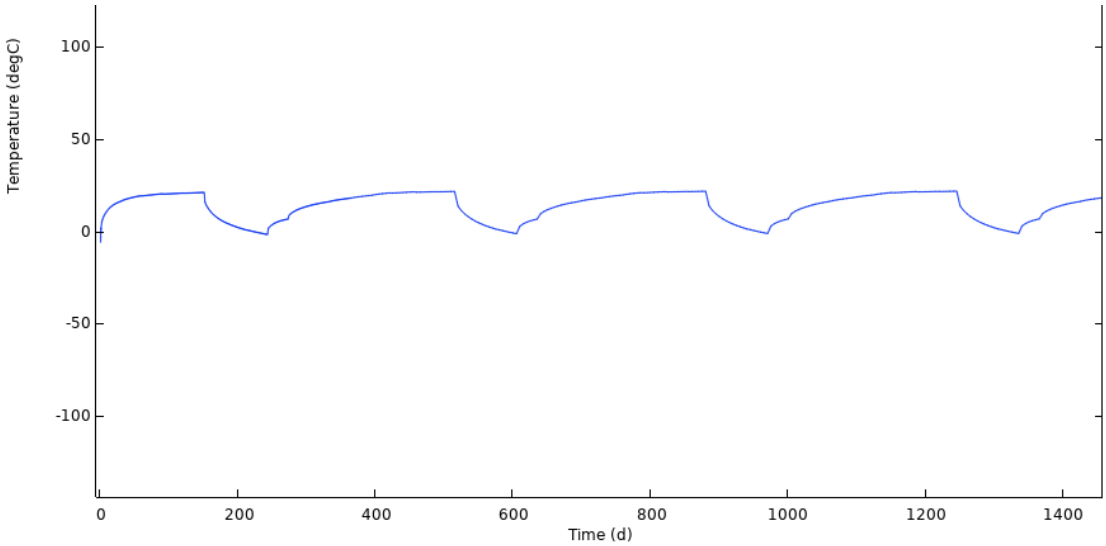

Figure 16 Inlet temperature

The load distribution used can be considered as balanced since the areas of the thermal load plot above and under the zero Watts is pretty much the same, which says that the amount of heat (energy) extracted and injected to the ground are similar. In the other hand, unbalanced systems appear when the demand for heating and cooling is not the same, something that is not optimum for the geothermal systems because it affects the thermal equilibrium of the soil medium.

3.4 Soil and wall

The profile of the soil is assumed to be homogeneous throw-out the whole depth of the structure. The geotechnical and thermal parameters of the soil involved in the case of study are shown in bellow.

Table 7 Soil parameters

Parameter	Value(s)	Unit	Description
λ_{ground}	2.8	W/(m.K)	Thermal conductivity of ground
ρ_{ground}	1988	kg/m3	Density of ground
Cp_{ground}	1053	J/(kg.K)	Specific heat capacity of ground
E	215	MPa	Young Modulus
C	15	KPa	Cohesion
n	0.3	-	Poisson ratio
f	38	degrees	Friction angle

As the wall was modelled as an ILE material, the cohesion and friction angle were not defined. Then the mechanical and thermal parameters for the wall involved in the computation were:

Table 8 Concrete parameters

Parameter	Value(s)	Unit	Description
$\lambda_{concrete}$	2.3	W/(m.K)	Thermal conductivity of concrete
$P_{concrete}$	2549	kg/m3	Density of reinforced concrete
$Cp_{concrete}$	876	J/(kg.K)	Specific heat capacity of concrete
E	33300	MPa	Young modulus
n	0.3	-	Poisson ratio

3.5 Software validation

The software used to perform this study was *COMSOL Multiphysics®* in its version 5.4. The same is a general-purpose simulation software for modelling all fields of engineering. It involves many modules, offering in this way many physics, from the electromagnetics, acoustic, structural, fluid, heat transfer and chemical between others.

COMSOL is not a geomechanics software, even though the case of study is mainly a geomechanics problem. This software is giving much flexibility, allowing the user to define freely each equation, boundary condition, constitutive model and relation to be solved.

In order to model the case of study regarding the thesis, a good level of confidence should be relied into the software used. For this purpose and for the sake of the understanding of the most suitable meshing, boundary conditions definitions and rest of model's features to be defined, it is a good practice to validate the software with trustable data.

For that purpose, two validations have been performed, one mechanical and one thermal.

3.5.1.1 Mechanical validation

3.5.1.1.1 Mechanical validation's case of study

The mechanical validation was followed through the modelling of the retaining wall described in (Barla, Di Donna et al. 2018), the one used for the purpose of this thesis. The geometry of the case studied is shown in Figure 17 Geometry of geothermal wall from (Barla, Di Donna et al. 2018).

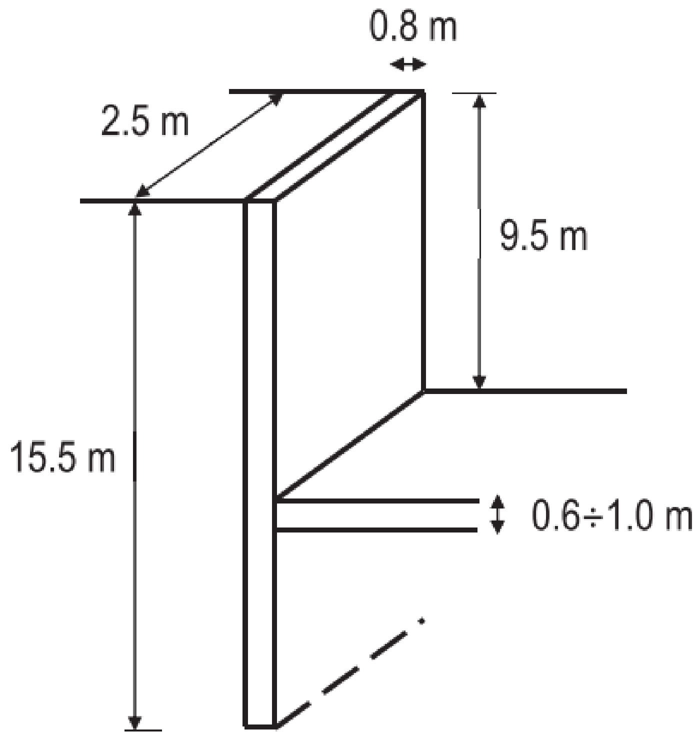

Figure 17 Geometry of geothermal wall from (Barla, Di Donna et al. 2018)

Although the model of the purpose of this thesis was a 3D model, this validation was a plain strain one, since the purpose of this is validating the mechanical physic only, avoiding the existence of many degrees of freedom that a 3D model would have.

For the model, the soil was considered to have an elastoplastic behaviour and the wall (concrete) a behaviour respective to an Isotropic Linear Elastic material.

In terms of the software nomenclature, the soil was set as an Isotropic Linear Elastic material, adding a Soil plasticity feature, which allows to compute the plastic strain, but non elastoplastic stiffness matrix is used during the computation. For this Soil plasticity feature, a Drucker Prager matching the Mohr Coulomb parameters was used, modelling an ELPLA behaviour.

The respective geotechnical parameters both for the soil and the wall were the ones shown in Table 9 Geotechnical parameters adopted for the mechanical validation:

Table 9 Geotechnical parameters adopted for the mechanical validation

Parameter	Unit	Ground	Concrete
Unit weight	[Kg/m^3]	1988	2549
Elastic modulus	[MPa]	215	33300
Poisson's ratio	[-]	0.3	0.2
Cohesion	[KPa]	15	-
Friction angle	[deg]	38	-

3.5.1.1.2 Modelling

To be able to model a solid continuum, usage of the "Solid Mechanics" feature from *COMSOL* was done.

That interface is based on solving Navier's equations, computing displacements, stresses and strains. The same physic can be applied to different parts of the domain as pleased, and different material behaviour and features as Soil Plasticity can be applied to them.

As said before, *COMSOL* is not a geomechanics software, and consequently, the modelling of different construction steps was not straightforward as would be with other software. To overcome this difficulty, was decided to model many study steps, involving one construction step to each study step. Modelling different study steps is equivalent as saying modelling different problems, involving different domains and boundary conditions in each one of them.

It is important to stand the difference between having many studies and having many steps. For a FEM model, the governing equations are solved to obtain the dependent variables in the nodes. For the case of having different studies, the variables that are solved for are totally uncoupled between the studies by default, while in the case of having different study steps, these variables can be coupled with ease. The coupling of variables was needed not only for the field of displacement (primary variables for a mechanical FEM model), but for the stresses as well (secondary variables). The fact of coupling the stresses was important at the moment to model the construction process.

Considering that, for the mechanical validation, a Stationary Study with five study steps was performed. Between these five study steps, can be mentioned:

1) Initial stress field:

   Whole geometry modelled under gravity forces with the purpose of the initialization the stress field with zero displacements.

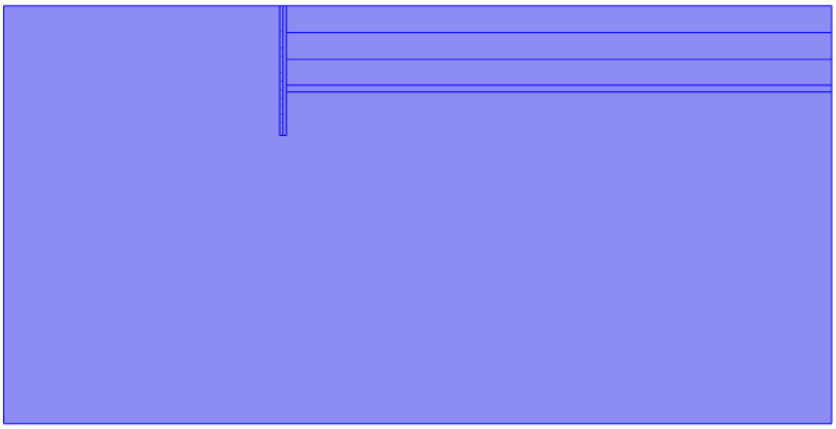

2) First excavation of 3.2 m:

   Was model the domain respective to the remaining geometry after 3.2 meters excavated.

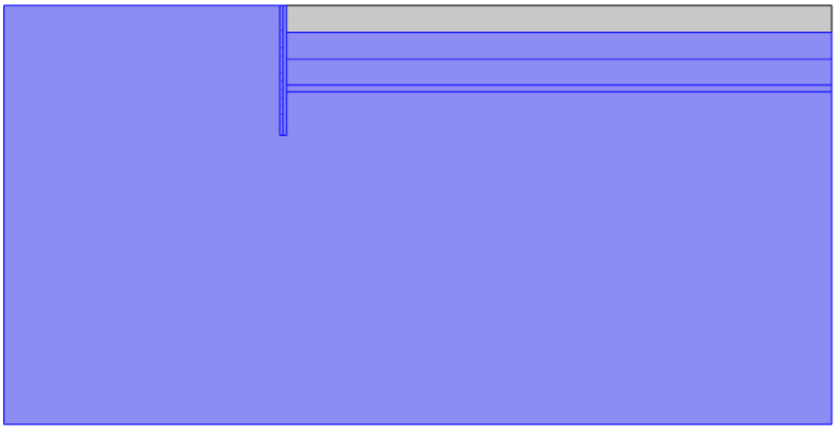

3) Second excavation of 3.2 m:

   Same as previous explanation but considering the geometry remained after 6.4 m excavate

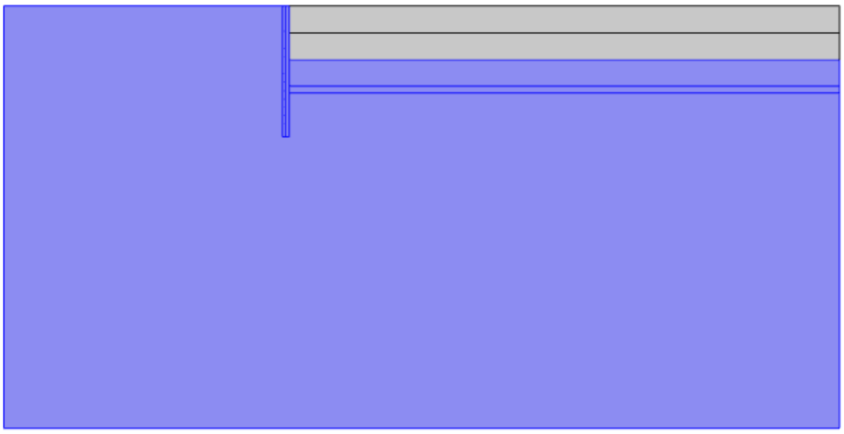

4) Third excavation of 3.1:

   Same as previous explanation but considering the geometry remained after 9.5 m excavated

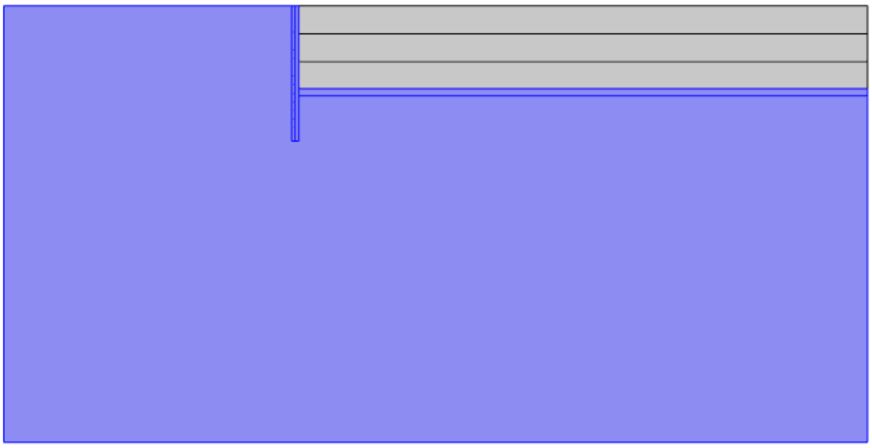

5) Slab installation:

   To simulate this step, were assigned concrete parameters to the finite elements in correspondence with the slab position and were given zero initial stresses to the same.

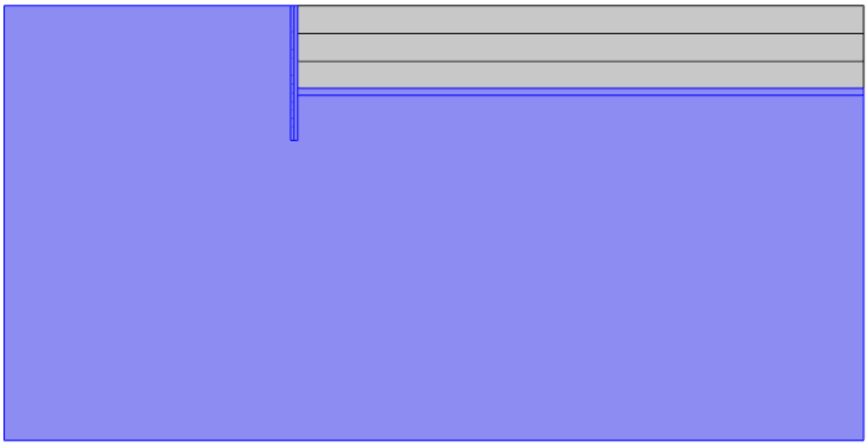

To ensure that the equilibrium was ensured at the beginning of each step and to couple of the stresses and strains was reached between the steps, resource to the “Initial Stress” feature was done. The use of initial stresses is acting in the equation **(2.5**) as the component S_{ext}. Can be noticed that this external stress tensor is not part of the constitutive model.

It is important to clarify that the components of the external stress tensor were the Second Piola Kirchhoff’s stress tensor components, which means that the stress components were defined in the material frame under the undeformed configuration, as the problem was not linear (as will be explained later).

The model’s size was chosen as 99 meters wide and 50 meters of height. With those measurements, was ensured that no undesired effect of the boundary conditions was present in the model.

The boundary conditions involved were set as Dirichlet’s boundary conditions for some of the boundaries, as free at top surface, rollers at the sides and fully constraint at the very bottom of the model and a single Force boundary condition set as Contact for all the boundaries involved in the interface between the wall and the soil. These boundary conditions can be observed in Figure 18 Boundary Conditions

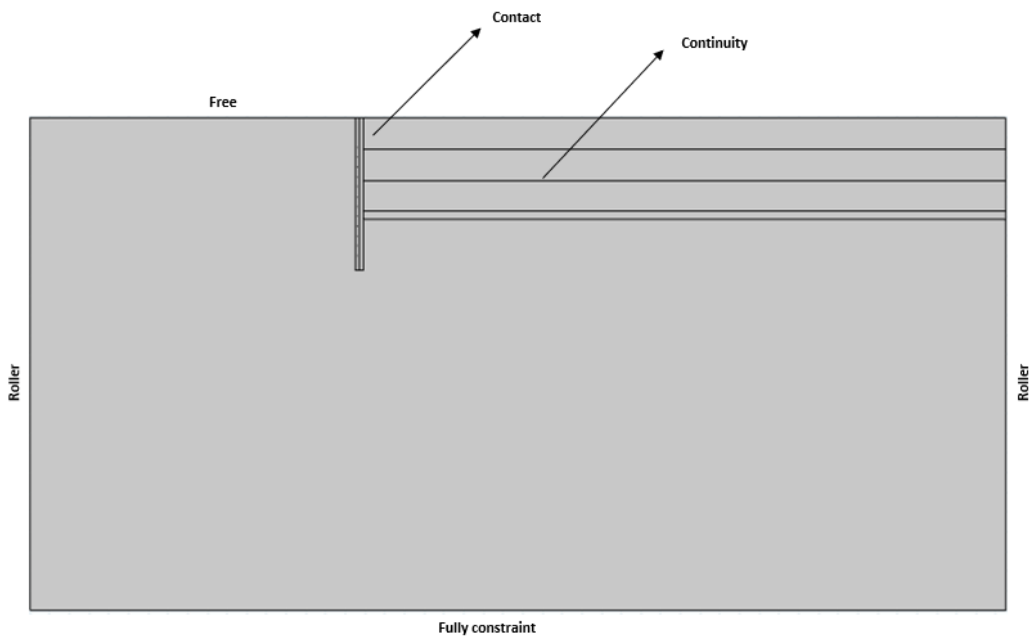

Figure 18 Boundary Conditions

3.5.1.1.3 Treatment of interfaces

One of the biggest difficulties faced during the modelling was the definition of the boundary condition between the wall and the soil. For this definition, the different options considered were:

- Continuity
- Prescribed displacement
- Contact

For the case of the continuity boundary condition, was found that the use of the same to model the interface soil-wall was not an accurate representation of the real behaviour. The main reason laid in the fact that the finite elements at the unexcavated side of the wall were "hanging" from the wall, bending the same to their side, instead of the excavated one.

The definition of a prescribed displacement was set as mapping the soil's nodes displacements into the wall nodes, ordering the soil to follow the wall in this way. It was a good representation of a frictionless interface as the component of displacement mapped was the one normal to the interface. But after comparing results, was decided not to use this boundary condition as the comparison was not good. This may be because the pressure between soil and wall was not obtained properly with this assumption since this may represent an infinite cohesion, and then the wall deflection and bending moment due to this lateral wall was not accurate.

Finally, was decided to use contact boundary conditions. For that purpose, during the model building, was used the software's feature "Contact pairs". The same allows to simulate two boundaries that may be in contact but cannot penetrate each other under deformation. The use of the same also allows to model friction for the interface surface and give stiffness to that interface as well. That boundary condition is the most like any "interface feature" used by any geotechnical software. The disadvantage about using contact boundary conditions is the fact that the problem becomes a non-geometrical linear problem, increasing the computational cost.

The use of Contact Pairs can be done through two different methods, either Augmented Lagrangian or Penalty method. For this model, resource to the second one was done, as the same represents the actual stiffness of a spring inserted between the boundaries of the interface, while the first one controls how hard the interface surface is during the iterations.

During the setting of the contact pairs, was needed to define a "source" and a "destination" for this feature. The software suggested that the source one should have the highest stiffness in correspondence to the normal direction of the boundary involved. Then the wall was selected as the source boundary.

For the definition of the stiffness of the respective springs inserted between the interfaces, was used the so-called characteristic stiffness of the interface. The software suggested to use the one representative of the destination domain material in a direction normal to the boundary. Then the stiffness for the interface surface was the one respective to the soil.

3.5.1.1.4 Wall's efforts

When modelling the wall itself, were analysed two options. The first one was using a physic/feature given by the software called "Beam", which is essentially an interface used to model slender structural elements having significant bending stiffness, giving as outputs displacements, rotations, stresses, strains and section forces.

The pros about this is that the efforts in the wall can be obtained with ease and no extra computation or considerations need to be taken. The cons about this physic, is that is a 1D element which won't allow to simulate the pipes inside the wall properly. The same happened in a 3D model while using the feature "shell". An extra and important disadvantage of that feature is that was not possible to define the boundary conditions in the nodes of the beam with ease.

Due to this fact was decided to model the wall as a continuum with the same physic "Solid Mechanics", allowing to represent the real geometry of the problem and introduce the pipes loops properly in the case of study. Then, to obtain the efforts in the structural element (Bending Moment and Shear), resource to Euler-Bernoulli theory was done. The equation **(3.1** was defined for the nodes in correspondence to the middle axis of the wall.

$$M = -EI\frac{d^2w}{dx^2} \tag{3.1}$$

With w normal displacement component of the node's axis

During the computation of all the stationary steps, the model was subjected to gravity forces in the vertical direction (y axis) as said before.

3.5.1.1.5 Outputs of the validation

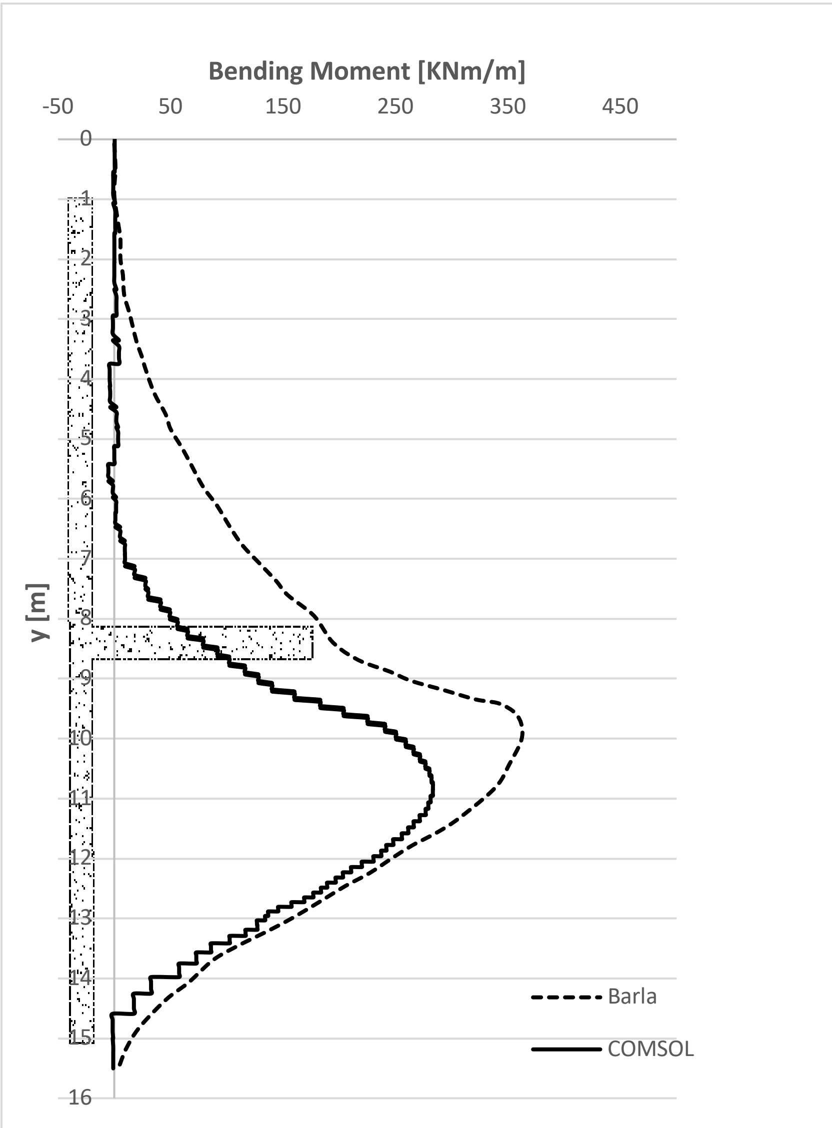

Figure 19 Bending Moment comparison

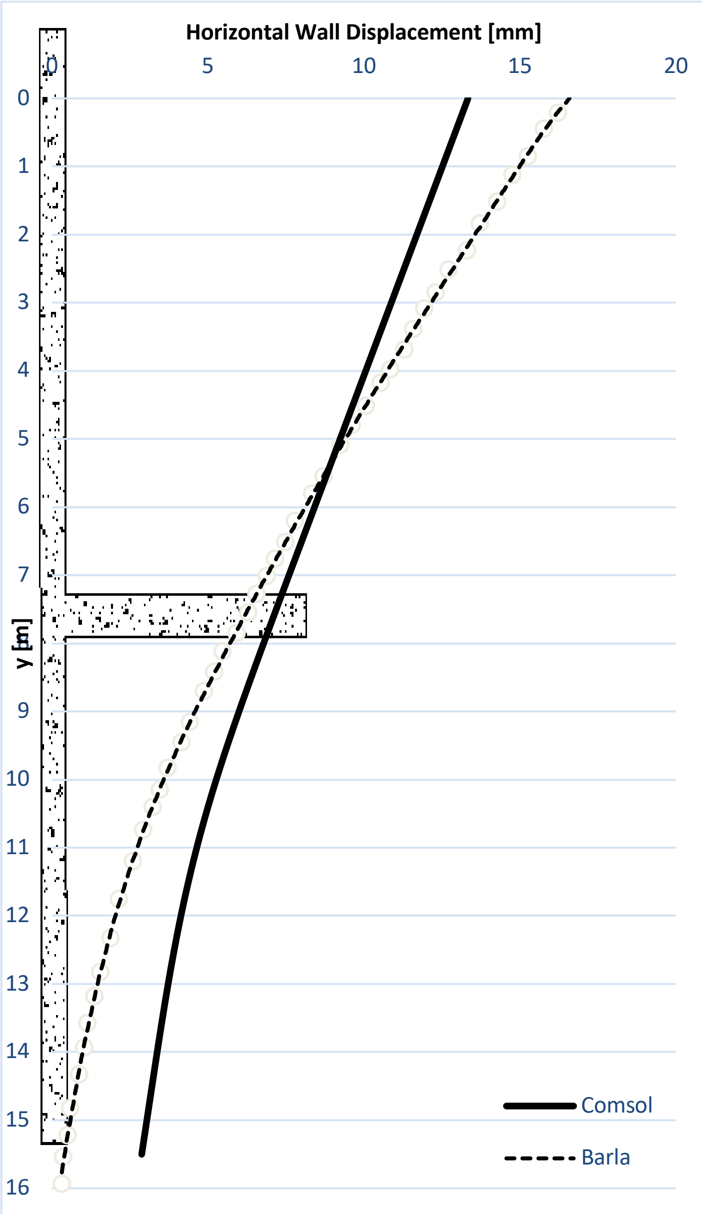

Figure 20 Horizontal Wall displacement comparison

In the last two figures, can be observed the comparison between the bending moment and horizontal wall displacement described in Barla, M., et al. (2018) with the ones respecting *COMSOL's* model. In the case of the wall displacement in the horizontal direction, the difference between the two models in terms of the top wall displacement is about 18 % and in terms of the maximum bending moment is about the 22 %. This difference may be due to the treatment of the interfaces.

For the case of *COMSOL*'s bending moment plot, the observed steps in the line are because the output's results are in correspondence with the nodes, which had a considerable distance between them due to the meshing.

3.5.1.2 Thermal validation

Regarding to the thermal validation of *COMSOL* software, were done two different validations.

The first validation was referred to the model built by Bidarmaghz. A, Makasis. N and other members of Porous Media Research Laboratory for the simulation of a Thermal Response Test from the University of Melbourne, while the second one was the thermal simulation of the geothermal wall described in Barla, Di Donna et al. 2018 sited already in paragraph 3.5.1.1 .

These two thermal validations had different purposes for the aim of the thermal validation itself. The first validation was done to validate the physics involved in the thermal heat exchange and fluid flow that were used in the case of study of this thesis. The second one, was done to validate the thermal part of the study described in Barla, M., et al. (2018).

3.5.1.2.1 Makasis's validation

The validation involving Bidarmaghz. A, Makasis. N work consist in modelling a Thermal Response Test (TRT) performed in an energy soldier pile retaining wall in Melbourne city. The model itself had the purpose to simulate soil-wall behaviour under heating and cooling loads, examining the thermal effect with the software *COMSOL*.

The geometry of the model and the mesh adopted for the same are shown in Figure 21 COMSOL FEM model for thermal validation (taken from Bidarmaghz. A, Makasis. N), while the data from the field and the comparison model-field data are shown in Figure 22 TRT data from field work (taken from by Bidarmaghz. A, Makasis. N)and Figure 23 TRT 1 linear regression (taken from Bidarmaghz. A, Makasis. N) respectively.

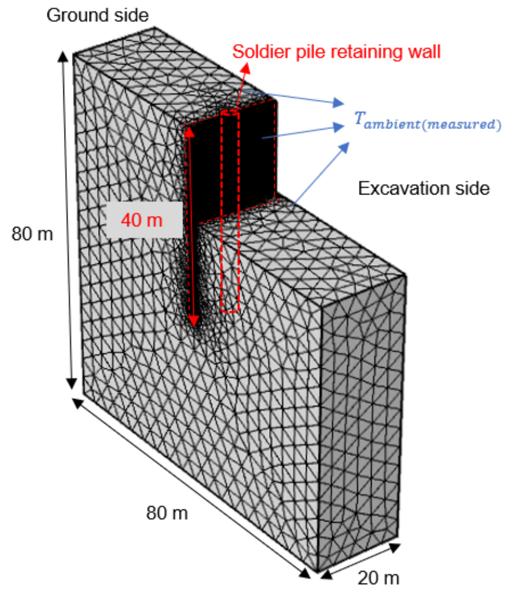

Figure 21 COMSOL FEM model for thermal validation (taken from Bidarmaghz. A, Makasis. N)

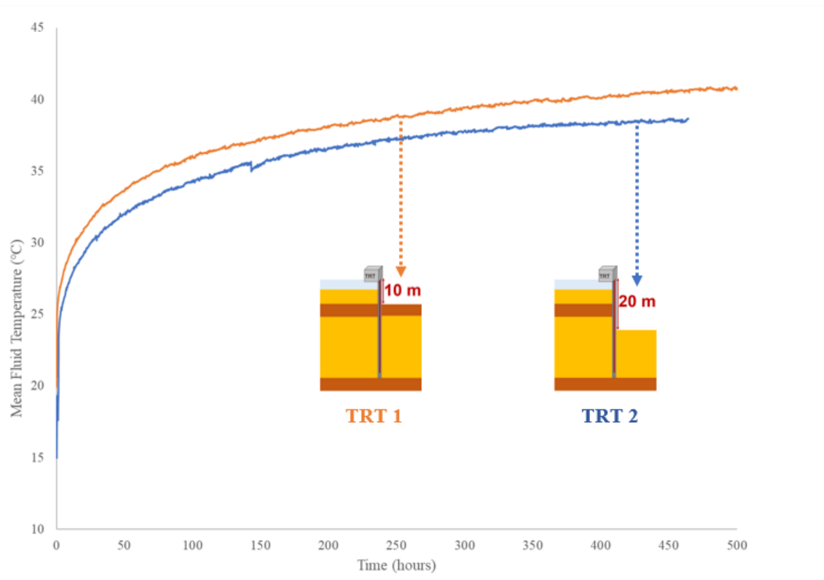

Figure 22 TRT data from field work (taken from by Bidarmaghz. A, Makasis. N)

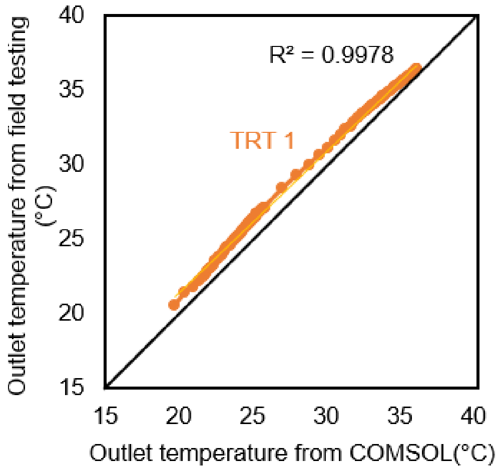

Figure 23 TRT 1 linear regression (taken from Bidarmaghz. A, Makasis. N)

For the same model, two physics were involved. The first one was the so-called "Heat Transfer in Solids", which is an interface used to model heat transfer in solids by conduction, convection and radiation. The governing heat equation for temperature corresponds to the differential form of the Fourier's law. With that interface, the heat exchange through the whole domain and the temperature boundary conditions were modelled. These last Temperature boundary conditions are shown in Figure 24 Thermal boundary conditions (taken from Bidarmaghz. A, Makasis. N).

For the computation of that physic the initial values were set with the same value as the Far field temperature. Afterwards, a time dependent study was performed.

During the mentioned computation, another physic was coupled with the Heat Transfer in Solids. This coupling was done with the interface "Non-isothermal Pipe Flow", which allows to compute the temperature, velocity and pressure fields in pipes, approximating the pipe flow profile by 1D assumptions. In this way, the temperature through the whole domain of the soil was coupled with the temperature that the carrying fluid had inside the pipes.

These last two mentioned physics were the ones used for the study case of this thesis, reason why they needed to be validated for the final 3D model before its application.

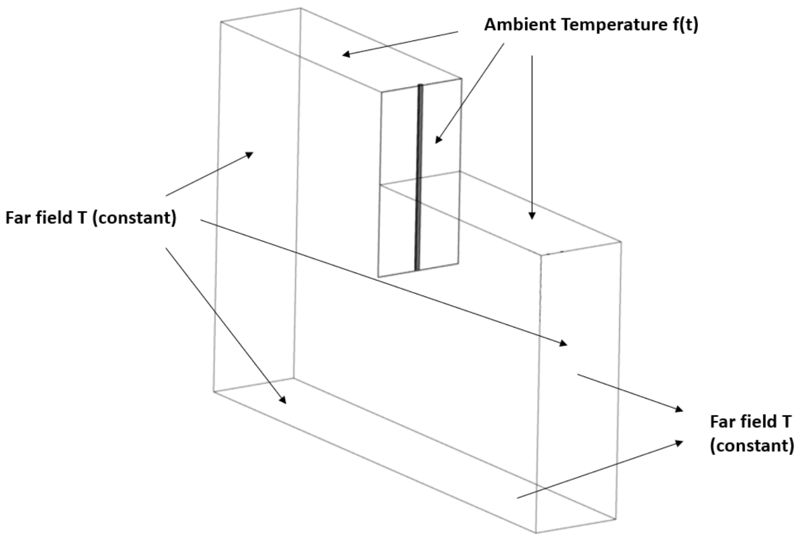

Figure 24 Thermal boundary conditions (taken from Bidarmaghz. A, Makasis. N)

3.5.1.2.2 Thermal diaphragm wall validation

Regarding the thermal validation upon the work done by (Barla, Di Donna et al. 2018), a model with a time dependent study with two study steps was performed. The same included only one physic, the already mentioned "Heat Transfer in Solids", for which, the boundary conditions were set as shown in Figure 25 Thermal boundary condition.

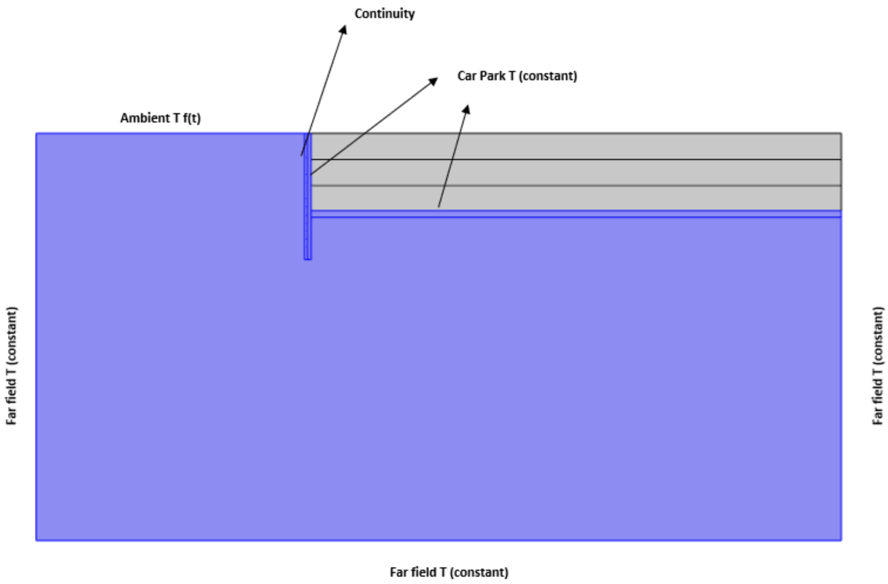

Figure 25 Thermal boundary condition

For the first step, the initial values were set as 14 ˚C for the whole domain, considered as the mean value year-round temperature. That temperature was also used to define the far field and car park temperatures. This first step was subjected to an “Ambient Temperature” on the top surface for 1095 days (3 years), with a daily time step. That study simulated the approaching to a thermal equilibrium due to the new excavated geometry, where the new geometry found a constant temperature of 14 ˚C in correspondence with the car park.

The mentioned ambient temperature was set as a trigonometric function and is shown in Figure 26 Ambient Temperature

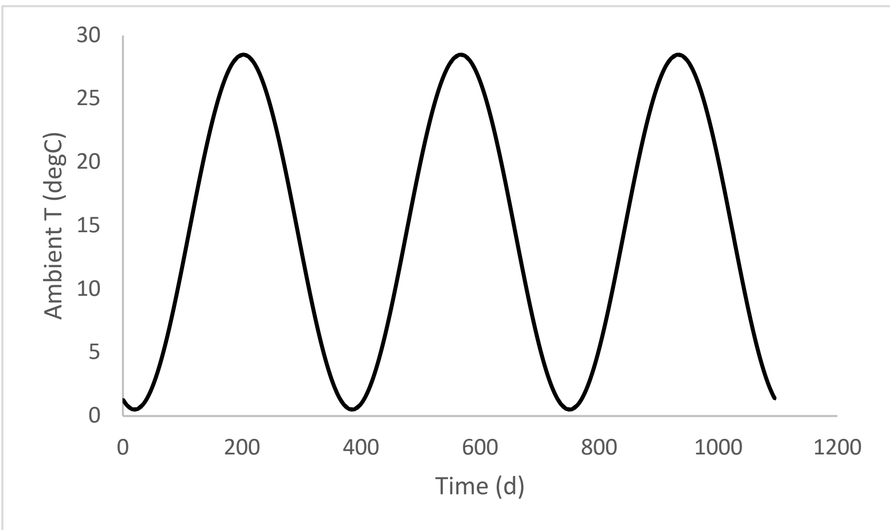

Figure 26 Ambient Temperature

The second study step was a time dependent one as well, in which the GSHP operation was simulated. To do so, a temperature function of time was assigned to the boundaries of the pipes. These pipes were modelled as circles of 25 mm simulating the cross section of the HDPE. In this case, the initial values for the domain's temperature were set as the output temperature of the previous study. The simulation of the GSHP was done for 1000 days (2 years and 270 days). The function applied to the pipes boundaries is shown in Figure 27 GSHP Temperature

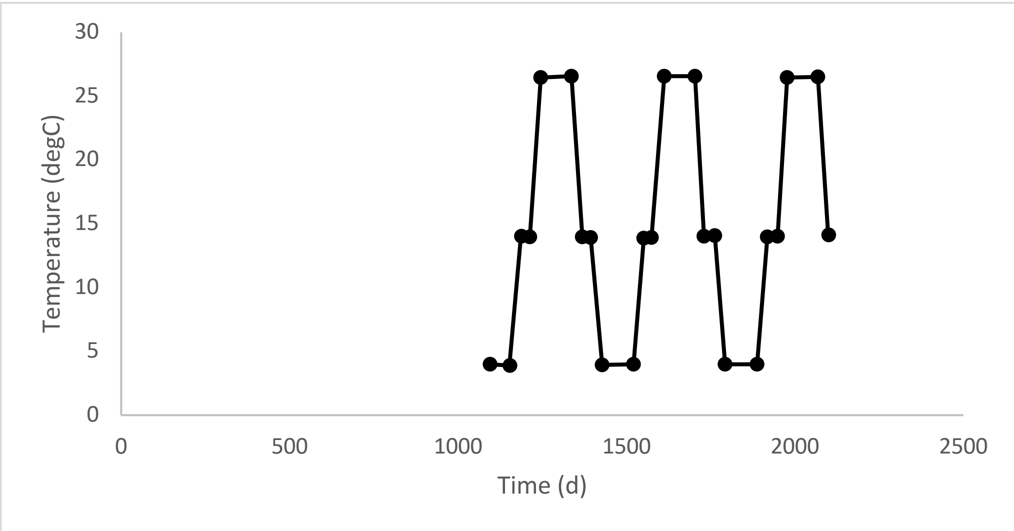

Figure 27 GSHP Temperature

It is important to clarify that the Ambient Temperature boundary condition was applied continuously, both for the first and second study.

To clarify where the GSHP Temperature boundary condition was applied and how the GHE was represented through the pipe's cross section, a simple scheme is shown below.

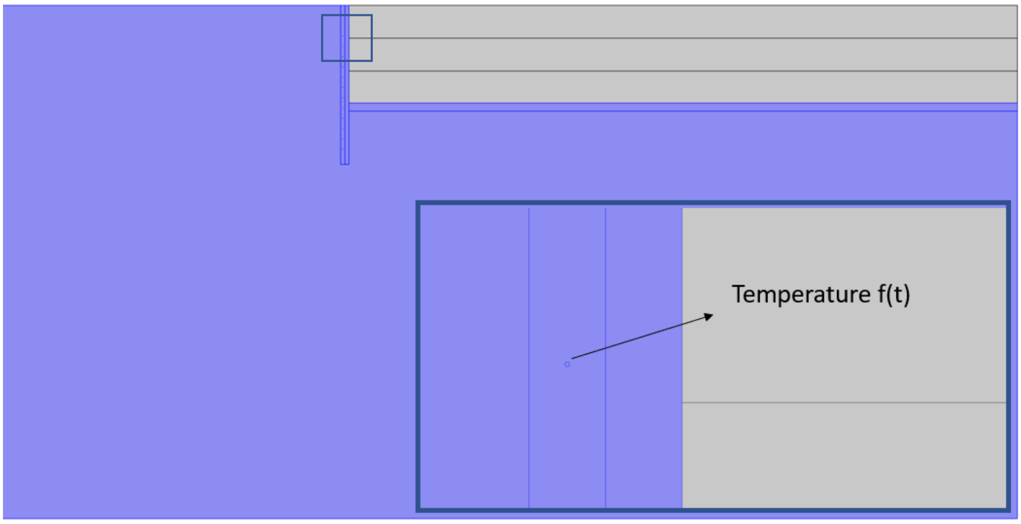

Figure 28 Thermal load (Barla, Di Donna et al. 2018)

To be able to compare the results obtained, *COMSOL*'s outputs and the respective to Barla, M., et al. (2018).are shown in Figure 29 Temperature distribution described in Barla, M., et al. (2018) in ˚C in the ground in August and Figure 30 COMSOL's Temperature distribution in ˚C in the ground in August respectively. The outputs represent the ground temperature distribution in the month of August and are basically the temperature contours in the day 1335 (which includes 3 years of ambient temperature and 240 of the GSHP operation).

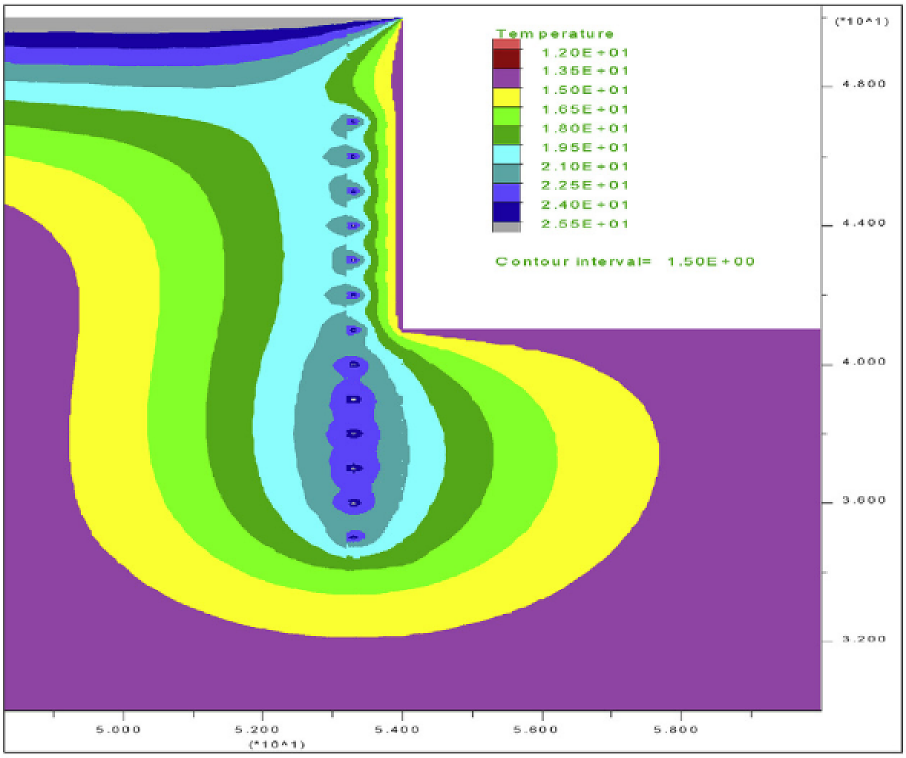

Figure 29 Temperature distribution described in Barla, M., et al. (2018) in ˚C in the ground in August

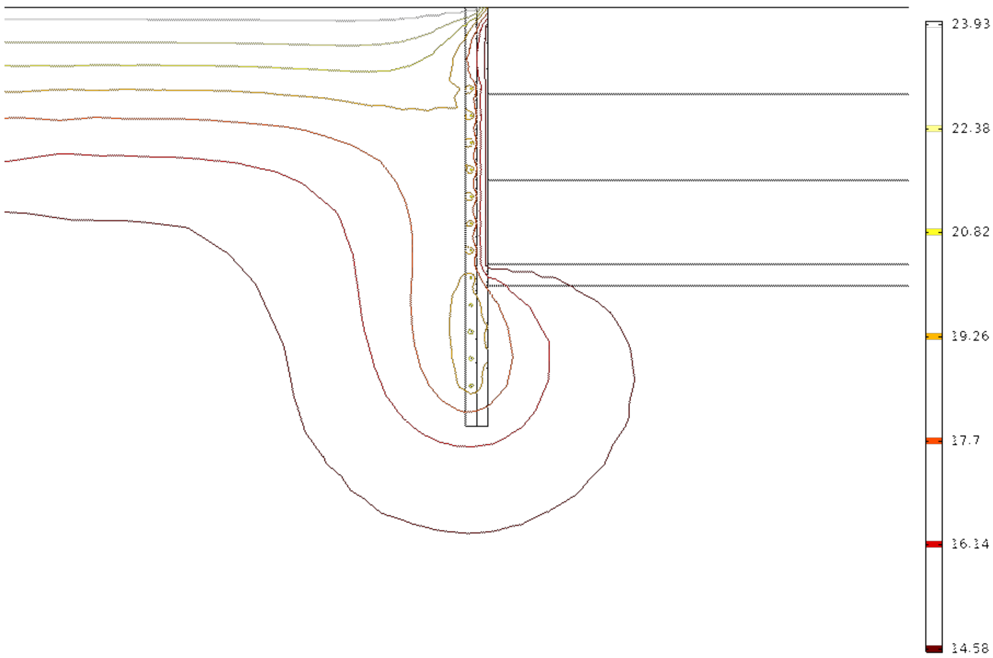

Figure 30 COMSOL's Temperature distribution in ˚C in the ground in August

3.6 General Methodology

To be able to model the thermo-mechanical effects in the retaining wall due to the thermal activation of the GSHP, the FEM model involves many studies, from stationary to time dependent, involving at the same time different physics.

The model for the entire simulation included:

1. Mechanical FEM study
2. Thermal FEM study
3. Thermo mechanical coupling FEM study

All these different FEM studies will be explained during the following chapters.

4 FEM Model

4.1 Mechanical modelling

4.1.1 Methodology

The very first study involved a stationary simulation of the excavation process and slab installation. The same has been done through the modelling of different stationary study steps, in which the domain of the side to be excavated was decreased in layers until the excavation depth was reached, and then, the foundation slab was installed.

Each study step, except of the first one which was destined to get the initial stress state, had as initial stress field the one of the previous steps, with the purpose to couple the steps and simulate the continuous excavation. The field of displacement for each step was coupled with the very previous one as well, getting the respective initial values as desired (as mentioned in paragraph 3.5.1.1.2).

A little flow chart is shown below to schematize these study steps that were mentioned before and show how the variables were coupled between them.

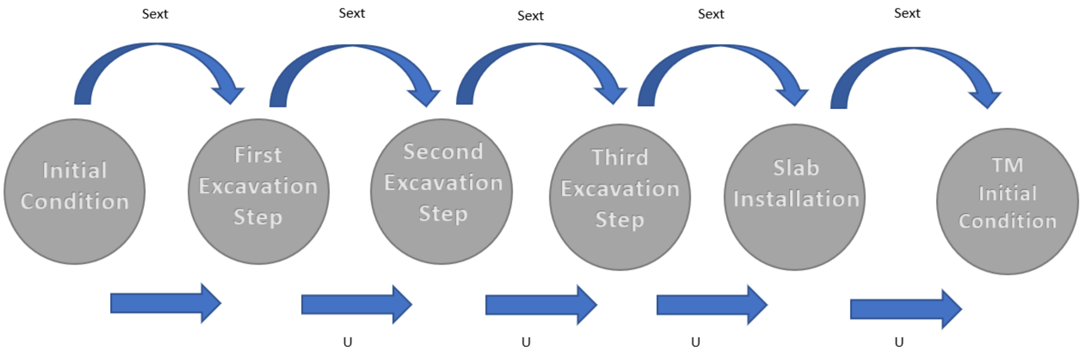

Figure 31 Study Steps for Mechanical Modelling

In the chart can be seen an extra study step that was not mentioned before. The same allows to get the final mechanical output (displacement and stresses) that will be coupled with the thermal part during the thermo mechanical modelling. The reason of its existence is having a study step where only the thermal effects into the mechanical part can be observed. If the study step chosen to be coupled was the Slab Installation one, the outputs of the thermo mechanical computation would show the results due to the slab installation plus the thermal stresses and then the effects of the thermal activation of the GSHP wouldn't be that clear.

It is important to mentioned that even though the field of stresses Sext from the first step (Initial Condition) was taken as initial values for the second one (First Excavation Step), it didn't happened with the field of displacements U, since the displacements in the initial condition should be considered as zero, to represent the original geometry of the problem. That is why, at the bottom of the chart can be seen that the component of displacements of the Initial Condition is not passed into the rest of the steps. Nevertheless, the component of displacement of the Initial Condition is needed to compute the initial stresses, since in a mechanical FEM model the dependent variables in the nodes are displacement components and the stresses are computed from them. The initial values for the displacements are initial guesses to help the software. The initial mechanical condition is accounted through the stresses coming from previous steps. That is why the displacement at each study are differential of displacements and not absolute ones.

For a better understanding of what have been just said, some comments about the mathematical formulation will be done.

4.1.2 Physics involved

The mechanical modelling of the problem is based on the Solid Mechanic's physic available in *COMSOL*. The Solid Mechanics physic is intended for general structural analysis of 3D, 2D, or axisymmetric bodies. It is based on solving Navier's equations, and results such as displacements, stresses, and strains are computed. The same accounts for geometric nonlinearity and advanced boundary conditions such as contact, follower loads, and non-reflecting boundaries. At the same time offers material models for plasticity, hyper elasticity, creep, and concrete.

In this physic, the dependent variables for which the model is solving are the components of the field of displacements defined in the nodes. Then, through the respective shape functions they are interpolated into the FEM's elements.

The equations governing the physic are:

- Equilibrium equations

$$\nabla . \sigma + F = 0$$

- Compatibility equations

$$\mathcal{E}_X = \frac{\partial u}{\partial x}$$

$$\gamma_{xy} = \frac{\partial u}{\partial y} + \frac{\partial v}{\partial x}$$

$$\mathcal{E}_y = \frac{\partial v}{\partial y}$$

$$\gamma_{yz} = \frac{\partial v}{\partial z} + \frac{\partial w}{\partial y}$$

$$\mathcal{E}_Z = \frac{\partial w}{\partial z}$$

$$\gamma_{XZ} = \frac{\partial w}{\partial x} + \frac{\partial u}{\partial z}$$

- Constitutive laws

For the case of homogeneous, isotropic linear elastic material without thermal effect is:

$$\sigma_x = \frac{E[(1-v)\varepsilon_x + v\varepsilon_y + v\varepsilon_z]}{(1+v)(1-2v)}$$

$$\sigma_y = \frac{E[(1-v)\varepsilon_y + v\varepsilon_x + v\varepsilon_z]}{(1+v)(1-2v)}$$

$$\sigma_z = \frac{E[(1-v)\varepsilon_z + v\varepsilon_x + v\varepsilon_y]}{(1+v)(1-2v)}$$

$$\tau_{xy} = G\gamma_{xy}$$

$$\tau_{yz} = G\gamma_{yz}$$

$$\tau_{zx} = G\gamma_{zx}$$

- Yielding function

- Plastic potential function

. For the case of this model, tetrahedral elements were used with quadratic serendipity shape functions to interpolate the variables between the nodes. This means, that the stresses and strains were not constant inside each FEM element, since the derivative of displacements (variables solved for), which represent the strains that will later compute the stresses, were not constants due to this shape function.

4.1.3 Parameters

The mechanical parameters involved in the model are the ones shown bellow.

Table 10 Geotechnical parameters

Parameter	Unit	Ground	Concrete
Unit weight	[Kg/m^3]	1988	2549
Elastic modulus	[MPa]	215	33300
Poisson's ratio	[-]	0.3	0.2
Cohesion	[KPa]	15	-
Friction angle	[deg]	38	-

4.1.4 Initial and boundary conditions

For the mechanical model, the variables that are solved for are the field of displacements in correspondence with the nodes as said. The initial values of the field of displacements was set as zero for the Initial Condition Step, and for the following ones, the variables were taken from the previous steps.

Regarding the boundary conditions, them were set as Dirichlet's boundary conditions for some of the boundaries, as free at top surface, rollers at the sides and fully constraint at the very bottom of the model and a single Force boundary condition set as Contact for all the boundaries involved in the interface between the wall and the soil. These boundary conditions can be observed in the following figure, which shows a cross section of the 3D model.

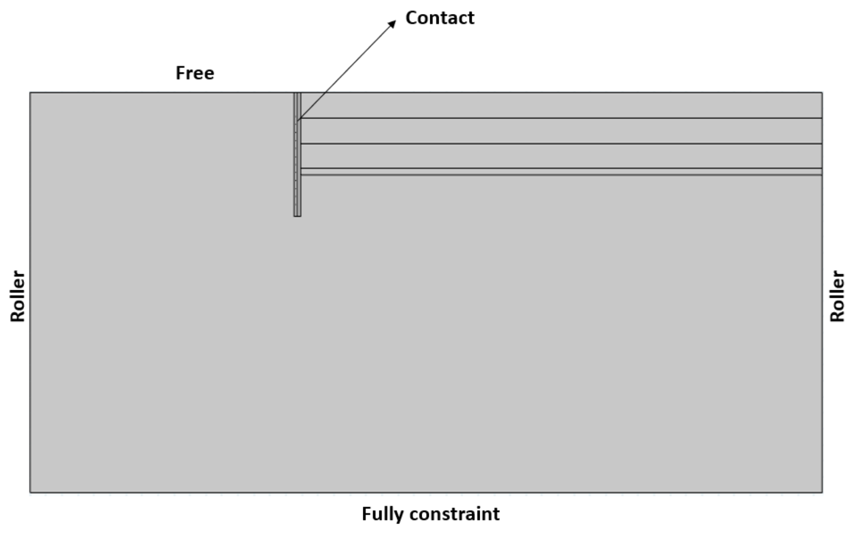

Figure 32 Mechanical Boundary Conditions

Symmetry boundary conditions were set at the sides of the model (in the depth direction of the last picture) to simulate the continuation of the thermal wall. The setting of this boundary condition will affect later the mechanical outputs compared to the plain strain model.

4.1.5 **Mechanical loads**

The simulation of construction and the operation of the diaphragm wall in terms of mechanics is subjected to a gravitational field, developing the respective stress field. The decision of modelling the retaining wall with gravitational forces is because this is a shallow geotechnical structure, in which the changes in the field of stresses with depth can't be disregarded as the case of a deep tunnels.

This field of stresses is the main component of the performance of this kind of structures. In other words, the field of stresses obtained at the end of the excavation will be the load at which the diaphragm wall will be subjected, reason why modelling with gravitational forces and modelling the respective construction steps is really important.

4.1.6 **Treatment of interfaces**

During the modelling of the energy wall, special attention was taken to the consideration of the soil-wall's interface since it governs big part of the system behaviour. For its consideration, different options have been considered.

This was a big issue because the software used is a universal software, in the terms that is not a geotechnical one. In this way, the treatment and consideration of the interfaces was analysed for a long period of time, trying different boundary conditions to represent geotechnical interfaces.

During that period, the different options considered were:

1) Modelling continuity between the domains

   In this way there are common nodes in both faces, belonging to both domains

2) Modelling pairs

   They are modeled while not forming a union of the geometry's objects involved in the model, creating two different boundaries giving the possibility to connect them in different ways. They can be:

   a) Identity pairs: Makes the fields across two connected boundaries continuous

b) Contact pairs: Boundaries that can come into contact but can't penetrate each other

As mentioned, while using pairs, the definition of different boundary conditions can take place. Examples of them can be contact, fixed constraint, roller, prescribed displacement and prescribed load.

Modelling continuity between both domains, soil and wall, was concluded to be not a proper model, as the finite elements of the unexcavated part seemed to hang from the wall, flexing it to their side, instead of pushing it to the excavated part.

The use of identity pairs with a prescribed displacement boundary condition was analysed as well. The same was used with a feature called "general extrusion" with which, the displacement field was mapped and copied to the boundary of the wall, simulating in this way frictionless interface with no detachment of soil. The same model was unsuccessful, probably because of continuity of stresses or because it represented an infinite cohesion.

The last model of interface and the chosen one was the model of contact pairs. The same allows contact and detachment while allowing a continuity in the field of stresses. At the same time, it allows to incorporate friction features, to be able to consider its contribution in the complete behaviour of the system (even though friction was not used in a first instance). The disadvantage of this boundary condition is in terms of computational cost, since transforms the problem into a nonlinear problem. Some comments of that will be done later.

It is important to mention that even though the software provides a membrane element feature, which is a 2D representation that allows to develop a model for the deformation of thin walled structures) was decided not to use it. The reason why, was that during the thermal activation of the GSHP, the modelling of pipes embedded into the wall should take place. For doing that, an entire 3D representation of the wall must take place.

4.1.6.1 Contact boundary condition

Contact can be modeled between a group of boundaries. There are different kind of algorithms for that purpose. The ones considered and available were augmented Lagrangian method and a penalty method.

In the augmented Lagrangian method, the system of equations is solved in a segregated way. An additional iteration level is added where the usual displacement variables are solved separated from some of the contact variables. The algorithm repeats this procedure until it fulfills a convergence criterion.

In the penalty method, no extra degrees of freedom are needed. These results are just computed from the displacements and the penalty stiffness. This means that no special solver strategies are necessary. This last method mentioned was the used in the case of study.

To understand why the problem becomes nonlinear due to this boundary condition lets stand first the conditions that must remain true to keep a problem linear.

These conditions are:

1. The relationship between stresses and stresses are linear

2. The stiffness matrix is not affected by changes in geometry of the boundary that occurs during the loading

3. Boundary conditions do not change during the loading

From a constitutive point of view the first conditions is wasn't violated since the model of plasticity was done with an ELPLA behavior, in which the constitutive relation remains linear. For the case of the second assumption, can be said that will remain true since the problem solved is included into a small strain theory problem.

Finally, the reason why the problem becomes nonlinear due to the contact is the last assumption since the boundary condition is changing with the loading, going from contact to a free boundary condition, affecting the assembly of the stiffness matrix. This is the reason why it is not possible to solve the system of equations directly (with a Direct Solver).

4.1.7 Model of the wall

As was mentioned before, the wall was modelled as a solid continuum Since the same was not modelled with any plate feature, the obtention of the efforts was not that straight forward.

To get the efforts in the wall, reference was done to Germain-Lagrange's plate theory. The wall was considered as a plate since has a small thickness compared with the other dimensions. Accounting to the plate theory, a meshed surface was modelled in correspondence with the center of the wall since the base of the theory is computing the efforts based in the deflection of the middle surface in a perpendicular direction.

To get the efforts it is important to mention the Flexural rigidity, which is an analogy to the Inertial Moment in the case of a beam. The expression of the same is the following one:

$$D = \frac{E\ H^3}{12(1-v^2)}$$

Then, the expression for the bending moment and shear efforts are the following ones:

$$Mx = -D\ (\frac{\partial^2 w}{\partial x^2} + v\frac{\partial^2 w}{\partial y^2})$$

$$Mxy = -D\,(1 - v)\frac{\partial^2 w}{\partial x \partial y}$$

$$Qx = -D\,\frac{\partial}{\partial x}(\frac{\partial^2 w}{\partial x^2} + v\frac{\partial^2 w}{\partial y^2})$$

4.1.8 Numerical solver used

As mentioned, the only reason why the problem was nonlinear was the fact that the contact boundary conditions were used. The nonlinearity was geometrical and not from a constitutive point of view. For that reason, the deformation frame takes an important place and governs part of the problem.

Even though the problem was considered as nonlinear, since the Penalty method was used non iterative or special solvers were needed as was mentioned before. Then the solver used for the mechanical study was MUMPS (multifrontal massively parallel sparse direct solver). That solver was the default one, and when tried in a first instance gave good results

4.2 Thermal modelling

4.2.1 Methodology

This model involved one-time dependent study composed by a single study step. The same computed the following coupled physics:

- Heat Transfer in Solids
- Non isothermal pipe flow

Both will be explained with the inclusion of some mathematical formulation.

This time dependent study was computed for 4 years, with the following time steps:

- 1/24-day time step computed for one day

- 1-day time step computed for one year

- 5 days time step computed the last three years

Can be observed that the “time mesh” is not uniform, and it varies from a hourly step to a five days step. The reason why that is to obtain a smoothness in the computation and allow the model to converge.

4.2.2 **Physics involved**

The thermal modelling involves the coupling between heat transferred in the GHE components, structural elements and surrounded ground to the fluid flow within the pipes.

The physics used were:

1) *Heat transfer in solids*

Used to model heat transfer by conduction, convection, and radiation. Domains can be modelled as solid or fluid. The temperature equation defined in solid domains corresponds to the differential form of the Fourier's law that may contain additional contributions like heat sources.

The equations involved in this physic are the ones listed below.

$$\rho_m C_{p,m} \frac{\partial T_m}{\partial t} = \nabla . (\lambda_m \nabla T_m) \tag{4.1}$$

2) *Non isothermal pipe flow*

Used to compute the temperature, velocity, and pressure fields in pipes and channels of different shapes. It approximates the pipe flow profile by 1D assumptions in curve segments, or lines. The equations involved in this physic are continuity and momentum equations for incompressible fluid and the one related to the heat transfer through convection and conduction in the carrying fluid flow listed below.

$$\nabla.\,(A\rho_w\boldsymbol{v}) = 0 \tag{4.2}$$

$$\rho_w\left(\frac{\partial v}{\partial t}\right) = -\nabla p - f_D\frac{\rho_w}{2d_h}|v|v \tag{4.3}$$

$$\rho_w AC_{p,w}\frac{\partial T}{\partial t} + \rho_w AC_{p,w}v\nabla T = \nabla\left(A\lambda_w\nabla T\right) + f_D\frac{\rho_w A}{2d_h}|v|v^2 + Qwall \tag{4.4}$$

$$with\ Qwall\ = f\ (T_m, pipe\ wall, T)$$

For the consideration of the fluid's flow inside the pipes, it was assumed to be fully developed, that is why this physics representing 1D elements were used, which represent properly this assumption.

For these physics, the heat transfer was modelled by conduction, for the soil, GHE wall and fluid while convection was only considered for the carrying fluid inside the pipes of the GHEs.

It is important to stand that when the groundwater flow is neglected, the heat transfer is done purely by conduction, and not convection as the soil is considered as a whole, and the voids and grain are considered all together for thermal purposes, allowing only conduction.

The equations of nonisothermal pipe flow are numerically solved for temperature, velocity and pressure fields, which are the primary variables at the nodes for the physic.

The coupling between these two thermal physics happens thanks to the modelling of a wall heat transfer, in which the heat exchange across the pipe walls is set. Then the carrying fluid temperature, pressure and velocity starts to interact with the external temperature (the temperature of the wall and soil).

4.2.3 **Parameters**

The thermal parameters involved in the model are the ones shown in Table 11 Thermal parameters of ground and Table 12 Thermal parameters of concretefor the soil and concrete respectively.

Table 11 Thermal parameters of ground

Parameter	Value(s)	Unit	Description
λ_{ground}	2.8	W/(m.K)	Thermal conductivity of ground
Cp_{ground}	1053	J/(kg.K)	Specific heat capacity of ground

Table 12 Thermal parameters of concrete

Parameter	Value(s)	Unit	Description
$\lambda_{concrete}$	2.3	W/(m.K)	Thermal conductivity of concrete
$Cp_{concrete}$	876	J/(kg.K)	Specific heat capacity of concrete

4.2.4 Initial and boundary conditions

For the thermal model, the variables that are solved for are the temperature in correspondence with the nodes for the Heat Transfer in Solids and for pressure, tangential velocity and temperature for the Non Isothermal Pipe Flow.

The initial values for temperature for the Heat Transfer in Solids interface was set as 14 ˚C and for the case of the Non Isothermal Pipe Flow the initial values were 14 ˚C for the temperature, 101325 Pa for the pressure (atmospheric pressure) and 0 m/s for the tangential velocity. It is important to stand that even the two physics are solved for temperature, those dependent variables are not the same.

Regarding the boundary conditions, for the case of the Heat Transfer in Solids, were the ones shown in the following figure.

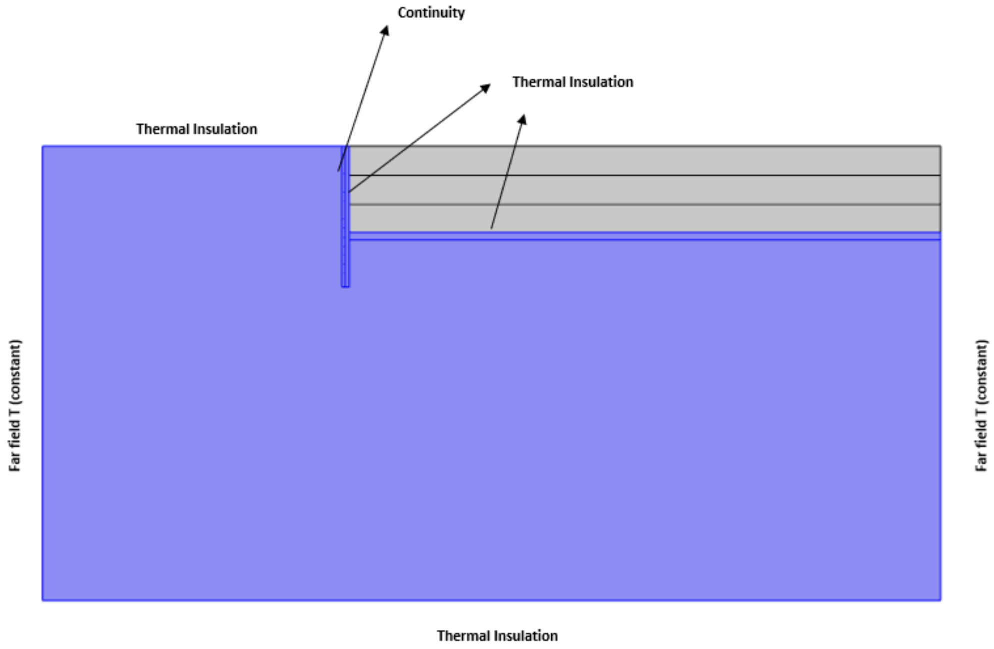

Figure 33 Heat Transfer in Solids Boundary Conditions

Symmetry boundary conditions were set at the sides of the model (in the depth direction of the last picture) to simulate the presence of side pipe's loops.

For the case of the Non Isothermal Pipe Flow the following boundary conditions were defined:

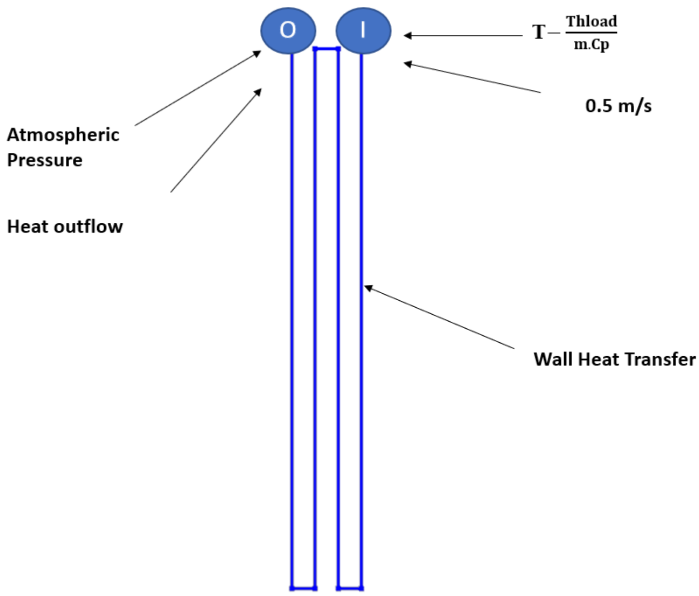

Figure 34 Non Isothermal Pipe Flow Boundary Conditions

In the last picture “O” stands for outlet while “I” for Inlet.

In correspondence with the Outlet point we find:

- Atmospheric pressure

  Shows how that point is connected afterwards with the respective secondary system of the GSHP in terms of pressure

- Heat outflow

  Provides a suitable boundary condition for convection-dominated heat transfer at outlet boundaries. With this boundary condition the temperature gradient in the normal direction is zero, and there is no radiation. This is a good approximation of the conditions at an outlet boundary in a heat transfer model involving fluid flow.

In the case of the Input point we find two different boundary conditions, which are explained bellow:

- $T - \frac{Thload}{m.Cp}$

  Express the value given to the inlet temperature, since the first term is the value of the outlet temperature and the second term is the delta of temperature desired due to the thermal load, expressed in temperature terms.

- 0.5 m/s

  Expresses a constant velocity of the circulating fluid in correspondence with the inlet.

An extra boundary condition is set in correspondence with the whole pipe loop allowing the heat exchanging between the carrying fluid and the domains that surround it.

4.2.5 Thermal load distribution

The thermal load distribution represents the amount of thermal energy that the system is aimed to provide. This is a key element of shallow energy geo-structures, since they not only determine the amount of energy that will be produced but also the solicitations at which the structure will be subjected.

The thermal load distribution adopted was the one used by (Makasis 2018) during a research in Melbourne city, scaled to match the dimensions of this wall and make sure that the GSHP worked between its operation limits. The same is shown in Figure 35 Thermal Load distribution.

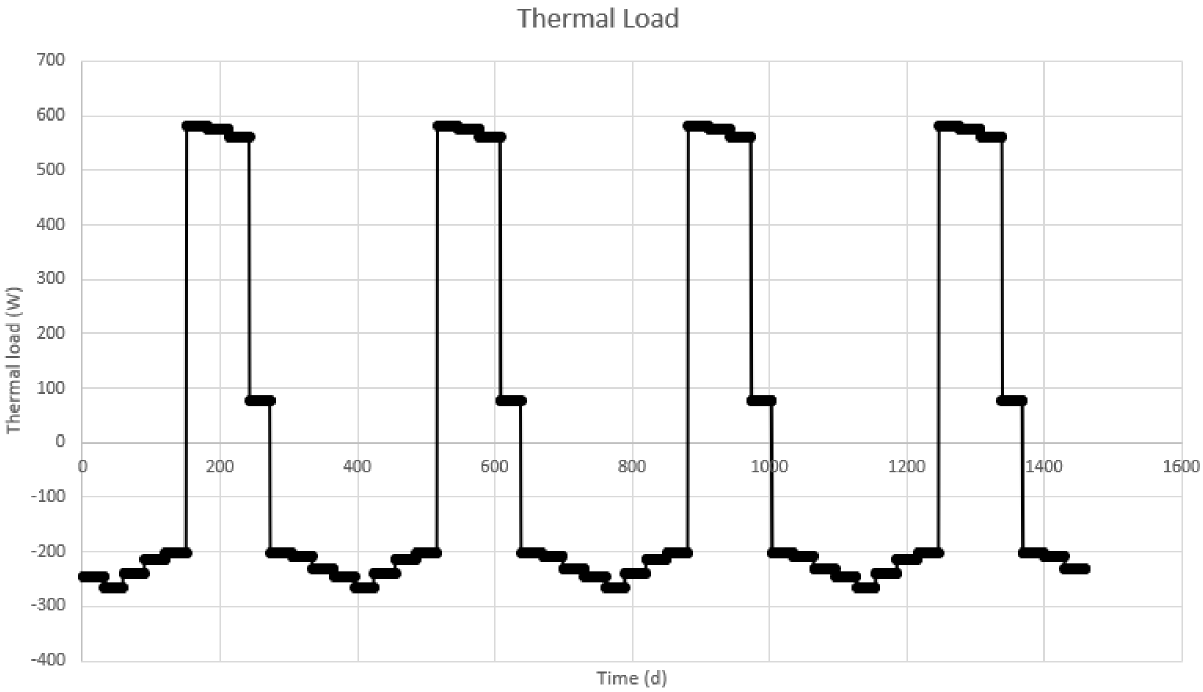

Figure 35 Thermal Load distribution

4.2.6 Geometry

The whole domain and the GHE geometries are shown below for a better understanding.

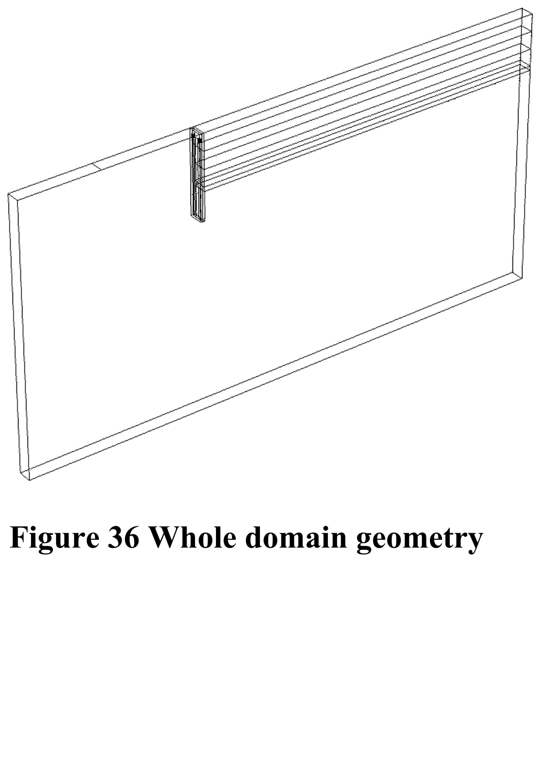

Figure 36 Whole domain geometry

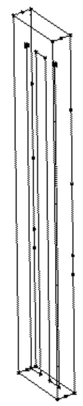

Figure 37 GHE geometry

A better description with dimensions of the GHE and the pipe's loop is shown below:

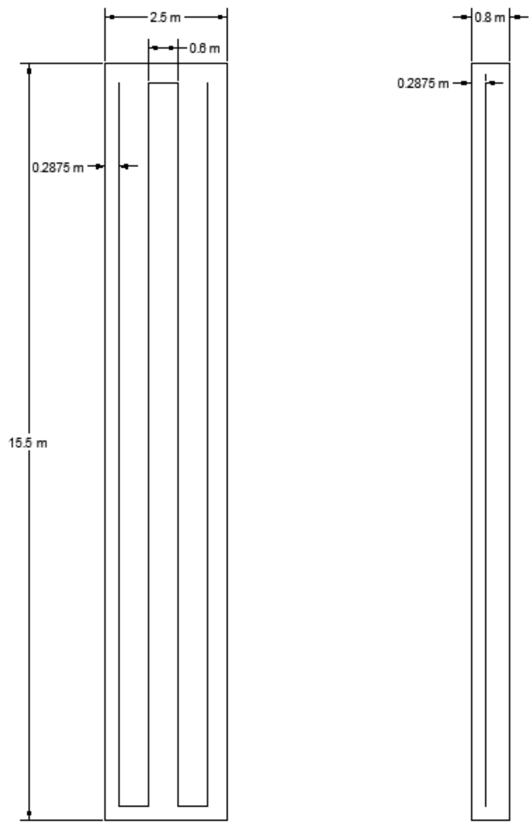

Figure 38 GHE dimensions

4.2.7 Numerical solver used

For the case of the thermal model, were handled two different physics that needed to be coupled. That coupling involves the fact of solving four dependent variables (two temperatures, one pressure and one tangential velocity).

For that purpose, was selected a Fully Coupled approach. The same forms a single large system of equations that solve for all of the unknowns (4 dependent variables) and includes all of the couplings between the unknowns within a single iteration.

The solver used for that approach was a MUMPS solver, the same that was used for the mechanical model.

4.3 Thermomechanical modelling

4.3.1 Methodology

The thermo-mechanical model involves the solution of two temperatures, pressure, fluid velocity and displacements, in total 5 different dependent fields of variables. These 5 fields of variables can be divided into thermal ones and mechanical ones, having 4 thermal variables and 1 mechanical one (one field, which involves 3 components).

While talking about the thermo-mechanical coupling, should be bear into account that one coupling is already present and won’t be mentioned. That coupling is the respective of the four thermal variables, between the Heat Transfer in Solids and the Non isothermal pipe flow.

The coupling works by using the temperature result of the coupling between the last two thermal physics to compute the thermal strain and thermal stresses that will affect the mechanics.

In order to couple the three physics, “Heat Transfer in Solids”, “Non isothermal pipe flow” and “Solid Mechanics”, an extra time dependent was set. That study had only one study step, with the single aim to couple all the physics mentioned.

The mentioned study step had the same time discretization as the thermal model:

- 1/24-day time step computing one day
- 1-day time step computing one year
- 5 days time step computing the last three years

The thermo-mechanical coupling was done in only one way, where the temperature was impacting in the mechanic part, but none mechanic effects were giving extra temperature changes. The reason of that, is that in these kinds of semi-static problems, the amount of energy produced by these stresses won't generate much temperature changes. The respective influence of the stresses in the energy equation was mentioned in paragraph 2.6.2.

A simple schematization of what was mentioned before is shown below.

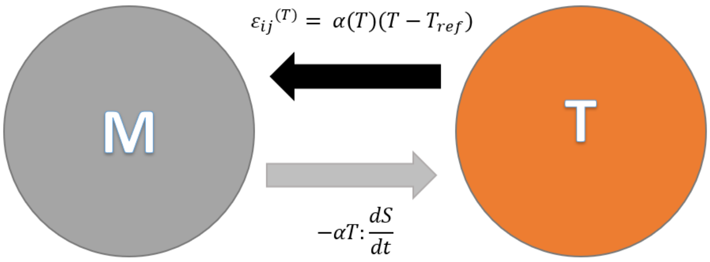

Figure 39 Schematization of the Thermo Mechanical coupling

4.3.2 **Coupling formulation**

In order to couple the thermal and mechanic part, the software allows to account for Thermal Expansion and Temperature Coupling.

With the Thermal Expansion, the effect of the thermal changes into the domains is considered. That is accounted through the following expression:

$$\varepsilon_{ij}{}^{(T)} = \alpha(T)(T - T_{ref})$$

In the case of this model, the coefficient of thermal expansion was set as the Secant coefficient and was considered to be constant. It is important to clarify that even though this model computed two fields of Temperatures, the one respective to the physic Heat Transfer in Solids was the one that accounted for the thermal expansion, since the one of the Non Isothermal Pipe Flow defined the temperature in the nodes in correspondence with the pipes only (carrying fluid).

The Volume reference temperature Tref, was set as 14 °C, equal as the initial values for the temperature and the far field boundary conditions. That temperature is the one that accounts for no thermal strains.

The mentioned Temperature Coupling allows to map the temperature values computed from the Heat Transfer in Solids physic into the Solid Mechanics one, specially to the last study step of the Mechanical model.

4.3.3 Parameters

The parameters involved in the model were the ones described into the mechanical and thermal modelling. For the case of the secant coefficient of thermal expansion, the values are shown in the following table:

Table 13 Coefficient of Thermal Expansion

Parameter	Value(s)	Unit	Description
$\alpha concrete$	1.2E-5	1/K	Coefficient of thermal expansion of concrete
$\alpha ground$	1E-5	1/K	Coefficient of thermal expansion of ground

4.3.4 Initial and Boundary Conditions

For the case of the initial conditions, the ones were the respective to the mechanical model and the thermal one. Same with the boundary conditions.

The already mentioned Volume reference temperature can be considered as an initial condition in terms of thermo-mechanics. The same stands the temperature at which no dilation or contraction is present.

4.3.5 Numerical Solver used

For the case of the thermo mechanical model, there are many variables that the model is solving for. Due to that fact, the matrix that needs to be computed is very large.

To account for the last inconvenient and help the software to compute all the variables field was decided to use a Segregated approach, instead of a Fully

Coupled one, as was the case of the thermal model. The Segregated approach will not solve for all of the unknowns at one time, it subdivides the problem up into Segregated Steps. Each step represents a single physics or multiple physics.

These individual segregated steps are smaller than the full system of equations that are formed with the Fully Coupled approach. The Segregated steps are solved sequentially within a single iteration, requiring less memory.

The Segregated approach included in this model two segregated steps:

- Segregated step 1

  Includes the four variables regarding the thermal part (two temperatures, one pressure and one tangential velocity)

- Segregated step 2

  Includes the field of displacement

The numerical solvers used respectively in this case were:

- PARDISO Solver
- MUMPS Solver

5 Results and conclusions

5.1 Mechanical outputs

The outputs that will be analysed for the mechanical point of view of the retaining wall are in terms of field of displacements and efforts.

It is important to consider that, although the geometry and parameters considered for the model are the same of the case of study of the mechanical validation (plane strain study), the outputs may be different since this is a 3D model, where symmetry was modelled in correspondence with the third dimension. These outputs may show the result of the contribution of side wall panels, or in another terms, the model of a middle wall panel.

5.1.1 Wall's deflection

For the case studied, the displacement of the wall in the horizontal direction was analyzed. The consideration of the same is very important in terms of the structure's serviceably, since excessive wall's displacements can produce cracks or other serviceability problems. The wall's displacement tolerance is in terms of the building's purpose and changes with every construction code.

The plot of the wall's deflection with correspondence with the "Slab Installation" stage is shown below.

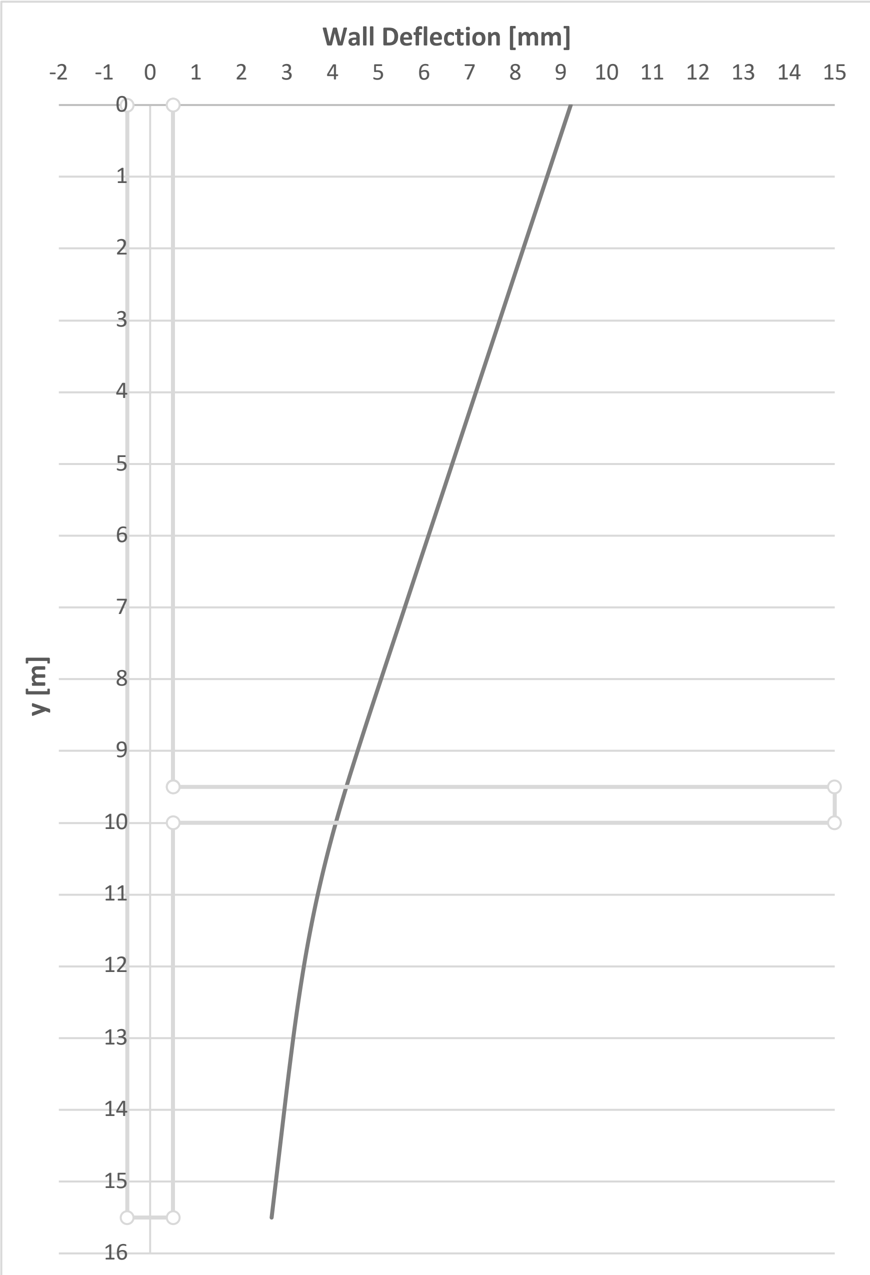

Figure 40 Wall's Deflection

As may be observed the maximum wall deflection is in correspondence to the top of the wall and is equal to 9.2 mm. As can be observed, the wall has a displacement at the very bottom as equal, due to the equilibrium of horizontal forces (active and passive thrust).

5.1.2 **Efforts**

As was mentioned in paragraph 4.1.7, the efforts in the wall were accounted in terms of the plate's theory. The main effort analyzed is the Bending moment in correspondence with the out of the wall's plane direction.

The plot for the outputs at the final study step, in correspondence with the slab installation is included bellow.

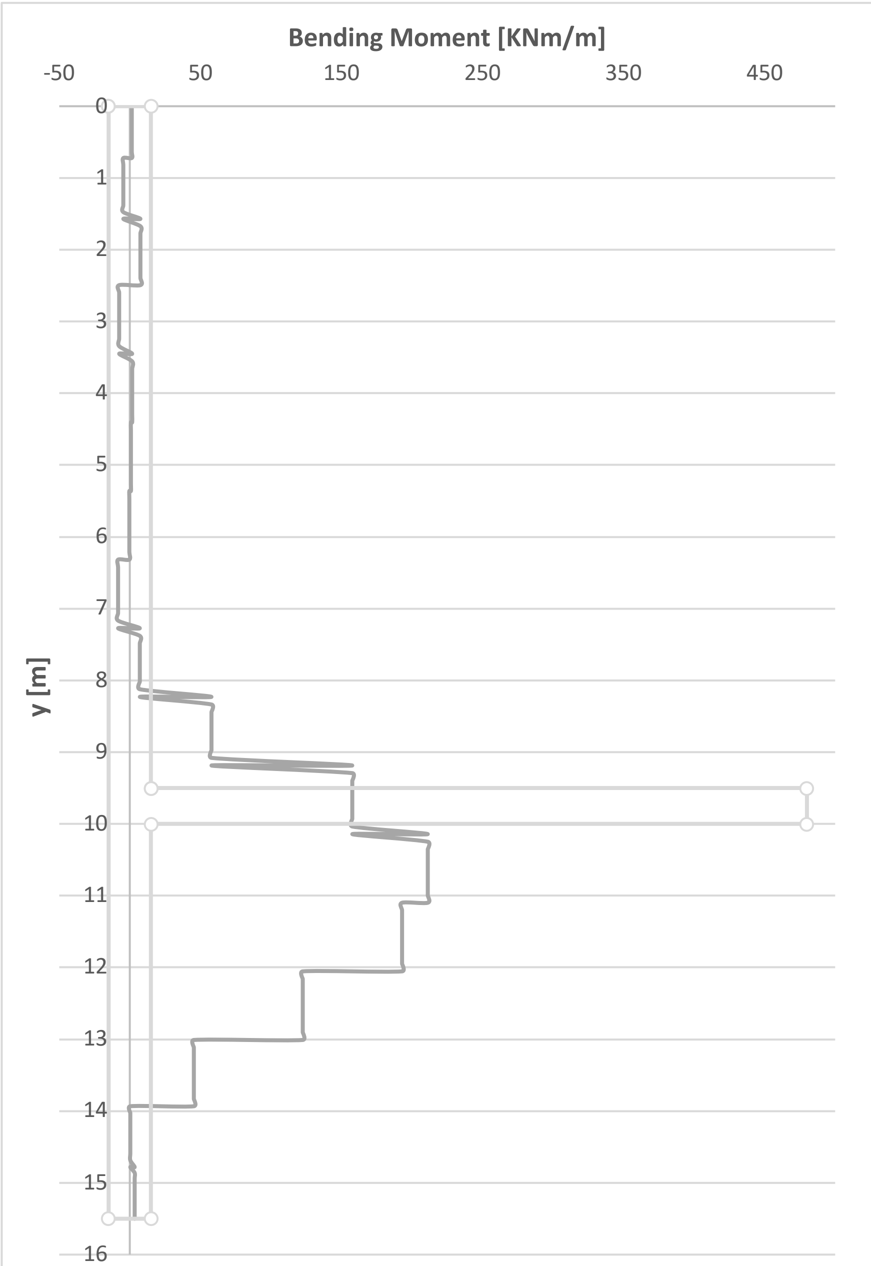

Figure 41 Bending Moment for the Slab Installation step

Can be observed that the bending moment concentrates in the area of the foundation slab and not exactly at the middle of the same. The reason why this is that this slab imposes a displacement and rotation constraint in terms of its stiffness, allowing a certain rotation and displacement that produce the resulting bending moment.

The normal stresses in KPa along the wall's depth related with the last construction step are shown below.

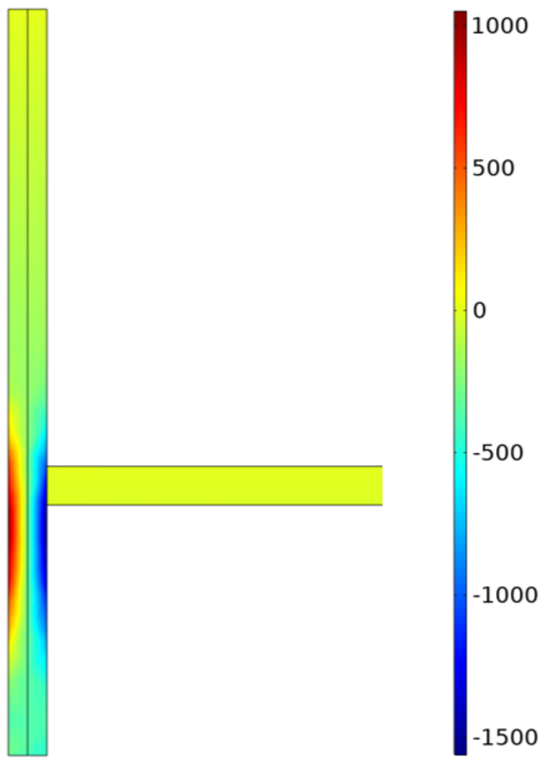

Figure 42 Normal stresses along the wall for the Slab Installation step

As can be observed there are tensile stresses in correspondence with the unexcavated side and compressive ones along the excavated side, as expected, since the wall is bending towards the excavated one.

Can be observed that the concentration of stresses is not perfectly in correspondence with the slab as the wall and the slab are not fully connected, not giving a total displacement constraint.

5.1.3 Yielding Surface

Was mentioned in the respective explanation of the case of study of this thesis that the soil was modeled as an ELPLA material with a Drucker Prager soil yielding criterion matching the Mohr Coulomb parameters. In that way, the plastic strains were computed by the model.

In the figure bellow are shown the contours for the effective plastic strains in correspondence with the Slab Installation step, to observe where is located the potential slide surface.

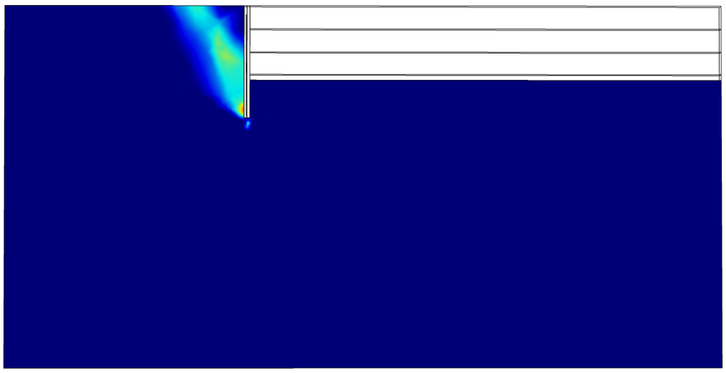

Figure 43 Effective Plastic Strain after Slab Installation

As can be seen in the last figure, the failure surface is roughly at 60 degrees, which sounds logical in reference to Figure 12 Mohr's circles at rest, active and passive states (Al-Khafaji & Andersland, 1992).

According to the Mohr's circle, the failure surface should be at an angle of $45° + \frac{\varphi}{2} = 45\,° + \frac{38}{2} = 59\,°$ with respect to the horizontal.

5.2 Thermal outputs

Referring to the thermal model, as both physics were modelled with different dependent variables at the nodes, two different temperatures were obtained.

The temperature related with the physic "Heat Transfer in Solids" is referred to the temperature through all the material domains included soil and reinforced concrete wall and slab, while the temperature related to the physic "Non isothermal Pipe Flow" is referred to the carrying fluid's temperature. Since the GHE allows the heat transfer between this carrying fluid and the rest of the domains there is a link between these two temperatures.

Both temperatures will be shown and analysed bellow. For the seek of a clear representation not all the time steps computed will be shown. For a first instance will be shown the respective with some of the interested points. For this purpose, the interested time steps analysed during the first year of the GSHP operation are shown in the plot bellow.

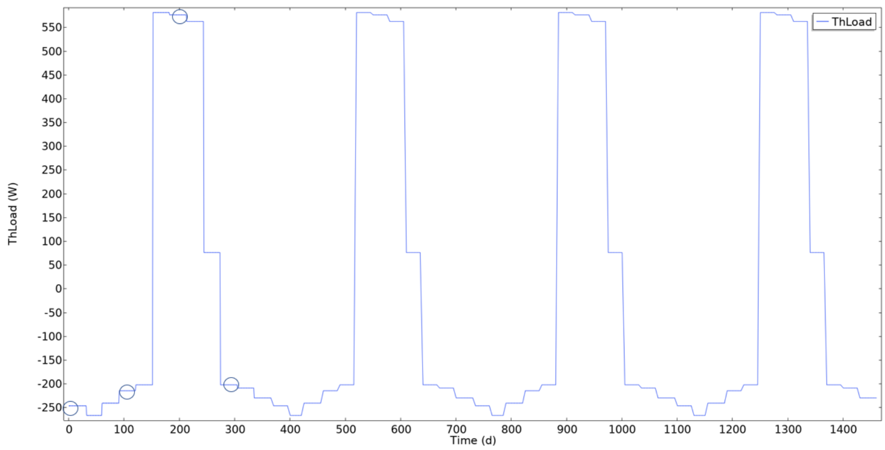

Figure 44 Points of interest

5.2.1 **Solid's temperature**

For a better representation will be plot the whole domain's temperature distribution from the side of the outlet point, which in a big scale plot doesn't differ much from the inlet point side view to get a general outlook of the thermal activity. After that, a detail of both sides of the wall and of the front of the same will be done.

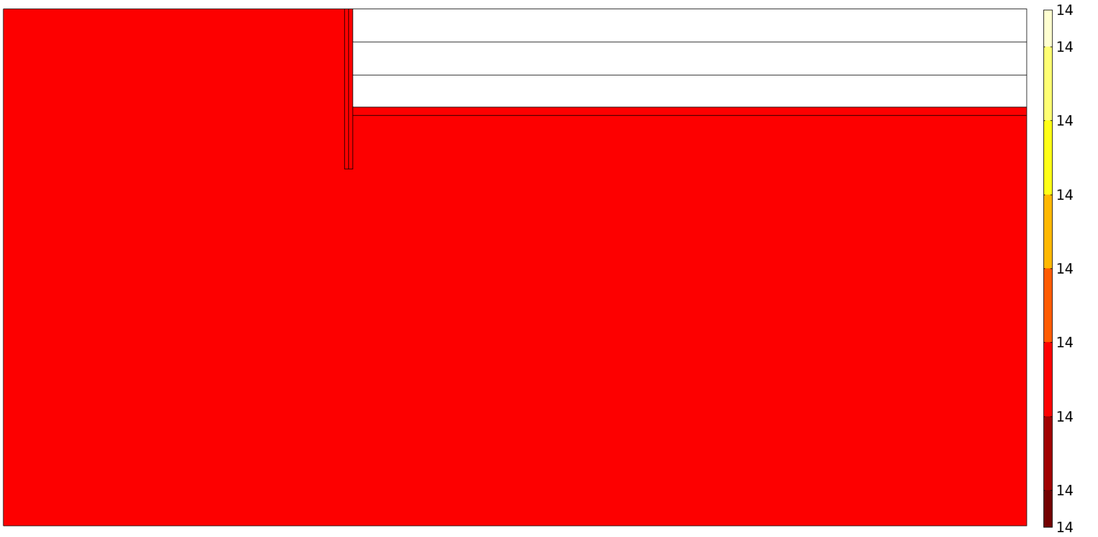

Figure 45 Initial Condition

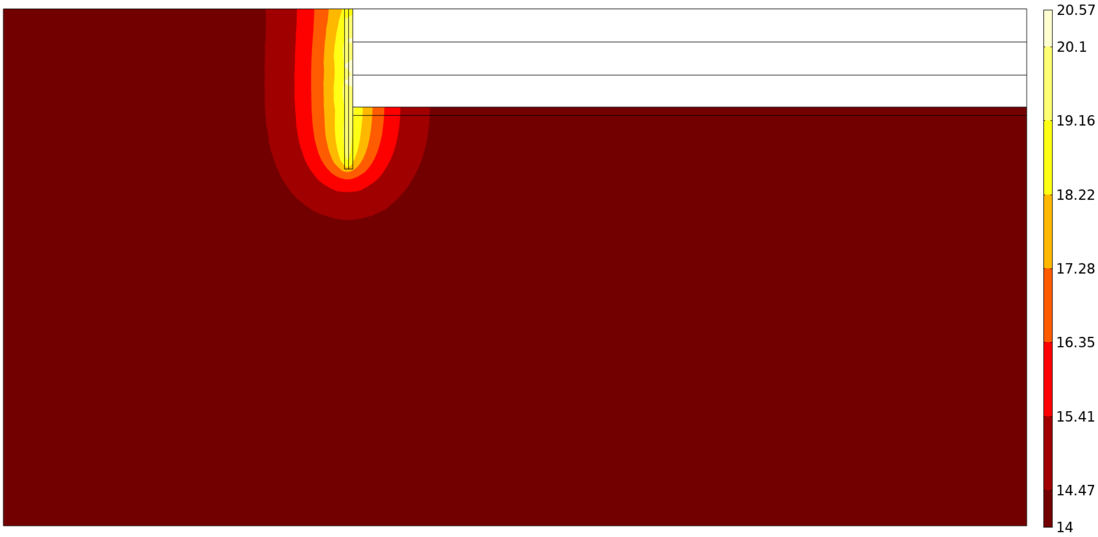

Figure 46 First Period of Heating (day 130)

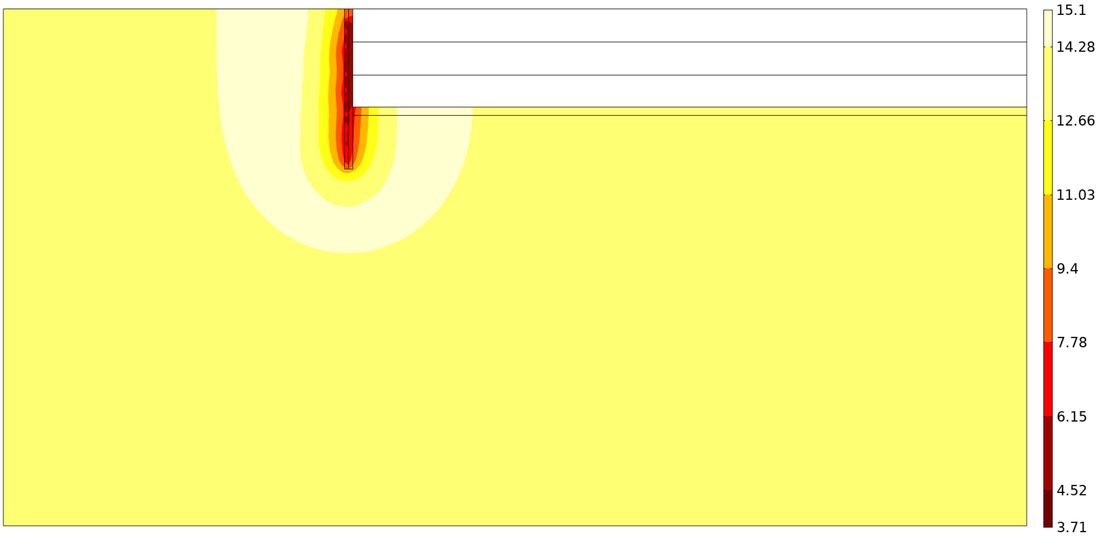

Figure 47 First period of Cooling (day 200)

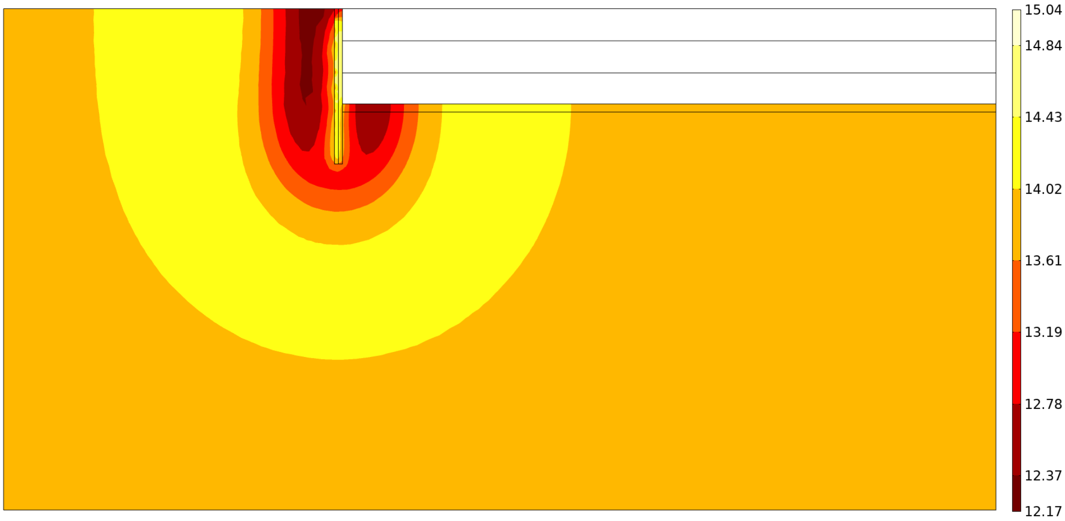

Figure 48 Second period of Heating (day 300)

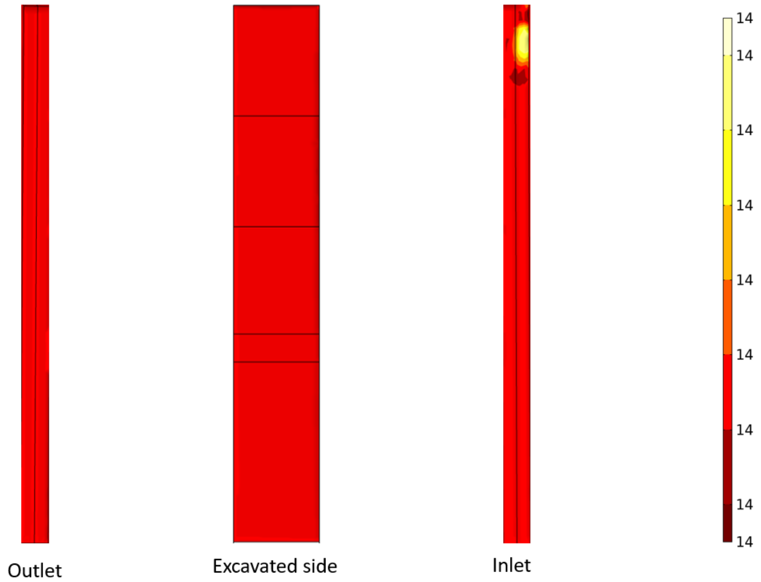

Figure 49 Initial Condition Wall's temperature contours

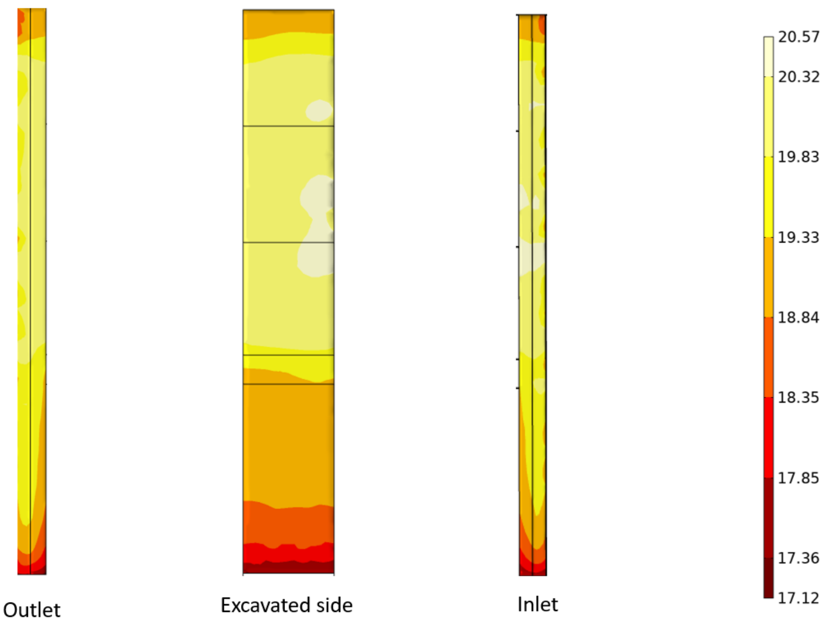

Figure 50 First period of heating Wall's temperature contours

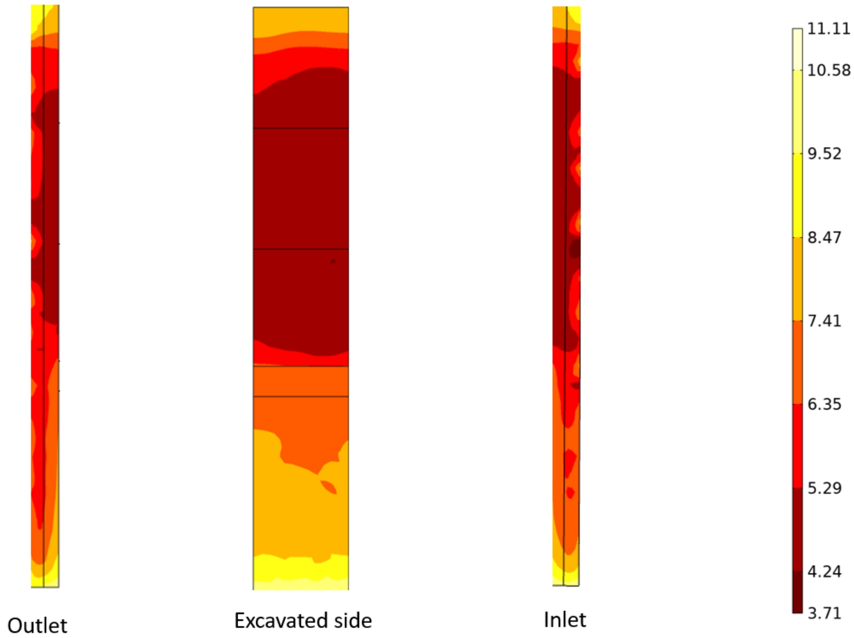

Figure 51 First period of cooling Wall's temperature contours

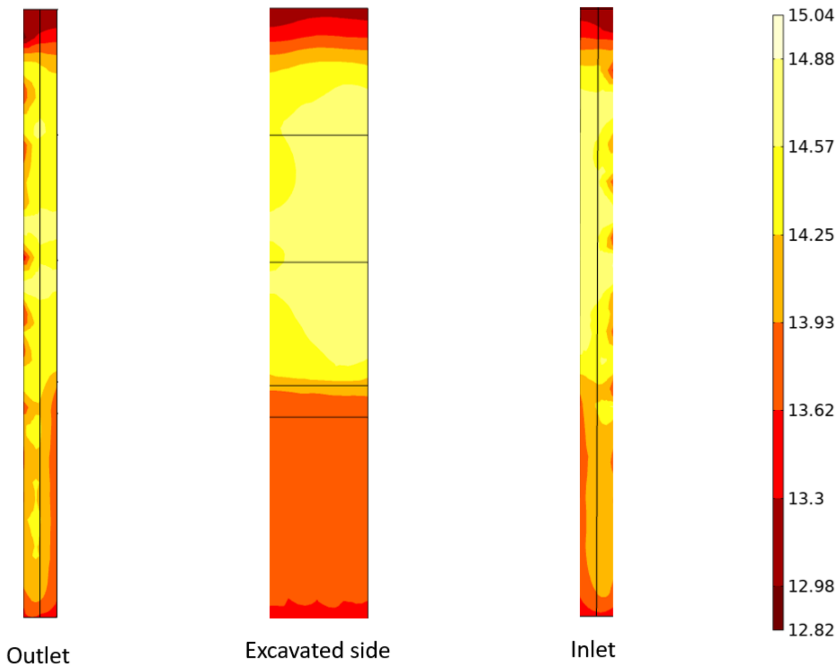

Figure 52 Second period of heating Wall's temperature contours

As can be seen in the detail plot of the wall for the initial condition, it seems that there is thermal activity at time zero in correspondence with the inlet point of the GSHP, but it can be neglected since it is only a plot deficiency.

In a general view of the detail's plots can be observed that there is not a perfect symmetry at both sides of the wall in terms of temperature distribution. The reason why this is because the fluid is starting with a certain temperature in correspondence with the inlet point, and the same is changing as the carrying fluid is flowing through the pipes towards the outlet point. The fact that symmetry boundary conditions were set at the sides of the wall should be taken into account bearing in mind that the effect of side thermal wall panels are contributing as well.

For the case of the front view of the wall's temperature distribution, the plot is referred to the excavated side, where thermal insulation was defined. As can be see, the temperature distribution is quite smooth. In the other hand, as can be seen in the left edge of the Outlet plot or the right edge of the Inlet plot which represents the interface soil-wall, the temperature distribution in the contact is not quite smooth. Can be observed little zones of concentration of temperature. This can be understood in terms of the meshing and the contact mechanical boundary condition. The reason involved in the mesh, is due to the fact that the meshing of the soil's side is much coarser compared to the one of the wall's one. Then, as there is a continuity thermal boundary condition in that interface, the software is interpolating values within the coarse elements of the soil affecting the overall temperature distribution giving those points of concentration of temperature.

It is important to clarify that the mesh used was for the sake of the convergence of the model. Many meshes have been tried until the final one was chosen. The mesh used is shown below.

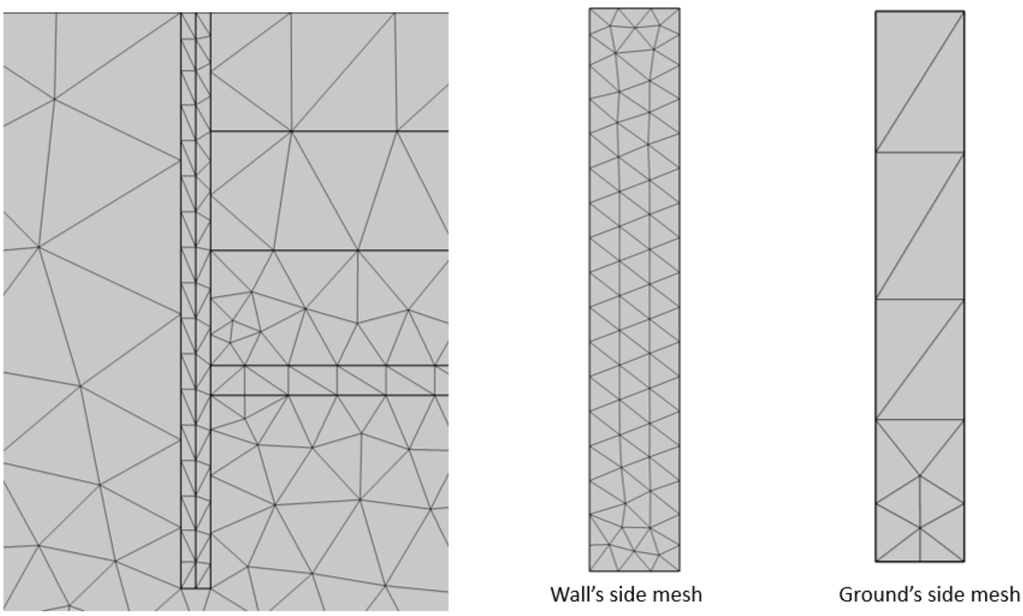

Figure 53 Interface meshing

An important observation that must be stand that will affect the wall's deflection during the thermo-mechanical analysis is the fact that the top of the wall remains around two degrees of difference compared to the middle part of the same. The reason why is because the pipe loop starts at a depth of 1.2 m from the top of the wall and then, the top of the wall involves not direct thermal activity and is surrounded in both boundaries by thermal insulation.

5.2.2 Carrying fluid's temperature

At a first instance, this temperature will be analysed through the plotting of the Inlet and Outlet temperatures in correspondence with the pipe's loop for the first year. Afterwards, will be shown the plots respective to the carrying fluid temperature in correspondence with the time steps shown for the solid's temperature.

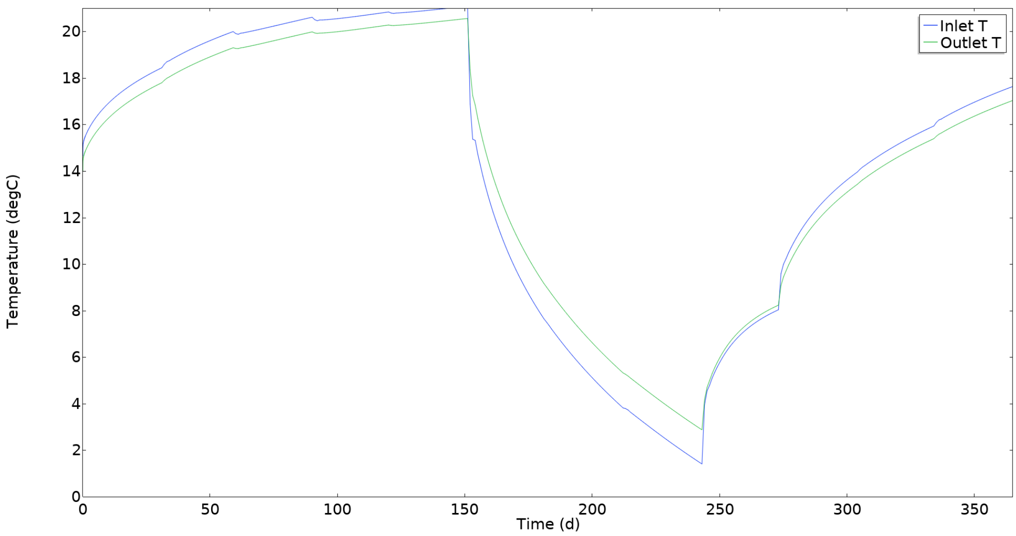

Figure 54 Inlet and Outlet temperature for the first year

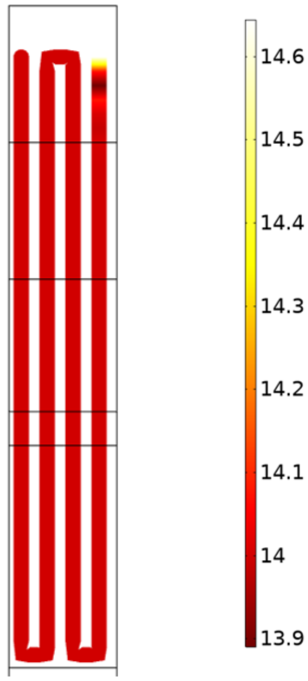

Figure 55 Carrying fluid's temperature Initial's value

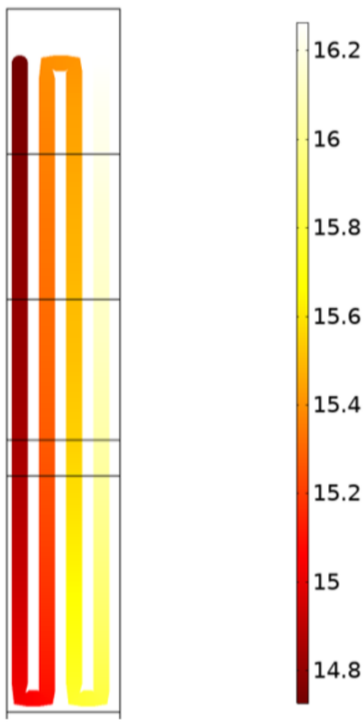

Figure 56 Carrying fluid's temperature for first period of Heating (day 130)

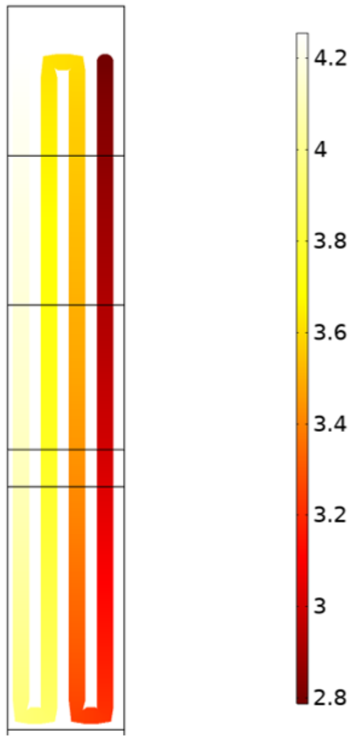

Figure 57 Carrying fluid’s temperature for first period of Cooling (day 200)

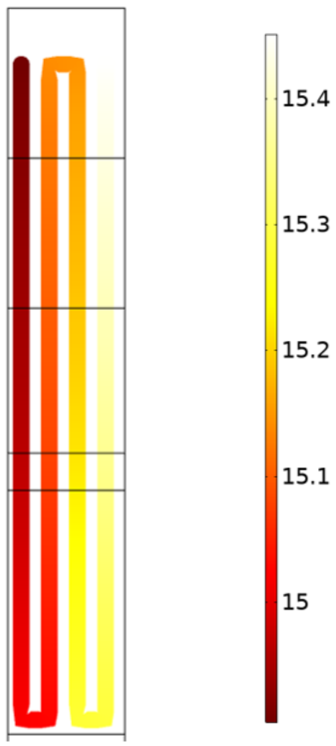

Figure 58 Carrying fluid’s temperature for second period of Heating (day 300)

Considering that in the last four plots the right top of the loop corresponds to the inlet point and the left one to the outlet one, a relation between those plots and the first one showing the whole year temperature distribution in those points can be done.

As can be seen, for the heating periods corresponding to days 130 and 300, the inlet's temperature is above the outlet one, which expressed in terms of the first plot, the inlet line showing the temperature is above the outlet one. That means that the GSHP systems is putting heat into the ground, cooling the carrying fluid and the building afterwards, For the case of day 200 =, can be seen that the opposite is happening.

There are periods of time when both temperatures, inlet and outlet have about the same value. The reason why that is because the overall system including ground and GSHP is experiencing the change from a heating load to a cooling one, or the other way around. This fact can be observed in the two following plots.

The same phenomena will happen for different time periods in the operation time of the GSHP, equalling temperatures between inlet and outlet at different values.

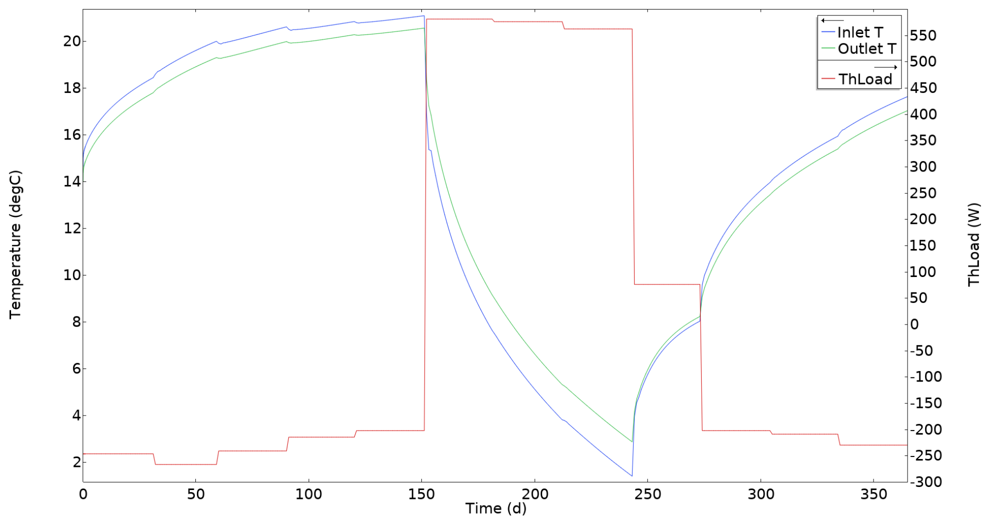

Figure 59 Inlet and Outlet temperature referred to the thermal load time

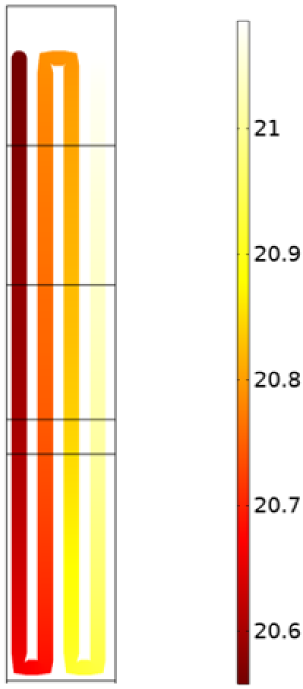

Figure 60 Carrying fluid's temperature for day 151

As can be observed in the first plot, around day 151 the inlet temperature equals the outlet one. It happens exactly at time step 151.26, but it is not possible to plot the data for that time step, since that was not a computed time step. The second plot is showing the carrying fluid's temperature for the closest time step computed. As can be seen both tops of the loop, right and left, are about the same temperature, around 21 degrees.

5.2.3 Carrying fluid's pressure

As the pipe's loop includes a flux, the head pressure loss can be analysed as well. This head pressure loss impacts in the temperature computed as these two variables are coupled within a thermodynamic system. A plot of the head pressure loss will be shown for the first period of heating in correspondence of day 130 only to show the presence of the atmospheric pressure in correspondence with the outlet point as was said during the explanation of the thermal boundary conditions.

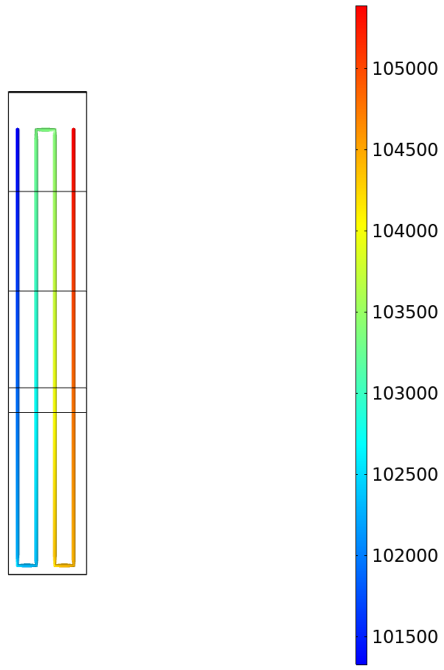

Figure 61 Head pressure loss in correspondence with the first period of Heating (day 130)

As can be observed, a pressure of 101500 Pascals is in correspondence with the outlet point (right top of the pipe loop).

5.3 Thermo Mechanical outputs

5.3.1 Initial values

As was said before, for the thermo-mechanical computation, the solver takes the mechanical values of the last mechanical model step as initial values or initial guess for the thermo-mechanical model. After that, the coupling is set between the mechanics and thermal physics during the time dependent study.

It is important to bear in mind, that the initial values taken by the solver within the thermo-mechanical model have a shift with respect with the mechanics outputs obtained with the mechanical model. This shift can be observed in the two following plots.

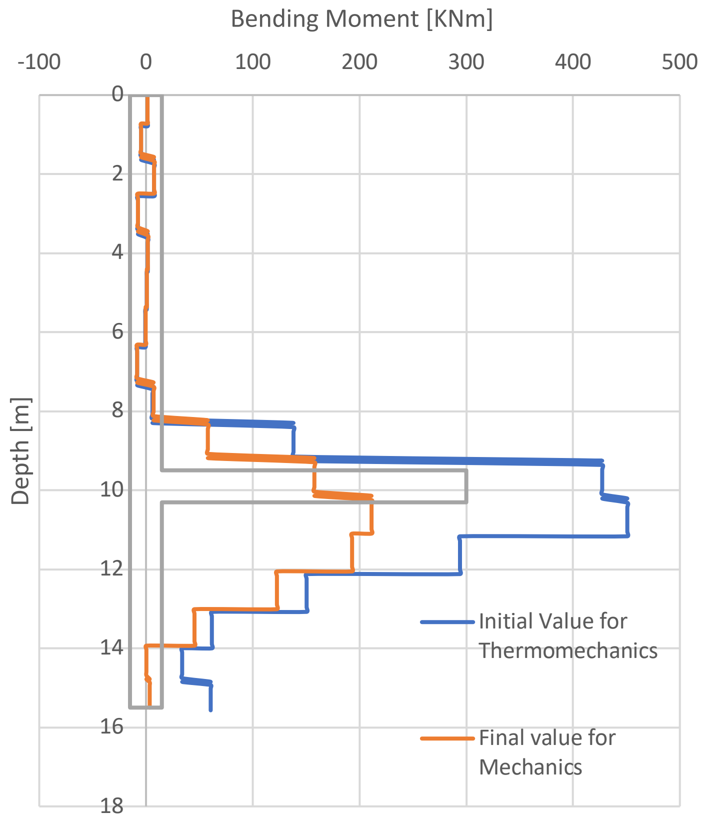

Figure 62 Bending Moment initial values for Thermo-mechanics

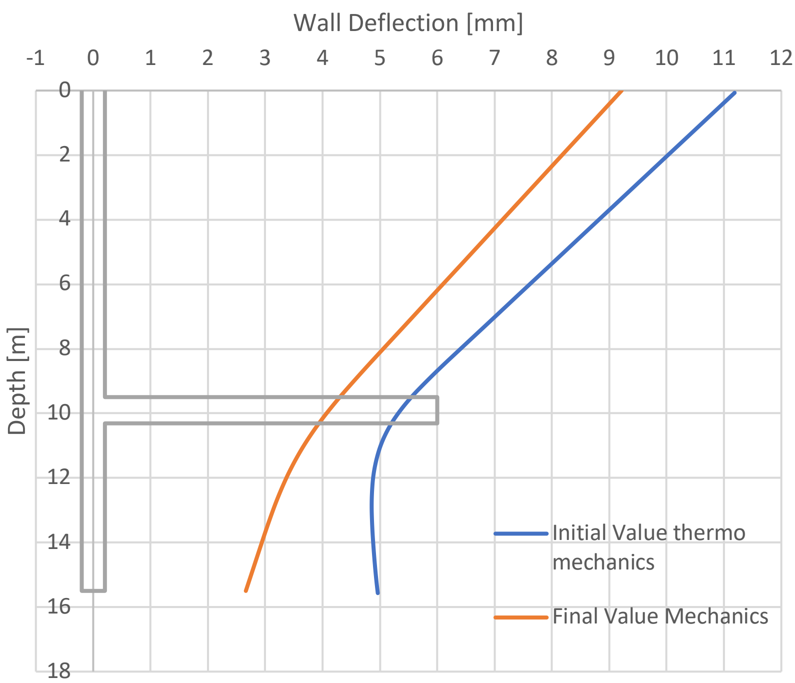

Figure 63 Wall deflection initial values for thermo-mechanics

As may be observed in the plots there is a shift of 240 KNm for the case of the maximum value of bending moment and a shift of 2 mm for the maximum of the wall's displacement. Many solvers and options about getting initial values were considered to avoid this unsuccessfully. This is a reason to not consider the absolute values of this thesis as design values.

For the aim of this thesis, the overall behaviour of the thermal wall can be still appreciated and reflect the thermo-mechanical behaviour properly (not in terms of absolute values). The reason why this is that no plasticity at all is considered during the thermo-mechanical modelling and then the effects can be observed in terms of the trend of the variables.

Since no plasticity is considered for the thermo-mechanics, it is clear that the whole constitutive behaviour becomes linear and then, no plastic strains are raised, avoiding in this way the redistribution of stresses due to these "extreme values". The main reason about not considering an elasto plastic behaviour for the thermo-mechanical model is due to the computational cost that demands. On top of that, a geothermal system of this characteristics undergoes thermal changes that the soil has already experienced and then the yielding due to this small thermal change can be disregarded.

The fact of not considering plasticity during the thermo-mechanical model doesn't affect the thermal stresses neither since thermoelectricity theory has been considered. Within this theory, the thermal strains contribute as linear elastic strains to the mechanical ones. Then the elastic strains of the thermo-mechanical domain are defined as:

$$\varepsilon_{ij} = \varepsilon_{ij}{}^{(M)} + \varepsilon_{ij}{}^{(T)}$$

5.3.2 **First Year Analysis**

During this section, the outputs will be referred to four-time steps of interest. Between them:

- Initial value
- Day 130
- Day 200
- Day 300

The reason why of choosing those time steps is that they belong to different periods of the GSHP operation. The first one allows to have a reference for the comparison of the thermo-mechanics effects. The second one belongs to the first phase of the heating of the GSHP (cooling the building and heating the ground) while the time step referred to day 200 belongs to the first phase of cooling (heating the building and cooling the ground). For the case of the last one, the same is referred to the second phase of heating of the GSHP (again, cooling the building and heating the ground).

A clear identification of the time steps that have been just mentioned is shown below:

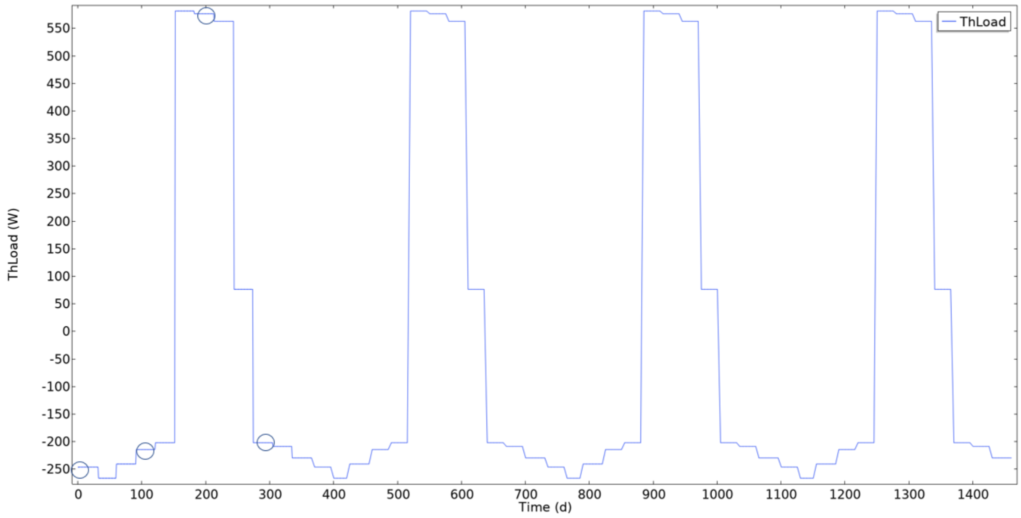

Figure 64 First year's points of interest

5.3.2.1.1 Wall Deflection

The outputs referred to the wall deflection during the first year of the GSHP activation is shown below.

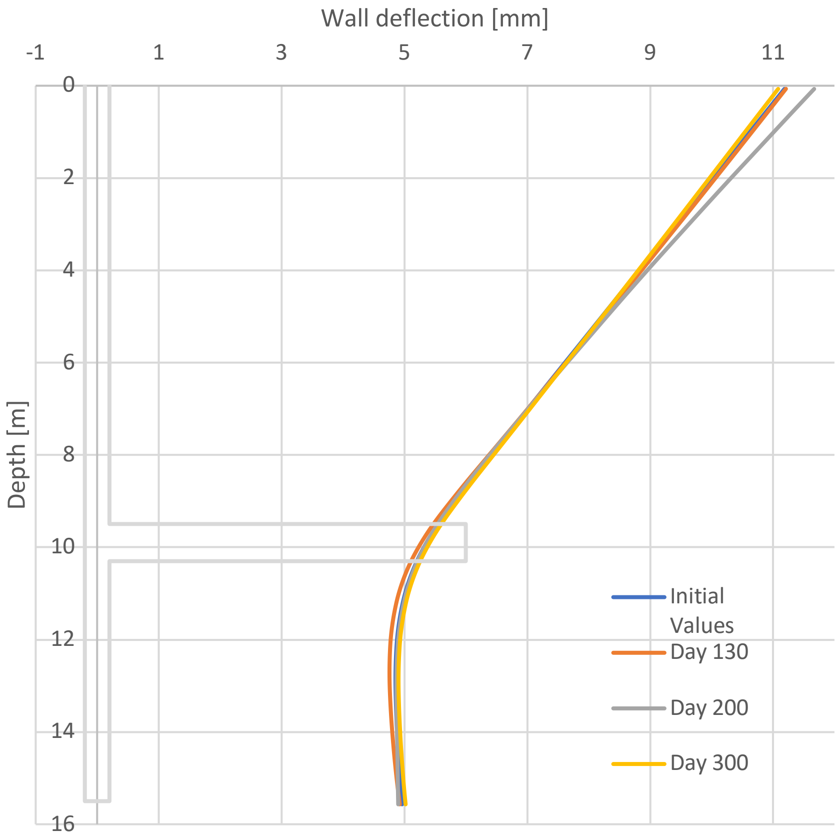

Figure 65 Wall Deflection during the first year of the GSHP operation

In the last plot, can be observed that when the GSHP is extracting heat from the ground (day 200), the top of the wall is moving the most towards the excavated side, while for the day 300 during the heating operation of the GSHP (heating the ground), the wall is moving to the unexcavated part.

This may sound unexpected thinking that heating an element produces its thermal expansion, but the reason is that the boundary conditions defined keep the top of the wall at a different temperature compared to the rest of the wall, where the pipe loop is located. The top of the wall remains around two degrees of difference compared to the middle part of the same. The reason why is because the pipe loop starts at a depth of 1.2 m from the top of the wall and then this top part of the wall involves not direct thermal activity. On top of that, the very top is surrounded in both boundaries by thermal insulation. Then, this top temperature is producing these wall deflections

To have a better view of this fact, the wall's temperature distribution is shown below for the different time steps mentioned:

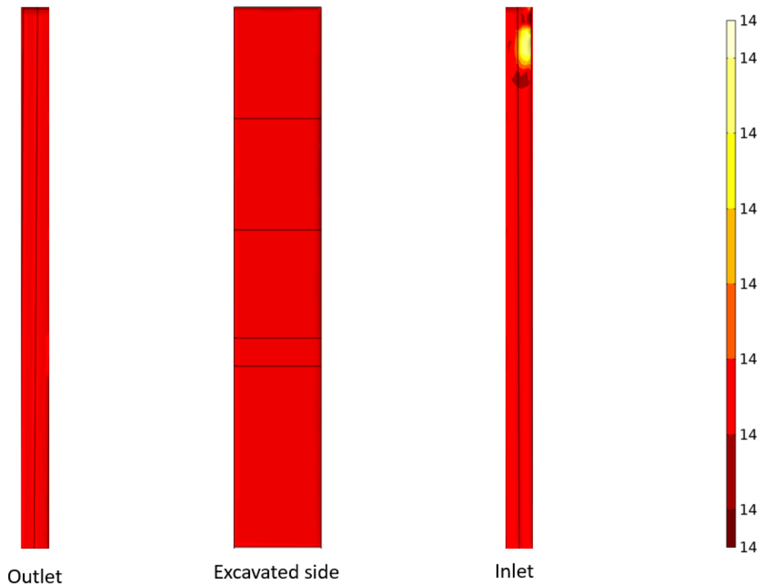

Figure 66 Initial Condition Wall's temperature distribution

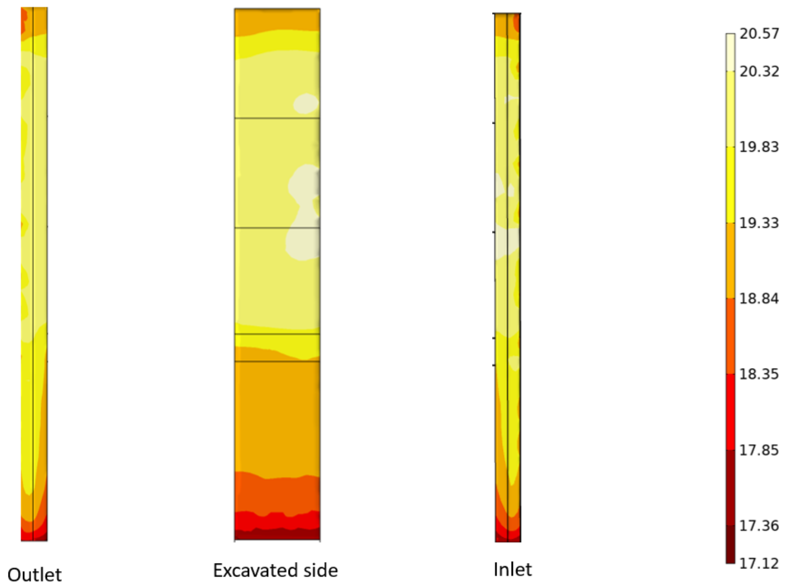

Figure 67 Day 130 Wall's temperature distribution

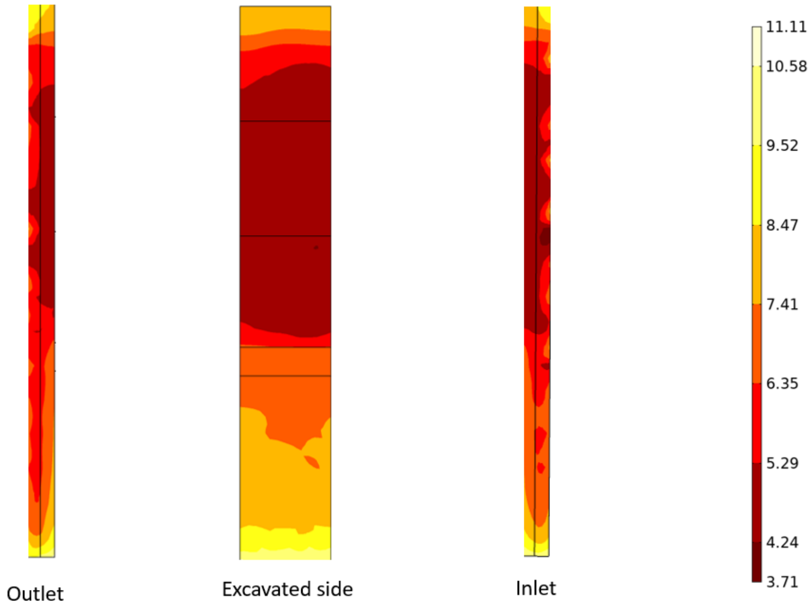

Figure 68 Day 200 Wall's temperature distribution

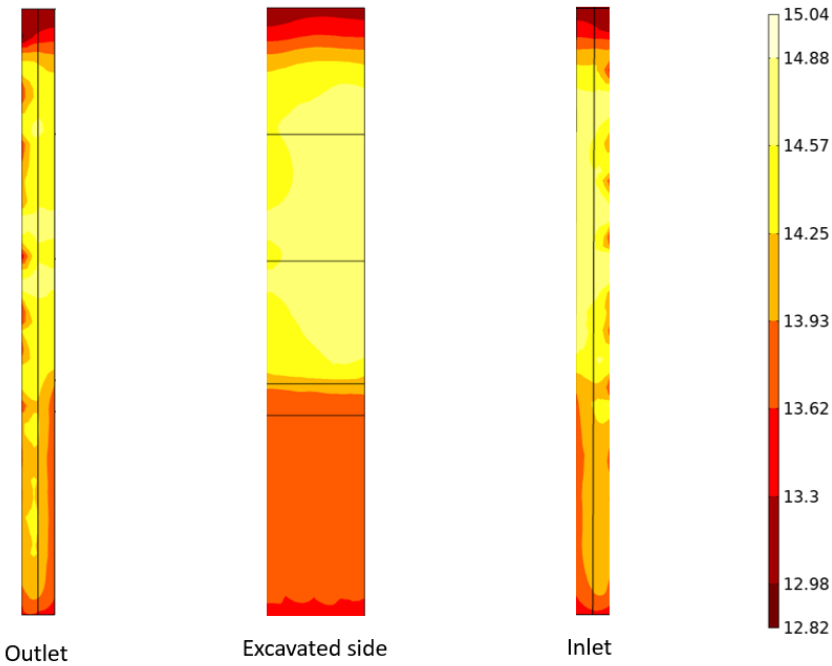

Figure 69 Day 300 Wall's temperature distribution

The same phenomena happens all over the time: i.e. in distribution can be observed the wall's temperature distribution during the cooling operation where the

GSHP is extracting heat from the ground. Can be observed that at the top the temperature is higher compared to the middle depth of the wall. Then, the wall is deflecting to the excavated side.

The behaviour of the top of the wall for the whole year and the thermal load are plot together below for a better outlook of the thermo-mechanical phenomena.

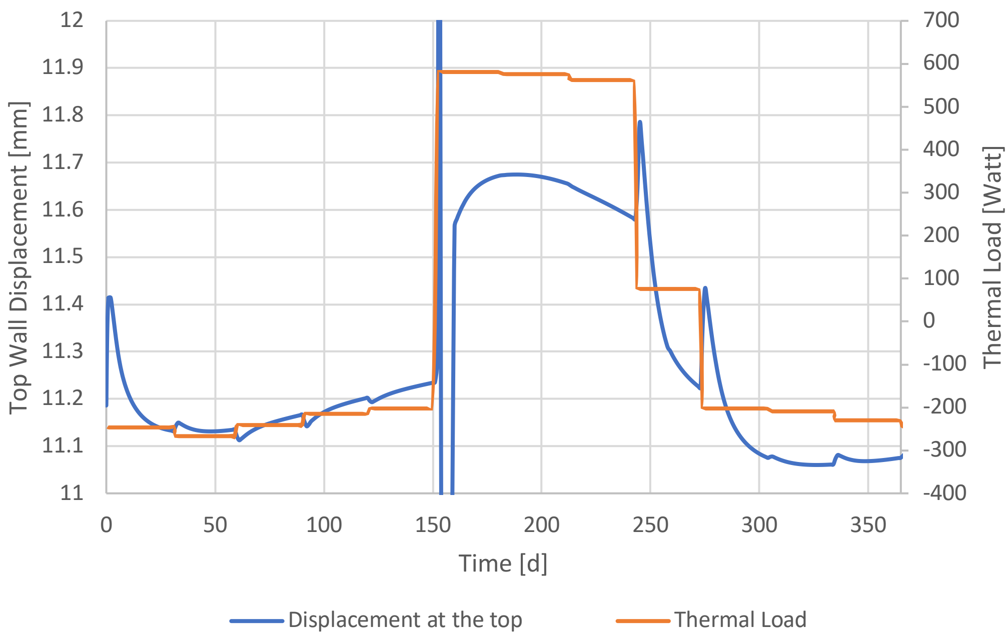

Figure 70 Top Wall displacement for the first whole year of GSHP operation

In the last plot can be observed that disregarding the pick values, the wall's deflection oscillates around the initial value within an interval of less than a millimetre for the thermal load considered.

Considering that over zero watts the load corresponds to a cooling activity of the GSHP (cooling the ground) and below it corresponds to a heating one, it can be observed the fact mentioned below. As the soil is heated up, the top wall displacement decreases, and as it is cooling down, the same is increasing.

Around day 250 and 270 are observed two picks. The reason of their presence is due to the fact that the thermal load has a sudden change between two-time steps and the thermal strains are calculated straightforward without letting the system find equilibrium. These picks will be smoother afterwards for the following years.

At the very beginning corresponding to the first days of operation can be observed a pick as well. This is happening because the solver is getting wrong values up to a certain time where it gets steady and start calculating properly these values.

5.3.2.1.2 Bending Moment

The outputs referred to the wall's bending moment during the first year of the GSHP operation is shown below.

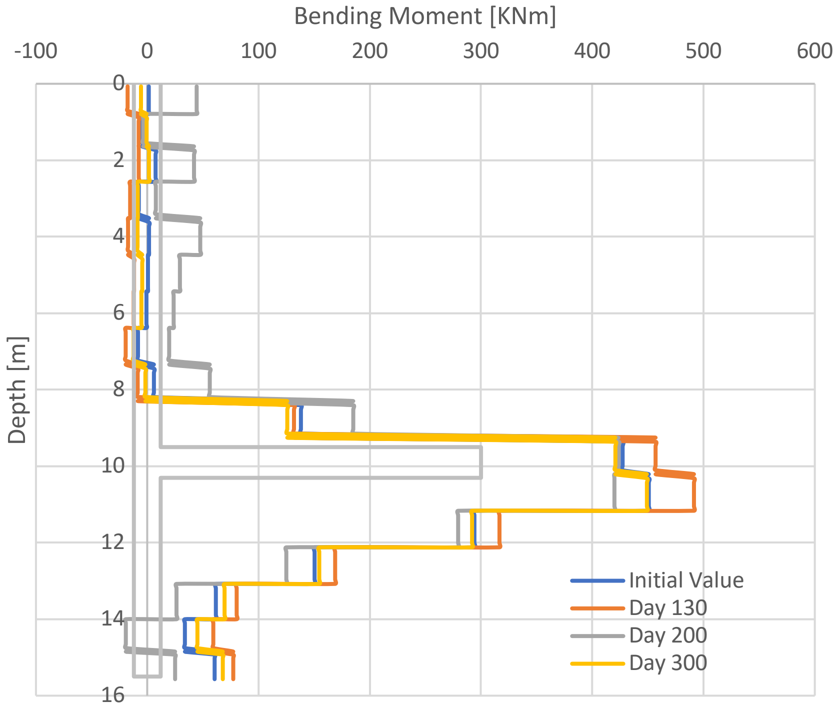

Figure 71 Bending Moment during the first year of the GSHP operation

In the last plot can be observed that the bending moment is changing mostly in correspondence with the slab, at about 9.5 meters of depth. That makes sense, since the slab acts as a constraint to the wall, not allowing the free expansion or contraction, rising the stresses' absolute value in that area of the wall but not much, as the slab is not constraining totally the rotation, it is just a stiffer contact compared to the soil.

For the case of the time step related with the cooling operation of the GSHP, the bending moment is changing also at the top and the very bottom of the wall as suggested by (Barla, Di Donna et al. 2018). This may be explained due to the fact that during the cooling operation of the wall, the domain is shrinking instead of expanding, increasing the thrust to the wall. It is obvious that when it expands, the fact that there is an excavated side where there aren't displacement constraints, gives rise to none extra stresses in correspondence with the excavated depth (top part of it), but it does affect in terms of wall's displacements.

The behaviour of the wall in terms of bending moment for the whole year and the thermal load are plot below for a better outlook of the thermo-mechanical phenomena.

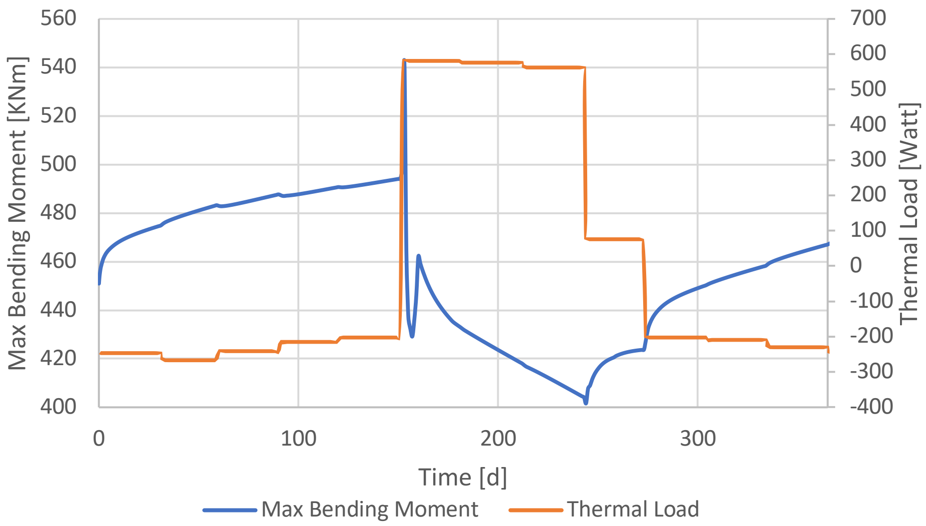

Figure 72 Bending Moment for a whole year of GSHP operation

The presence of the pick values in correspondence with the big changes on the thermal load can be appreciated as well as in the case of the wall deflection.

In the last plot can be observed that the bending moment, disregarding the pick values, oscillates around the initial value within an interval of 100 KNm.

The plot is referred to the maximum value, which is happening at different depths all over the time, but mostly around the slab were the constraint is present. Can be observed that the maximum value is increasing during the heating period and goes to lower values during the cooling one.

Thinking that the thermal activity is concentrated at the middle depth of the wall, the bending moment is affected because of a constraint thermal expansion in correspondence with the slab during heating, and a constraint thermal contraction because of the soil presence in the unexcavated side during cooling.

5.3.3 **Four-year GSHP Operation**

The operation of the Ground Source Heat Pump has been analysed for a time of four years. The results of that model are shown below.

5.3.3.1.1 Wall's maximum displacement

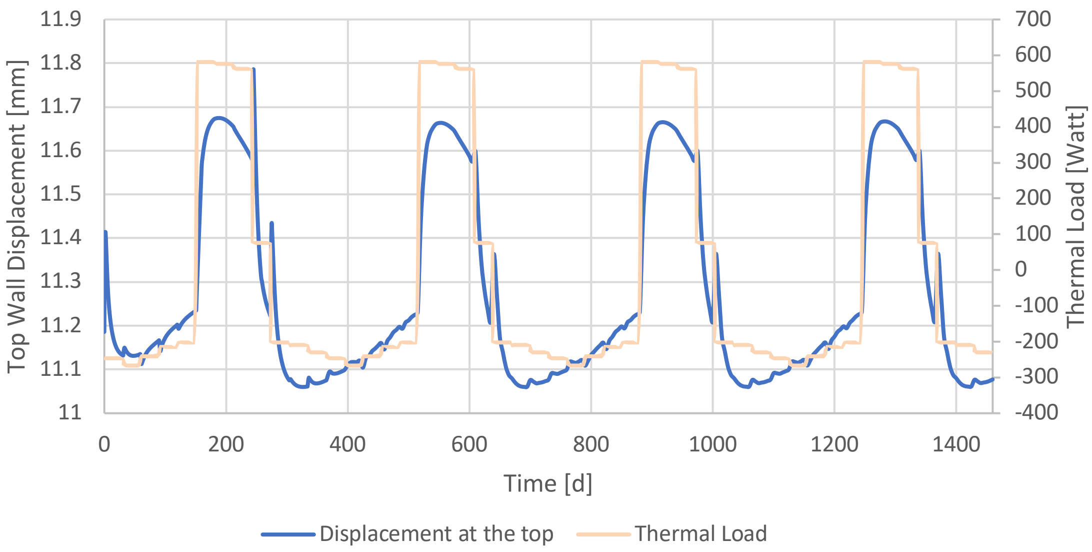

Figure 73 Top wall displacement for a four years operation of the GSHP

As can be observed in the last plot, the wall's maximum displacement remains pretty much the same through the four-year time. Both maximum and minimum values don't have a significant change through the four years' time.

The fact that the maximum and minimum value remains the same through the time is related with the presence of a balanced thermal load, which keeps the temperature equilibrium between the same interval. The presence of the balanced thermal load can be observed in terms of the areas over and under the 0 Watts of thermal load. As observed, those areas are roughly the same, showing that the heating and cooling demand are pretty much the same.

As seen, the picks of the top of the wall displacement' plot in correspondence with the big thermal load changes are smoother for the last three years, compared with the first year.

In the last plot can be observed that the maximum values of the top wall displacement, correspond to the first third of the cooling period while the lower maximum value ones correspond to the heating period coming right after the cooling ones.

The wall deflection for the whole wall depth is plot below for the end of each year (day 365,730,1095 and 1460) to show that not only the top wall displacement is the same but the whole wall deflection as well.

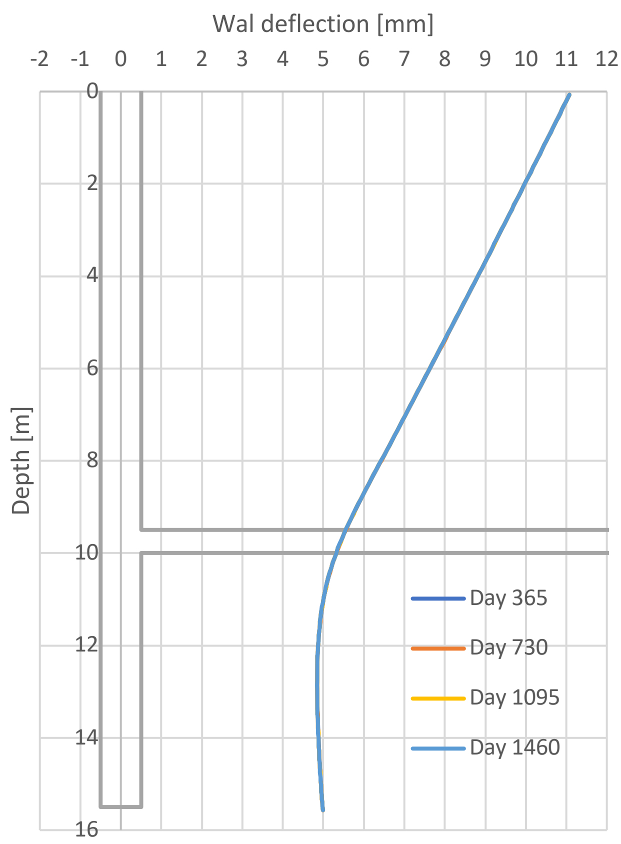

Figure 74 Wall deflection at the end of each year

5.3.3.1.2 Bending moment

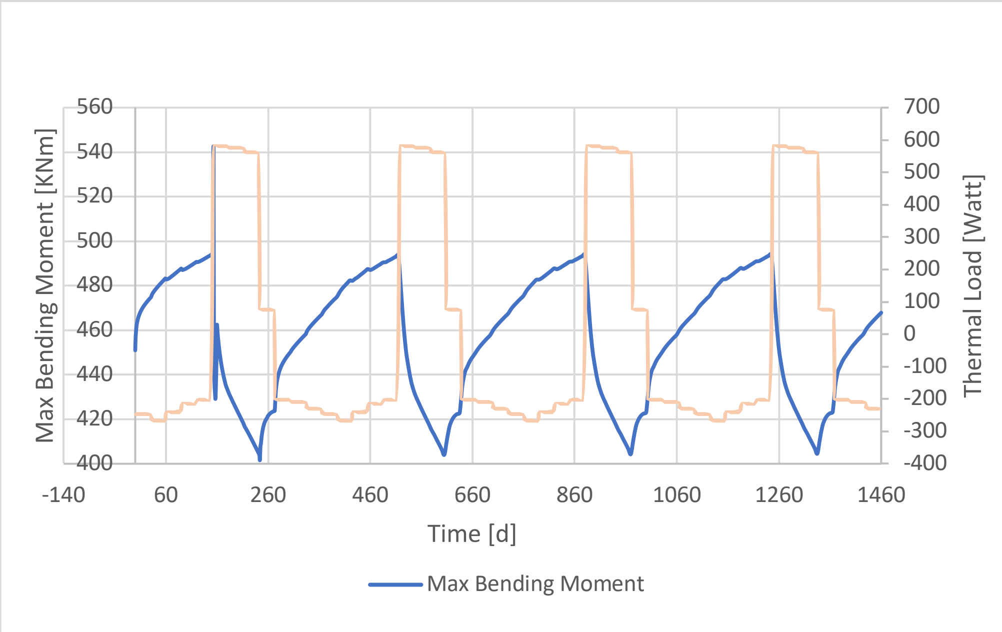

Figure 75 Maximum bending moment for a four years operation of the GSHP

Something important to observe in this plot is that the bending moment trend is quite similar to the inlet and outlet temperatures one included in 5.2.2 (Carrying fluid's temperature) . That is not happening for the case of the top wall displacement.

In the last plot can be observed that the maximum bending moment values correspond to end of the heating periods and the lower maximum values to the last third of the cooling period, when the thermal load is almost zero.

As in the case of the wall's deflection can be observed that the wall's maximum bending moment remains pretty much the same through the four-year time. The fact of the picks getting smoother in the following years is present too.

The reason of the balanced thermal load regarding the maximum and minimum values changes involved in the top displacement applies for the bending moment trend as well.

The bending moment effort for the whole wall depth is plot below for the end of each year (day 365,730,1095 and 1460) to show that not only the maximum and minimum values are the same but the whole bending moment distribution as well.

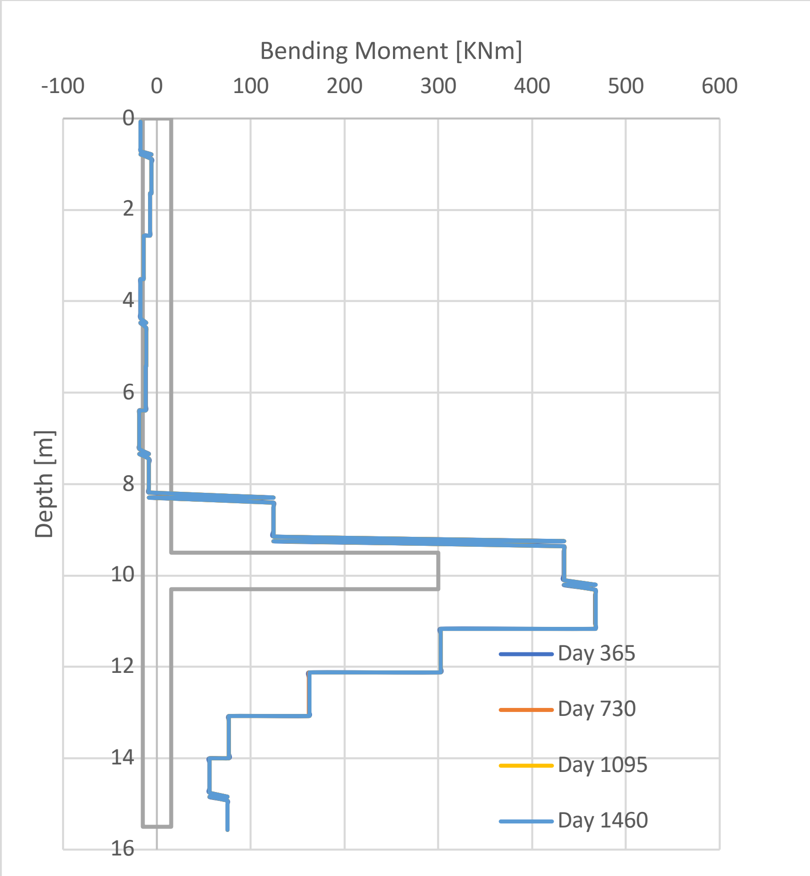

Figure 76 Bending Moment at the end of each year

5.3.3.1.3 Inlet and Outlet Temperature

This mentioned fact about the oscillation around constant values for the four-year's time and the not over accumulation or over extraction of heat can be seen clearly through the plot of the inlet and outlet temperature. The same is shown below for the four years computed:

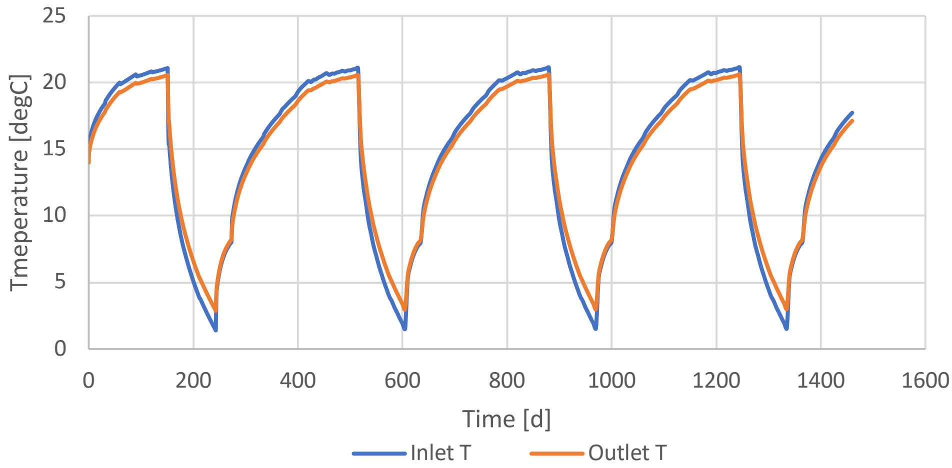

Figure 77 Inlet and Outlet temperatures

The fact that there is no accumulation or over extraction of heat produces that the maximum and minimum values remain in the same interval during the years for temperatures, wall's displacements and wall's efforts.

For a better understanding of the effects of unbalanced thermal loads a reference to (Makasis 2018) work will be done.

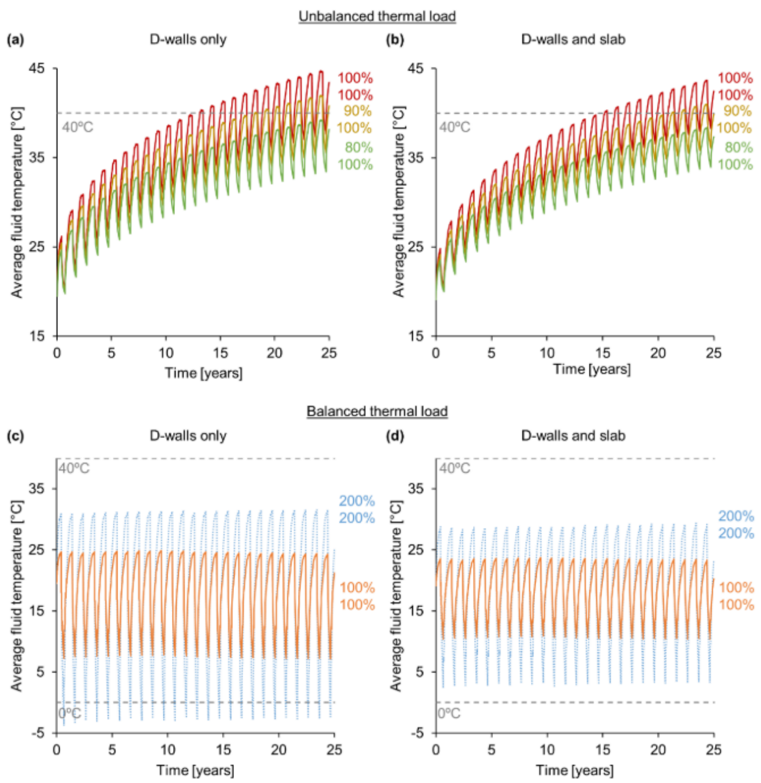

Figure 78 Fluid temperature results providing different amounts of energy

As can be observed in plot a) and b), the average fluid temperature increases when an unbalanced load takes place, while it remains within the same interval for a balanced one. The changes in the average fluid temperature is coupled to the changes in the ground and wall temperature as well. Knowing that, it is logical that for an unbalanced load, the maximum and minimum values of bending moment and wall deflection change between the operation years.

5.3.4 Conclusions

During the last chapter, the outputs of a thermal diaphragm wall under a balanced thermal load has been analysed. Through the same, the relevance of the balanced thermal load in the results has been explained. The balanced case should be considered as a different case from the unbalanced one in terms of maximum and minimum values reachable.

Under these conditions, a thermal diaphragm wall undergoes thermal effects in terms of displacements and efforts. For this case, the impact of the thermal activity was stronger in terms of efforts respect to the displacements. This allows to think that this thermal activity won’t affect the serviceability of the structure as much as the efforts ideally.

Regarding the efforts, it would be recommendable to consider the maximum bending moment changes, as for the case of a balanced load is considerable, and then, knowing that there may be accumulation of thermal effects for unbalanced loads, its change may be important.

With the results obtained can be observed that the modelling of the geothermal system doesn’t need to be done for long periods of time for the case of the balanced load, while for the case of unbalanced, this may be the main thing to focus on.

During the modelling of this structure, could be observed that the thermal boundary condition of the top surface in correspondence with the unexcavated side is essential. That boundary condition affects the thermo mechanical response of the structure conditioning not only the absolute value of the variables involved, but the whole behaviour as well. It is recommendable to analyse deeply that boundary condition, considering how the neighbour structures affect that surface in terms of temperature for a proper thermo-mechanical modelling.

References

"<CRC Continuum Mechanics for Engineers>."

Barla, M. and A. Di Donna (2018). "Energy tunnels: concept and design aspects." Underground Space **3**(4): 268-276.

Barla, M., et al. (2018). "Energy and mechanical aspects on the thermal activation of diaphragm walls for heating and cooling." Renewable Energy.

Coletto, A. and D. Sterpi (2016). "Structural and Geotechnical Effects of Thermal Loads in Energy Walls." Procedia Engineering **158**: 224-229.

Lade, P. V. (2005). Overview of Constitutive Models for Soils. Soil Constitutive Models**:** 1-34.

Lund, J. W. and T. L. Boyd (2016). "Direct utilization of geothermal energy 2015 worldwide review." Geothermics **60**: 66-93.

Makasis, N. (2018). Further understanding ground source heat pump system design using finite element methods and machine learning techniques, University of Melbourne.

ACKNOWLEDGMENTS

This study was supported by the PMRL group of the University of Melbourne. The collaborative work of this effort significantly improved the quality of this thesis. The thermal modelling was advised by this group, who has been involved in thermal response of soils in many projects all over Australia.

I would like to thank specially to Guillermo Narsilio from the University of Melbourne and a member of the PMRL group, who has accompanied my work from the beginning. Also, I would like to thank Nikolas Makasis who has advised me any time I needed about the software I have used and took time to listen to me for any doubt I had as all the members of the PMRL group. Finally, I want to mention the presence of Yu Zhong, Yu Zhou, Wenbin Fei, Yaser Motamedi from PMRL group, specially Gregorius Aditya who was a member with which I had a really good connection and gave me motivation every morning at the office.

In particular I want to mention Marco Barla from the Politecnico di Torino, my former teacher from the subject “Numerical methods for geotechnical engineering” who has taught me everything a knew which was essential for the development of this work, and also for awakening my interest into geotechnics, as I was a structural engineer before starting his subject.

This thesis is a gift to my mother Silvia who has always been with me in the path and guided me through every decision I made.